

NEUROBEHAVIORAL AND GENE EXPRESSION EFFECTS OF EARLY
EMBRYONIC METHYLMERCURY EXPOSURE IN YELLOW PERCH (*Perca
flavescens*) AND ZEBRAFISH (*Danio rerio*) LARVAE

by

Francisco X. Mora

A Dissertation Submitted in
Partial Fulfillment of the
Requirements for the Degree of

Doctor of Philosophy
in Freshwater Sciences

at

The University of Wisconsin-Milwaukee

August, 2015

ABSTRACT

NEUROBEHAVIORAL AND GENE EXPRESSION EFFECTS OF EARLY EMBRYONIC METHYLMERCURY EXPOSURE IN YELLOW PERCH (*Perca flavescens*) AND ZEBRAFISH (*Danio rerio*) LARVAE

by

Francisco X. Mora

The University of Wisconsin-Milwaukee, 2015

Under the Supervision of Professor Michael J. Carvan III

Methylmercury (MeHg) is a pervasive and persistent neurotoxic environmental pollutant known to affect the behavior of fish, birds and mammals. The present study addresses the neurobehavioral and gene expression effects of MeHg in yellow perch (*Perca flavescens*) and zebrafish (*Danio rerio*) embryos. The rationale for this study originated from an interest to understand the behavioral and molecular phenotypes of environmental MeHg exposure in the yellow perch, an ecologically and economically relevant species of the North American Great Lakes region. Both MeHg and the yellow perch coexist in a common ecosystem: the North American Great Lakes. However, the effects of this organism-contaminant interaction are poorly understood. The zebrafish was utilized here as a surrogate model for yellow perch, due to its ease of rearing, whole sequenced genome and its status as an NIH endorsed model organism. The objectives of this study were to understand the effects of MeHg on behaviors that are critical for survival both in yellow perch and zebrafish. Among the behavioral paradigms tested, this study addressed fundamental behaviors for the survival of young larval fish, namely swimming and prey capture. Furthermore,

this study screened for gene expression alterations in the same cohorts of fish for which behavioral analysis was performed; this was done to gain insight into the gene pathways involved in MeHg-induced neurotoxicity, as well as to expand the knowledge about biomarkers of MeHg exposure in the yellow perch. Here, we have uncovered important differences and similarities between the effects of MeHg exposure in yellow perch and zebrafish larvae, both in terms of behavioral and molecular responses to MeHg. The findings of this study suggest that environmentally relevant MeHg exposure can adversely affect the behavior of yellow perch larvae and impair fundamental survival skills. Furthermore, this study determined that although it would be challenging to relate behavioral endpoints between yellow perch and zebrafish, molecular responses between these two species could be more conserved.

Key words: yellow perch, zebrafish, methylmercury, behavior, molecular biomarkers.

© Copyright by Francisco X. Mora, 2015
All Rights Reserved

TABLE OF CONTENTS

ABSTRACT	ii
LIST OF FIGURES	ix
LIST OF TABLES	x
ACKNOWLEDGEMENTS.....	xi
CHAPTER 1: INTRODUCTION TO THE DISSERTATION.....	1
Rationale and relevance of the study	1
Overview of the dissertation	4
Figures	7
CHAPTER 2: THE NICOTINE-EVOKED LOCOMOTOR RESPONSE: A PARADIGM FOR BEHAVIORAL NEUROTOXICITY SCREENING IN ZEBRAFISH (<i>Danio rerio</i>) EMBRYOS AND ELEUTHEROEMBRYOS	9
Abstract	9
Introduction.....	11
Materials and methods	14
Fish husbandry.....	14
Nicotine-evoked Locomotor Response (NLR) dose curve.....	15
Recording apparatus.....	16
Modulation of the NLR by chronic low-dose exposure to nicotine in 48 hpf embryos	17
Analysis of the NLR in macho zebrafish mutants	17
Methylmercury exposure regimes	18
Free swimming of methylmercury exposed 6 dpf zebrafish eleutheroembryos	18
NLR of methylmercury exposed 48 hpf zebrafish embryos.....	19
Statistical analyses.....	19
Results	20
Nicotine-evoked locomotor response (NLR) dose curve	20
NLR in chronic low-dose nicotine-exposed embryos and “macho” mutants....	21
Free swimming and NLR of MeHg exposed eleutheroembryos and embryos.	22
Discussion	23
Figures	26
Tables.....	36

CHAPTER 3: PARENTAL WHOLE-LIFE-CYCLE EXPOSURE TO DIETARY METHYLMERCURY IN ZEBRAFISH (<i>Danio rerio</i>) AFFECTS THE VISUALMOTOR RESPONSE, LOCOMOTION AND FORAGING OF OFFSPRING.....	39
Abstract	39
Introduction.....	40
Materials and methods	43
Fish husbandry.....	43
MeHg food preparation.....	44
Dietary MeHg exposure regimes	44
Assessment of embryo mortality and early life stage (ELS) toxicity	46
Analysis of Hg contents in diets and tissues	47
VMR assay.....	47
Analysis of 7 dpf larval zebrafish swimming behavior	48
Routine swimming and prey capture at 8, 12 and 16 dpf	49
Data processing and statistical analysis.....	50
Results	52
Embryo mortality and early life stage (ELS) toxicity scoring.....	52
Mercury analyses	52
VMR assay.....	52
Analysis of 7 dpf larval zebrafish swimming behavior	53
Routine swimming and prey capture at 8, 12 and 16 dpf	54
Discussion	55
MeHg accumulation in tissue	55
VMR assay.....	55
Routine swimming behavior and prey capture (separate swimming from prey capture and narrate developmentally).....	57
Relevance of observed behavioral endpoints in predator-prey dynamics	59
Figures	60
Tables.....	74
CHAPTER 4: EFFECTS OF EARLY EMBRYONIC MeHg EXPOSURE IN THE LOCOMOTION, VISUALMOTOR RESPONSE AND FORAGING OF YELLOW PERCH (<i>Perca flavescens</i>) LARVAE	76
Abstract	76

Introduction.....	77
Materials and methods	80
Yellow perch broodstock and egg husbandry.....	80
Static waterborne MeHg exposure regimes	81
Analysis of 17 dpf larval yellow perch swimming behavior	82
Visual-motor response assay	82
Routine swimming and prey capture at 25 dpf larvae	83
Data processing and statistical analysis.....	85
Results	86
Discussion	88
Figures	91
Tables.....	103
CHAPTER 5: GENE EXPRESSION ALTERATION ASSOCIATED WITH EARLY EMBRYONIC MeHg EXPOSURE IN YELLOW PERCH (<i>Perca flavescens</i>) AND ZEBRAFISH (<i>Danio rerio</i>) LARVAE	104
Abstract	104
Introduction.....	106
Materials and methods	109
Experimental organisms and tissue collection.....	109
RNA Isolation and quality assurance.....	110
Illumina TruSeq RNA Library Preparation and Sequencing of zebrafish RNA	110
RNA-Seq data analysis	111
Selection of biomarkers of MeHg exposure for yellow perch.....	113
RT-qPCR primer design for yellow perch	114
Primer optimization for RT-qPCR.....	116
Yellow perch RT-qPCR	117
Results	119
Zebrafish whole-embryo RNA-Seq.....	119
Yellow Perch RT-qPCR.....	120
Discussion	121
Figures	125
Tables.....	130

CHAPTER 6: SUMMARY OF THE DISSERTATION.....	138
REFERENCES	149
APPENDICES	160
Appendix 1: Maternal MeHg transfer from ovaries to zebrafish embryos	160
Appendix 2: Fecundity of MeHg exposed zebrafish females and mortality of their offspring	161
Appendix 3: ELS tox scores of embryonic zebrafish from MeHg exposed parents	162
Appendix 4: Significantly up-regulated genes in 1ppm MeHg treated zebrafish embryos.	163
Appendix 5: Significantly down-regulated genes in 1ppm MeHg treated zebrafish embryos.....	164
Appendix 6: Significantly up-regulated genes in 3ppm MeHg treated zebrafish embryos.	166
Appendix 7: Significantly down-regulated genes in 3ppm MeHg treated zebrafish embryos.....	169
Appendix 8. Significantly up-regulated genes in 10ppm MeHg treated zebrafish embryos.	173
Appendix 9. Significantly down-regulated genes in 10ppm MeHg treated zebrafish embryos.....	175
Appendix 10: Gene ontology (GO) enrichment analysis of biological functions affected by MeHg exposure in zebrafish embryos.	179
Appendix 11: Gene set enrichment analysis (GSEA) results for each MeHg exposure concentration tested in zebrafish embryos.	181
Appendix 12: RNA yields and RIN values of zebrafish whole-embryo RNA extractions.....	188
Appendix 13: RNA yields and RIN values of yellow perch whole-embryo RNA extractions.....	189
Appendix 14: RT-qPCR primers utilized for the analysis of gene expression in yellow perch embryos.....	192
Appendix 15: Accession numbers of proteins used to perform alignments in order to create degenerate primer pairs for yellow perch	193
Appendix 16: Degenerate primers for yellow perch obtained from protein alignment.....	194
Curriculum vitae.....	195

LIST OF FIGURES

Figure 1.1: Decline of the yellow perch populations	7
Figure 2.1: Characteristic kinematics of the nicotine-evoked locomotor response in zebrafish embryos	26
Figure 2.2: Custom-made behavior observation chamber	28
Figure 2.3: Nicotine-evoked locomotion dose response curves in 36 and 48 hpf zebrafish embryos	30
Figure 2.4: Validation of the nicotine-evoked locomotor response assay by testing it in the non-touch-responsive “macho” mutant zebrafish strain	32
Figure 2.5: Spontaneous swimming of 6 dpf MeHg-exposed zebrafish eleutheroembryos and the NLR of MeHg-exposed 48 hpf embryos	34
Figure 3.1: Whole life cycle MeHg exposure experimental design	60
Figure 3.2: Regression analysis of THg in embryos as a function of THg in ovaries	62
Figure 3.3: Parentally transmitted MeHg burdens affect the VMR of 6 dpf zebrafish offspring	64
Figure 3.4: Effects of parental dietary MeHg on the spontaneous swimming of 7 dpf zebrafish offspring	66
Figure 3.5: Maternal dietary MeHg burdens increase the swimming scoot frequency of the offspring	68
Figure 3.6: Monitoring of routine swimming of 8, 12 and 16 dpf and foraging efficiency assay	70
Figure 3.7: Prey capture is increased by MeHg exposure	72
Figure 4.1: Yellow perch MeHg exposure assay	91
Figure 4.2: Individual trajectory traces from a group of free swimming 25 dpf yellow perch larvae	93
Figure 4.3: Comparison of locomotor activity in 17 dpf yellow perch exposed to MeHg and tested in two different lighting conditions	95
Figure 4.4: Locomotor output of 21 dpf yellow perch throughout the VMR assay	97
Figure 4.5: Locomotor output of 25 dpf yellow perch prior to prey capture assay	99
Figure 4.6: Locomotor activity and prey capture efficiency of 25 dpf yellow perch	101
Figure 5.1: Schematic representation of the software packages used to create an RNA-seq analysis pipeline	125
Figure 5.2: Transcriptomic analysis of dysregulated genes in MeHg-exposed 5 dpf zebrafish embryos	126
Figure 5.3: Expression analysis of selected genes in yellow perch	128

LIST OF TABLES

Table 2.1: NLR dose response in 36 and 48 hpf zebrafish embryos	36
Table 2.2: Modulation of the NLR in 48 hpf zebrafish embryos by chronic, low-dose exposure to nicotine during development	37
Table 2.3: Effect of methylmercury on the NLR of 48 hpf zebrafish embryos	38
Table 3.1: G ₁ diet Hg concentrations and embryo burdens	74
Table 3.2: G ₂ diet Hg concentrations and embryo burdens	75
Table 4.1: THg concentrations and post-hatch mortality of 14 dpf yellow perch embryos.....	103
Table 5.1: Gene ontology (GO) enrichment analysis of the top 20 biological functions affected by MeHg exposure in zebrafish embryos	130
Table 5.2: KEGG enrichment analysis of genes affected by MeHg exposure in zebrafish embryos	131
Table 5.3: Phenotype enrichment analysis of dysregulated genes in MeHg exposed zebrafish	132
Table 5.4: Gene set enrichment analysis (GSEA) results for each MeHg exposure concentration tested in zebrafish embryos (Curated gene collection)	133
Table 5.5: Gene set enrichment analysis (GSEA) results for each MeHg exposure concentration tested in zebrafish embryos (Biological process collection)	134
Table 5.6: Gene set enrichment analysis (GSEA) results for each MeHg exposure concentration tested in zebrafish embryos (Cellular component and molecular function collections).....	135
Table 5.7: Gene set enrichment analysis (GSEA) results for each MeHg exposure concentration tested in zebrafish embryos (Human phenotype ontology collection)	136
Table 5.8: Dysregulated genes in zebrafish and yellow perch.....	137

ACKNOWLEDGEMENTS

I would like to express my most sincere gratitude to my PhD. Adviser Dr. Michel Carvan III. Since my first visit to his laboratory he has always conveyed a sense of welcoming and good will. I also thank each one of my committee members; Dr. Cheryl Murphy, Dr. Kurt Svoboda, Dr. John Janssen and Dr. Peter Tonellato. They have all been instrumental in my formation, and have bestowed on me great amounts of knowledge, each one in their area of expertise.

My dissertation work could not have been possible without funding from the United States Environmental Protection Agency, the National Oceanic and Atmospheric Administration's Ocean and Human Health traineeship and from the School of Freshwater Sciences of the University of Wisconsin – Milwaukee.

I acknowledge our close collaborators Dr. Niladri Basu and Dr. Jessica Head for their assistance in total mercury quantification in zebrafish and perch tissues. Also, I thank Gregory Barske and Randolph Metzger from the School of Freshwater Science's instrument shop for their role in the creation of several custom-made instruments that I used for behavioral analyses.

I thank Dr. Rebekah Klingler for her unconditional friendship and support throughout the last four years. Her guidance, assistance and discipline were crucial for the success of every single one of my bioassays, both in yellow perch and in zebrafish. I also thank her for being my molecular biology tutor and for teaching me good laboratory practices.

I give special thanks to my dear friends and lab mates MSc Abigail DeBofsky and MSc Jeremy Larson. Both of them paved the road for the optimization and standardization of the qPCR techniques that I employed to analyze gene expression in yellow perch; they were always willing to assist me or answer my questions. I also thank the Marcus Evan Waltz, Brady King and David Anderson from the Tonellato Lab for their assistance in the analysis of the zebrafish RNA-seq data. Your role in this project was instrumental.

Special thanks also to Rebecca Klaper, Angela Schmoldt, Raymond Hovey, Brittany Suttner and Christopher Suchocki from the Great Lakes Genomics Center (University of Wisconsin – Milwaukee) for their support with my molecular biology experiments and questions.

To my lab mates, Matthew Pickens, Thomas Kalluvila, Amanda Carson and Gayle Mentch, thank you very much for your friendship and support in fish husbandry activities. The laboratory would not have been the same without you.

I would also like to thank the current and former members of the Children's Environmental Health Sciences Core: Kris Kosteretz, Alisa Henry, Samantha Sullivan, Tyrone Gandhi, Mike Henderson, Joseph Lutz and Miguel Lewis. Your dedication to the welfare of our experimental fish and your camaraderie will never be forgotten.

To my closest friends and "allies in life": Jessica Schuld, Matthew Wolter, Jane Harrison and Doug Sours. Thank you for the company and the laughter. "All work and no play would have made Francisco a dull boy".

Finally, I thank my family, I would have not been able to get this far in life without their love and support, I thank my mother Aurelia Zamorano; your upbringing gave me the strength to believe in myself. To my departed father, Sergio Mora, your gentle heart and good humor are missed every single day, but we keep moving forward, just like you taught us. To my brothers, Luis, Sergio and Jorge, thank you for your support and wisdom, I am here for you, whenever you need me, always. Special thanks to my uncles Francisco and Victor who have been absolutely wonderful to me throughout my years in Milwaukee and remind me of my “papá” every single time I see them. Finally, to my “adoptive family”: Eileen Gordoux and Sarah Graycareck, the Katz-Bogan family the Buechs family and Louise Robinson. Thank you for the good times and the good food. It was never a dull moment around you.

CHAPTER 1: INTRODUCTION TO THE DISSERTATION

Rationale and relevance of the study

Mercury (Hg) is a widespread and pervasive heavy metal found in a variety of forms in freshwater and marine ecosystems around the world (Devlin, 2006). Naturally occurring processes such as volcanic eruption can release inorganic mercury into the atmosphere, but it was the onset of the industrial revolution that introduced new sources of anthropogenic-derived mercury emissions such as fuel combustion, waste incinerators, mining, and manufacturing. Among all of the sources of mercury, the most numerous and largest emitters are coal-fired power plants (Monson, 2009a).

Mercury enters the aquatic ecosystems primarily through atmospheric deposition (Risch et al., 2012a), after which anaerobic bacteria convert the elemental form of mercury into organic molecules (Alvarez et al., 2006a). MeHg is reported to be the most abundant form of environmental mercury and accounts for up to 99% of the total mercury fraction in analyzed tissues (Klaper et al., 2006). Fish begin experiencing adverse effects from MeHg exposure at a tissue concentration of 0.2ppm in wet weight (ww) (Wiener et al., 2012). Reported neurological effects of methylmercury in fish include abnormal startle response, and diminished visual perception (Smith et al., 2010), reduction of serotonin levels in the brain, inhibition of normal development of the hypothalamic serotonergic system, effects on locomotor activity and impairment of prey capture abilities (Alvarez et al., 2006a). Moreover, levels of ≥ 0.3 ppm ww in fish muscle

tissue result in consumption advisories; these advisories, in turn, have been reported in almost every body of water in the North American Great Lakes basin (Wiener et al., 2012).

The yellow perch was selected as a study organism not only due to its autochthony in an ecosystem historically affected by MeHg, but also due to its economical relevance. The yellow perch is valued for its meat and it is popular among anglers (Provencher and Bishop, 1997), however this has been antagonized by a drastic population decline of this species observed over the last 25 years (Figure 1.1; Wilberg et al., 2005). Before 1997 this species represented 85% of the recreational catch by number; more recently it has been estimated that the stock of adult yellow perch suffered a decline of 92% in the state of Wisconsin (Wilberg et al., 2005).

There are many acknowledged causes for the population decline of the yellow perch, namely overfishing (Marsden and Robillard, 2004), introduction of invasive species (Shroyer and McComish, 2000), and to alterations in the trophic chain leading to a scarcity of plankton for the young yellow perch larvae to feed upon (Dr. John Janssen, University of Wisconsin – Milwaukee, personal communication). Nevertheless, the role of environmental pollutants in the population dynamics of the yellow is seldom addressed or understood.

Exposure concentrations of MeHg that are substantially lower than those that cause mortality can cause observable effects in behavior (Scheuhammer et al., 2007a). These subtle sub-lethal behavioral effects can have enormous implications for the survival of whole populations (Alvarez et al., 2006a). It is not

unlikely that the presence of neurotoxic environmental contaminants such as MeHg could be exacerbating the problem of poor yellow perch recruitment¹ by subtly affecting the survival skills of the young larvae (e.g. capturing prey and avoiding predators). Moreover, by coupling behavior analysis with gene expression quantification it is possible to elucidate phenotypically-anchored molecular biomarkers of MeHg exposure, which can give insights into the putative molecular mechanisms of MeHg-induced behavior alteration.

The zebrafish was integrated into this study to perform behavioral and gene expression analysis in parallel with the yellow perch. Despite the enormous ecological and economical relevance of the yellow perch, exclusively utilizing this organism to carry out behavioral and gene expression analysis poses important methodological challenges. Yellow perch only spawn seasonally, it takes roughly 2-3 years for this species to reach sexual maturity, the rearing of larvae in controlled conditions can be extremely complicated and the species lacks a fully sequenced genome. In light of these challenges, the zebrafish was chosen as a surrogate model for yellow perch; this NIH endorsed model organism is easy to rear in a laboratory setting, it reaches sexual maturity in as little as three months and it has a sequenced genome (Hill et al., 2005; Spitsbergen and Kent, 2003). These assets of the zebrafish model facilitated the development of techniques

¹ **Recruitment:** The number of fish surviving to enter the fishery or to some life history stage (e.g. larval fish becoming juveniles, or juveniles becoming adults)

and a knowledge base of MeHg-induced behavioral and gene expression alteration, which could be then be used to carry out assays in yellow perch.

Understanding how MeHg affects gene expression and in turn how this differential gene expression affects behavior is a fundamental question that the present study poses to address. The knowledge produced by this study has immediate applicability, as it is crucial for the creation of mathematical models of wild perch population dynamics for environmental risk assessment of mercury emissions (Alvarez et al., 2006a). Additionally, the methodological framework of this study can be modified and expanded to assess the effects of various other contaminants in other species of interest.

Overview of the dissertation

The present document is organized into six chapters; all together they progressively explain key findings of this study, building up towards a final summary chapter. The content of each chapter is summarized below.

Chapter 1: Introduction to fundamental concepts; this chapter explains the rationale and relevance of the study and it concludes with the present overview of the dissertation.

Chapter 2: Preliminary experiments on the effects of sublethal MeHg exposure in the locomotor activity of zebrafish embryos and eleutheroembryos and discussion of putative anatomical mechanisms of MeHg-induced behavior alteration. This chapter also showcases an adaptation of a technique for early behavioral screening of zebrafish embryos [the Nicotine-evoked Locomotor

Response (NLR)] (Petzold et al., 2009; Thomas et al., 2009) and it introduces many of the methodological approaches for the quantification of behavior in fish embryos, which are revisited in further chapters.

Chapter 3: Analysis of MeHg-induced behavioral alteration in zebrafish eleutheroembryos, utilizing notions that were acquired from the experiments described in chapter 2. This chapter expands the repertoire of behavioral endpoints to include more complex paradigms such as the visual-motor response and prey capture. The study described in this chapter takes full advantage of the short generation times² in zebrafish and carries out an environmentally realistic whole-life-cycle dietary MeHg exposure.

Chapter 4: Elucidation of the effects of MeHg in yellow perch embryos, employing the methodological framework established in chapters 2 and 3.

Chapter 5: Analysis of the effects of MeHg in the gene expression of the siblings of the zebrafish and yellow perch utilized for behavioral analysis in the studies described in chapters 3 and 4. This chapter describes the high-throughput analysis of MeHg-induced gene expression alteration in zebrafish embryos, and then continues by describing the quantification of the expression of genes in yellow perch that were found to be dysregulated in the zebrafish model. Conclusive remarks are made about common gene pathways affected by MeHg exposure in both species of fish.

² **Generation time:** The average time between two consecutive generations in the lineages of a population. In zebrafish, generation times can be as short as 3 months.

Chapter 6: Summary of the dissertation. Here, the data described in each individual study is compiled into final conclusive remarks.

Figures

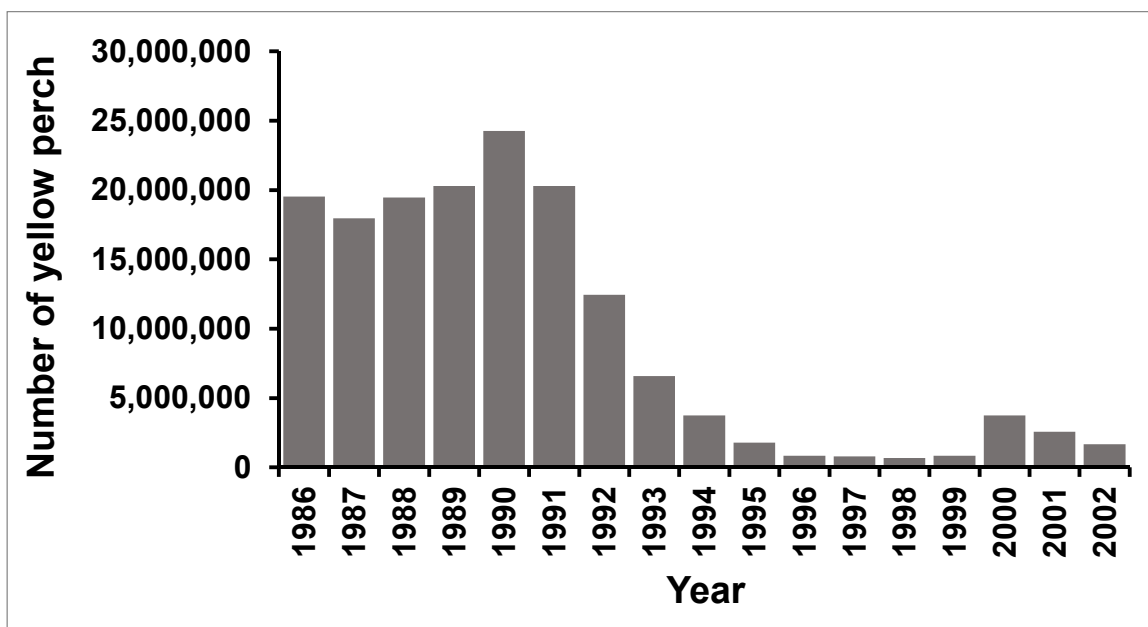


Figure 1.1: Decline of the yellow perch populations (Wilberg et al., 2005)

Figure 1.1: Decline of the yellow perch populations (Wilberg et al., 2005)

The populations of yellow perch have declined since the early 1990's. Wilberg and collaborators (2005) have estimated a decline of 92% of the catch of yellow perch in the state of Wisconsin.

CHAPTER 2: THE NICOTINE-EVOKED LOCOMOTOR RESPONSE: A PARADIGM FOR BEHAVIORAL NEUROTOXICITY SCREENING IN ZEBRAFISH (*Danio rerio*) EMBRYOS AND ELEUTHEROEMBRYOS

Abstract

The objective of this study was to develop a cost-effective and time-efficient approach for the assessment of the effects of sublethal doses of environmental neurotoxicants on the locomotor output of zebrafish embryos and eleutheroembryos. As a proof-of-concept, this study focused on the analysis of the behavioral effects of methylmercury (MeHg), due to the well-known neurotoxic effects of this environmental contaminant. Zebrafish embryos do not exhibit spontaneous swimming activity until roughly 5 days of age, however here we have tested and validated an assay to induce and quantify locomotor activity in 36 and 48 hours post-fertilization (hpf) zebrafish embryos by means of acute exposure to nicotine (30, 60, 120 and 240 μ M). To quantify behavioral endpoints, we utilized a webcam-based video acquisition system, paired with a free and open-source machine vision algorithm. The potential value of this Nicotine-evoked Locomotor Response (NLR) assay for the early detection of behavioral phenotypes was tested in 36, 48 and 72 hpf mutant zebrafish embryos of the non-touch-responsive “macho” (*mao*) strain. The NLR assay was successful at discriminating mutant embryos from their non-mutant siblings. Furthermore we concluded that the optimal experimental conditions for the NLR assay are to trigger the response in 48 hpf embryos utilizing 120 μ M of nicotine. To identify critical MeHg exposure concentrations that would induce subtle changes in spontaneous swimming behavior, we analyzed the locomotion of free-swimming 6 day post-fertilization (dpf) eleutheroembryos exposed to waterborne

methylmercury (MeHg; 0, 0.01, 0.03 and 0.1 μ M). Embryos exposed to 0.01 and 0.03 μ M of MeHg exhibited a significant increase in locomotor activity. Next, the NLR assay was tested in 48 hpf embryos that had been pre-exposed to the aforementioned concentrations of MeHg. As observed in 6 dpf eleutheroembryos, an exposure to 0.01 and 0.03 μ M of MeHg increased the locomotor output of 48 hpf embryos during the Nicotine-evoked Locomotor Response (NLR). In addition to the observed MeHg-induced hyperactivity in zebrafish embryos and eleutheroembryos, our results showcase the potential of the NLR assay as a valuable approach for neurotoxicity screening in early stages of the zebrafish development.

Introduction

Spontaneous swimming is arguably the most fundamental behavioral paradigm among the behavioral repertoire of zebrafish eleutheroembryos (Budick and O'Malley, 2000). It represents the interface by which organisms interact with their environment, as they are required to modulate locomotor output for most every complex survival task such as capturing prey and avoiding predators. Moreover, environmental contaminants play a role in the feedback loop between an organisms and its environment, as they can affect the way organisms behave and react to their surroundings (Kane et al., 2005). One such environmental contaminant is MeHg, which has been documented to cause locomotor abnormalities and abnormal startle response in zebrafish at concentrations significantly below lethal toxicity (Smith et al., 2010).

Although the most environmentally-realistic route of exposure to MeHg is through the diet (Depew et al., 2012), here we have made use of the many advantages of waterborne exposures. This approach is substantially quicker than a dietary exposure assay, it is much more cost-effective, it produces considerably less toxic waste and when performed early enough during the development of the embryos (≤ 2 hpf) it can effectively mimic the maternal transfer of MeHg (Weber et al., 2008), which would occur from the maternal ovary to the yolk of the embryos (Scheuhammer et al., 2007a). These qualities make, waterborne exposure an ideal approach to conduct preliminary screening assays, especially when critical behavior-altering doses of MeHg are not known for the aquatic organism of interest.

Historically, the use of behavioral screening in invertebrates and later in zebrafish was utilized to detect variable genetic phenotypes that affected normal behavior (Grunwald and Eisen, 2002). However, toxicologists have adopted these methods for toxicity screening due to the broadness and robustness of the results that can be obtained. For instance, quantification of the spontaneous swimming behavior of fish can be such a sensitive indicator of sublethal toxicity that alterations in swimming behavior caused by a neurotoxicant can be identified at concentrations as low as 0.7% of its LC50³ (Little and Finger, 1990).

The present study is not an exception to the aforementioned historical tendency to adapt screening assays from genetics to toxicology; the Nicotine-Evoked Locomotor Response (NLR) was first published as a behavioral screening method to study nicotine response genetics in zebrafish mutants (Petzold et al., 2009; Thomas et al., 2009), however here we have taken advantage of the locomotion-inducing effects of nicotine to test the potential value of the NLR assay as a screening tool for MeHg toxicology in 36 to 72 hpf zebrafish embryos – long before embryos develop a mature locomotor pattern (Figure 2.1). Apart from the obvious benefit of saving time, an advantage of carrying out behavioral experiments in zebrafish embryos as early as 36-48 hpf is that since the central nervous system (CNS) is not yet fully formed, the observed effects in locomotion more likely to be attributable to “more primitive” anatomical

³ **LC50:** LC stands for “lethal concentration”. LC50 is a standard measure of the toxicity equivalent to the exposure concentration of a toxicant required to kill half of the sample population of a specific test animal.

structures such as the spinal cord, the muscles, and the developing hindbrain (Saint-Amant and Drapeau, 2000).

To quantify the NLR we utilized a cost-effective approach comprised of a webcam-based video acquisition system paired with a free and open-source machine vision algorithm. Webcams are an affordable yet robust alternative to CCD cameras, capable of delivering excellent video quality and a sufficient frame rate to study spontaneous swimming in fish. Our machine vision algorithm of choice was the python-based “ctrax” (Branson et al., 2009); this software is available to be downloaded and used free-of-charge. Ctrax was originally designed as a tool for high-throughput analysis of locomotor activity of multiple fruit flies in the same arena; however the software performs remarkably well while tracking the NLR of multiple zebrafish embryos, as well as the free swimming of zebrafish eleutheroembryos.

Together, spontaneous swimming assay and the NLR, coupled with low-cost equipment and free and open-source software comprise a promising approach to carry out a simple diagnostic toxicity screening, which can later be supplemented with additional assays addressing more complex behaviors, if desired.

Materials and methods

Fish husbandry

Wild type zebrafish breeding stocks were obtained from EkkWill Waterlife Resources (EK strain; Ruskin, Florida, USA) and maintained in the laboratory for more than 15 generations. The “macho” (*mao*) mutant zebrafish strain was acquired from Dr. Angeles Ribera from the Anschutz Medical Campus of the University of Colorado, Denver. Both strains were maintained at 28°C on a 14h:10h light:dark cycle at the Children’s Environmental Health Sciences Core Center, located in the School of Freshwater Sciences of the University of Wisconsin – Milwaukee. All of the animal protocols were approved by the Institutional Animal Care and Use Committee (IACUC) of the University of Wisconsin – Milwaukee.

EK embryos were obtained by breeding adult zebrafish in a ratio of two females to one male (10 females and 5 males in each breeding tank). Macho strain zebrafish were bred in a ratio of one female to one male (1 female and 1 male in each breeding tank). The breeding tanks were constructed by removing the bottom of a 2L polycarbonate container (Cambro manufacturing company, Huntington Beach, CA) and replacing it with a plastic mesh, this container was in turn nested on top of a second 3L container. The mesh in the breeding tank allowed the spawned eggs to sink into the bottom container but restricted the adult fish from entering the bottom to eat the eggs. Adult fish would remain in their breeding tank over night at 28°C; the next morning, prior to the onset of

artificial dawn (8:00am), the breeding population was transferred into a 2L “spawning tank” containing fresh water to receive the newly spawned embryos. The adult fish would begin spawning at the onset of artificial dawn (9:00am), when the laboratory lights were automatically turned on. All embryos in this study were raised for up to 6 days post-fertilization in Petri dishes (100mmx15mm) containing E2 embryo medium (15mM NaCl, 0.5mM KCl, 1mM MgSO₄, 150μM KH₂PO₄, 50μM Na₂HPO₄, 1mM CaCl₂, 0.7mM NaHCO₃; pH 7.2) at a density of 200 embryos per dish; the embryo medium was exchanged daily.

Nicotine-evoked Locomotor Response (NLR) dose curve

Four doses of nicotine (30, 60, 120 and 240μM; Sigma, St. Louis, MO) were used to assess the NLR in zebrafish embryos in two different stages of early development (36 and 48 hpf). At each developmental stage, the embryos were manually dechorionated and then transferred into a recording vessel (89mm x 89mm x 25mm white semitransparent rubberized polystyrene weighing boat; Cole-Parmer, Vernon Hills IL, USA) containing 10ml of a nicotine solution. The embryos (n=12 embryos per vessel) were transferred with a fine-tip Pasteur pipette, ensuring that the clean medium necessary to carry the embryos over was kept consistent and to a minimum (~1ml) to avoid altering the concentration ratios of the nicotine solutions. The embryos were video recorded as soon as the tip of the glass pipette touched the nicotine medium.

Recording apparatus

The video recording apparatus consisted of a manifold holding four Logitech C920 (Logitech, Lausanne, Switzerland) web cameras pointing downwards into a Plexiglas tray that holds four weigh boats. Underneath the apparatus, a flat 22" Acer P221W computer monitor was used as a light source, which provided 58 lux of constant illumination; a sheet of velum paper was used as a diffusing filter. In order to block extraneous light and visual stimuli, the whole apparatus was surrounded by a custom made black polyethylene enclosure (Figure 2.2). All video recordings were streamed to a remote computer (Lenovo T410; Intel Core i5 CPU @ 2.53GHz, 4.00 GB RAM) at a resolution of 960x720 pixels and at a frame rate of 30 frames per second using the MATLAB (The MathWorks, Inc., Natick, MA) image acquisition toolbox.

The NLR of the embryos was tracked using the free and open-source machine vision algorithm "python-ctrax" (Branson et al., 2009) and tracking errors were manually corrected using the "fixerrors" MATLAB toolbox provided by the ctrax developers. The raw trajectory data was imported to a custom Microsoft Excel macro (Microsoft, Redmond, WA, USA) to calculate the maximum speed (mm s^{-1}) and the "latency of response" (time required to reach maximum speed; s) of each individual embryo. Twelve embryos were analyzed for each condition tested.

Modulation of the NLR by chronic low-dose exposure to nicotine in 48 hpf embryos

It has been observed that the tail beat frequency of zebrafish embryos during the NLR can be modulated if the embryos are reared in a low dose of nicotine (~1 μ M) for 24 hours prior to the NLR assay (Dr. Matthew Wolter, University of Wisconsin – Milwaukee; personal communication). Here we investigated if this observation translated into differences in maximum speed and latency of response.

Zebrafish embryos were grown in clean embryo medium for 24 hours and then transferred into media containing 0, 0.5 or 1 μ M of nicotine for an additional 24 hours. At 48 hpf, the embryos were submitted to the NLR assay using 120 μ M of nicotine to trigger the response. Twelve embryos were analyzed for each of the 24 hour low-dose nicotine pre-treatment regimes.

Analysis of the NLR in macho zebrafish mutants

Macho zebrafish mutants do not exhibit a touch response due to impaired sodium channel action potentials (Ribera and Nüsslein-Volhard, 1998). The known locomotor impairment in this mutant strain was utilized as a premise to investigate the potential of the NLR assay to discriminate between the maximum speed of embryos with and without locomotor abnormalities.

Embryos of the macho strain were raised to three different developmental stages (36, 48 and 72 hpf) in clean embryo medium and then manually dechorionated. Before carrying out the NLR assay, a quick phenotypic screening

on the embryos was done by performing a touch response test under a stereoscopic microscope (Olympus SZ61; Olympus Life Science Solutions, PA). After separating mutant embryos from their siblings without a phenotype, the two groups of embryos were tested with the NLR assay using a 120 μ M nicotine solution to trigger the response. Three replicates of this experiment were performed for each of the aforementioned conditions (12 embryos per replicate).

Methylmercury exposure regimes

To assess the effects of mercury exposure on both free-swimming and nicotine-induced locomotion, embryos were treated with methylmercury chloride (MeHg; Sigma-Aldrich Co., St. Louis MO, USA) from \leq 2-24 hpf using ethanol (0.01%) as vehicle at nominal concentrations of 0, 0.01, 0.03 and 0.1 μ M in E2. After MeHg treatment, embryos were rinsed three times in clean E2 and raised in E2 until needed for assessment.

Free swimming of methylmercury exposed 6 dpf zebrafish

eleutheroembryos

Newly spawned embryos were exposed to MeHg as described above, then raised to 6 dpf to assess the rate of travel (distance traveled in 5 minutes; mm 5min⁻¹) and activity (% of time active) of the free-swimming eleutheroembryos. A total of 120 fish per dose (10 fish per recording vessel; 12 vessels per dose) were video recorded and analyzed.

NLR of methylmercury exposed 48 hpf zebrafish embryos

The NLR assay was performed in MeHg-exposed 48 hpf embryos. 10 embryos per analyzed per recording vessel; 120 μ M of nicotine was used to trigger the NLR. The maximum speed, latency of response and distance traveled (in 2 minutes) was calculated for 50 embryos for each dose tested.

Statistical analyses

Statistical analyses were conducted with SigmaPlot software version 11.0 (Systat Software, San Jose, CA). All data was tested for normality using the Shapiro–Wilks test. If the data was found to be normally distributed, a one-way ANOVA was performed, subsequently a *post hoc* multiple pair-wise comparison between exposure groups was carried out with the Holm-Sidak method. Non-normal data was analyzed with ANOVA on ranks using the Klustal-Wallis method and multiple pair-wise comparisons between exposure groups were performed with Tukey's method.

Results

Nicotine-evoked locomotor response (NLR) dose curve

An NLR dose response curve was performed in two different stages of development of zebrafish embryos (36 and 48 hpf) to investigate the effect of varying doses of nicotine on the locomotor output of the embryos. Every one of the 96 embryos tested with this assay exhibited locomotor output in response to nicotine exposure, which highlights the efficacy of the NLR assay. Furthermore, embryonic developmental stage had an effect on the NLR. 36 hpf embryos achieved overall lower maximum speeds than 48 hpf embryos in all nicotine concentrations tested ($P < 0.001$). The NLR was affected by nicotine dose; 240 μ M of nicotine triggered a significantly higher maximum velocity in both 36 hpf ($H = 13.4$, $P = 0.004$) and 48 hpf embryos ($H = 38.1$, $P < 0.001$), relative to embryos exposed to 30, 60 and 120 μ M of nicotine, both at 36 and 48 hpf. High nicotine doses also reduced the latency of the embryos to reach their maximum velocity; 36 hpf embryos exposed to 240 μ M of nicotine reached their maximum velocities quicker than embryos exposed to 30, 60 and 120 μ M ($H = 29.9$, $P < 0.001$). Likewise, 120 and 240 μ M of nicotine decreased the latency to reach maximum velocity in 48 hpf embryos, compared to embryos exposed to 30 and 60 μ M ($H = 38.1$, $P < 0.001$) (Figure 2.3, Table 2.1; one-way ANOVA on ranks, Klustal-Wallis test). From a practical standpoint, 36 hpf embryos were more difficult to track with the ctrax algorithm due to their lack of pigmentation and significantly slower NLR; both of these factors can complicate the differentiation between moving embryos and the background. Furthermore, higher doses of nicotine

facilitated the analysis of the NLR, given that this reduces the time that the embryos remain immotile and aggregated during the first few seconds of the response, hence reducing mismatches and ambiguities in tracking. In 48 hpf embryos, a dose of 120 μ M of nicotine delivered a satisfactory NLR that was not significantly different to the NLR evoked by 240 μ M, for this reason we concluded that the optimal experimental conditions for the NLR assay as a screening tool would be to trigger the response with 120 μ M of nicotine utilizing 48 hpf embryos.

NLR in chronic low-dose nicotine-exposed embryos and “macho” mutants

Zebrafish embryos exposed to chronic low-doses of nicotine were utilized here to illustrate fundamentals nicotine pharmacology. Rearing zebrafish embryos in 1 μ M of nicotine for 12 hours prior to the NLR test resulted in significantly lower maximum velocities ($H=17.41$, $P<0.001$), coupled with a higher latency to reach maximum speed ($H=23.56$, $P<0.001$), relative to embryos reared in 0 and 0.5 μ M of nicotine. Embryos reared in 0.5 μ M of nicotine did not exhibit significant changes in maximum speed or distance traveled throughout 90 seconds of observation; however, they reached maximum velocities significantly quicker than the embryos from the 0 and 1 μ M nicotine exposure groups ($H=23.56$, $P<0.001$) (Table 2.2). Furthermore, the known locomotor abnormality of macho mutants was utilized here to test the capacity of the NLR assay to discriminate between organisms with and without locomotor impairments. The NLR was successful at discriminating mutant embryos from their non-mutant siblings. All zebrafish mutants of the macho strain tested with the NLR paradigm had significantly lower maximum speeds ($P<0.001$) (Figure 2.4). This proof-of-

concept experiment demonstrates the potential of the NLR assay to detect gross locomotor abnormalities in zebrafish embryos and it establishes a methodological framework to test for more subtle behavioral effects, such as the ones expected from environmental neurotoxicant exposure.

Free swimming and NLR of MeHg exposed eleutheroembryos and embryos

Prior to carrying out any NLR experiments in MeHg-exposed zebrafish embryos, an MeHg dose response assay was carried out by exposing embryos to 0, 0.01, 0.03, 0.1 μ M MeHg in order to identify critical doses of exposure that would cause significant behavioral alteration in free swimming 6 dpf zebrafish (Figure 2.5, Table 2.3). Eleutheroembryos exposed to 0.01 and 0.03 μ M of methylmercury exhibited a significantly increased rate of travel during the five minutes of activity tracking ($H=26.49$, $P<0.001$). Additionally, eleutheroembryos exposed to 0.01 μ M of methylmercury were more active than the rest of the exposure groups ($H=26.71$, $P<0.001$). Once these dose-dependent MeHg behavioral effects were established in free swimming 6 dpf embryos, the same doses of MeHg were utilized to assess the effect of MeHg in the NLR of 48 hpf embryos. The results obtained from this assay were similar to the observed in 6 dpf eleutheroembryos; 48 hpf zebrafish embryos exposed to 0.01 and 0.03 μ M of methylmercury had an increased rate of travel ($F=12.82$, $P<0.001$) and maximum speeds ($F=11.95$, $P<0.001$) compared to the 0 and 0.1 μ M exposure groups.

Discussion

As observed in the present study, exposure to MeHg has previously been reported to cause locomotor abnormalities in mummichogs, depending on the developmental stage at which the exposure occurred (Weis and Weis, 1995b). Mummichog larvae exposed to MeHg as embryos were found to swim more than controls (hyperactivity), while those that were only exposed as larvae swam less than the controls (hypoactivity) (Weis and Weis, 1995b). Hyperactivity after embryonic MeHg insult has also been observed in rainbow trout (*Oncorhynchus mykiss*), largemouth bass (*Micropterus salmoides*) (Sandheinrich and Miller, 2006) and in rodents (Giménez-Llort et al., 2001). More recently, a link has been suggested between prenatal MeHg exposure and the onset of attention deficit hyperactivity disorder (ADHD) in humans (Boucher et al., 2012).

Some characteristics of the onset of the NLR bear a noteworthy resemblance to the well-known touch-evoked response in zebrafish embryos, such as the swimming speed and tail beat frequency of these responses (Dr. Matthew Wolter, University of Wisconsin – Milwaukee, personal communication). Furthermore, both responses can be elicited early enough in development (roughly 36 hpf) that presumably both responses utilize the same rudimentary anatomical structures of the developing embryo to elicit locomotor output.

The hyperlocomotor response observed in both free-swimming 6 dpf zebrafish eleutheroembryos and 48 hpf embryos suggests that there is a common mechanism of MeHg-induced hyperactivity in both developmental

stages; furthermore, the effects observed at 6 dpf are likely the sequel of neurotoxic effects that occur at least as early in development as 48 hpf.

The mechanisms by which MeHg causes the observed hyperactivity are unclear; in fact, even the more fundamental question of how exactly MeHg acts as a neurotoxicant remains unanswered (Ho et al., 2013). However, our NLR assays in 48 hpf MeHg-exposed zebrafish embryos suggest that MeHg-induced hyperactivity is not associated with input from higher centers of the brain, but more likely to alterations in the spinal cord and the developing hindbrain.

The aforementioned notion is supported by seminal experiments conducted by Saint-Amant and Drapeau (1998), where different lesions would be inflicted along the body axis of 19-34 hpf zebrafish embryos to determine which anatomical structures were essential to produce locomotor output. Lesions that were rostral to the hindbrain had no effect on spontaneous contractions, touch-evoked response or swimming, demonstrating that the entire behavioral repertoire of embryonic zebrafish can solely be effectuated by the spinal cord and the hindbrain in the absence of the midbrain and forebrain.

To the author's knowledge, no previous studies have addressed the putative link between MeHg-mediated effects in the spinal cord and locomotor abnormalities. However, a link between oxidative stress in the cerebellum and hyperactivity has been observed in rodents (Stringari et al., 2006).

Regardless of the cellular and anatomical mechanisms of MeHg-induced behavioral alteration, the spontaneous-swimming and the NLR assay show promise as useful tools in behavioral toxicology screening.

Figures

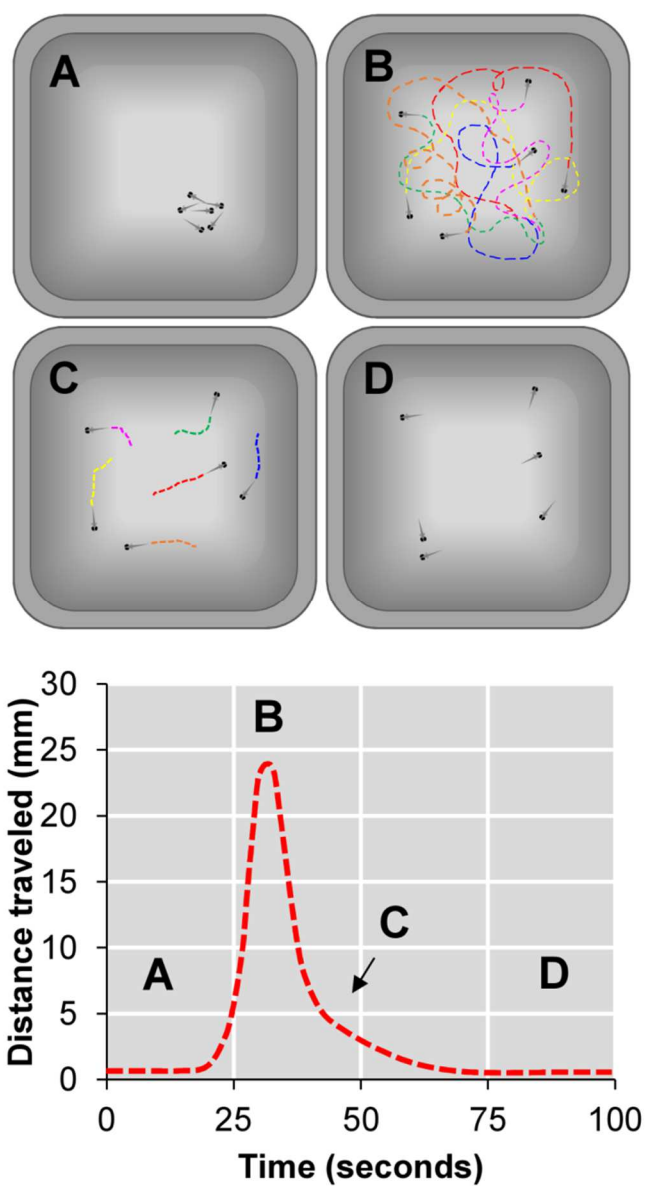


Figure 2.1: Characteristic kinematics of the nicotine-evoked locomotor response in zebrafish embryos

Figure 2.1: Characteristic kinematics of the nicotine-evoked locomotor response in zebrafish embryos

The NLR is a characteristic locomotor response triggered by an exposure to an acute concentration of nicotine (e.g., 30 to 240 μ M). This behavioral response is characterized by four phases: A) zebrafish embryos younger than 5 days post-fertilization do not exhibit free swimming, thus when exposed to an acute nicotine concentration the embryos first remain immotile for approximately 30 seconds; B) once the nicotine is absorbed, the embryos abruptly initiate a vigorous and continuous locomotor burst that lasts several seconds, many times advancing in a clock-wise spiraling trajectory; C) the locomotor response attenuates and many fish begin to erratically twitch without any forward propulsion; D) all embryos come to a complete halt.

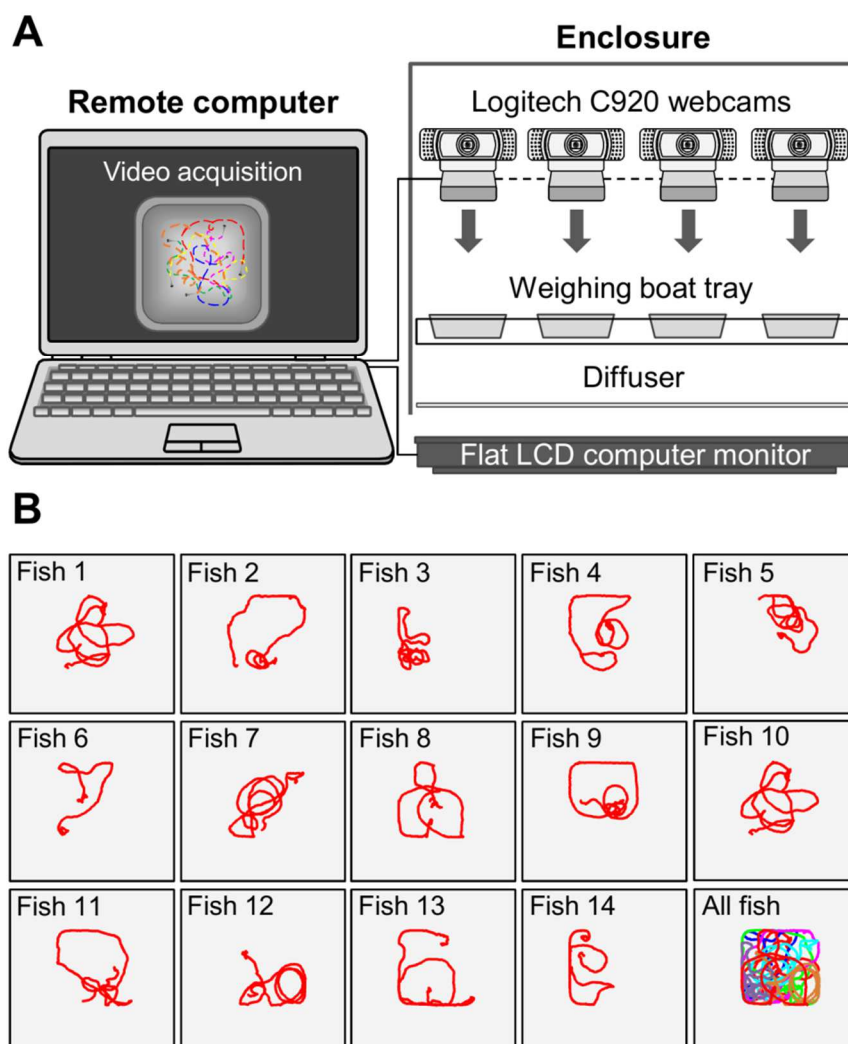


Figure 2.2: Custom-made behavior observation chamber

Figure 2.2: Custom-made behavior observation chamber

(A) The behavior observation chamber consists of a manifold of Logitech c920 webcams that point downwards onto a tray with weigh boats that serve as arenas for the swimming larvae. The webcams are connected to a remote computer and the video footage is streamed using the MATLAB image acquisition toolbox. (B) The ctrax tracking algorithm can quantify the locomotor activity of multiple fish embryos in the same arena simultaneously.

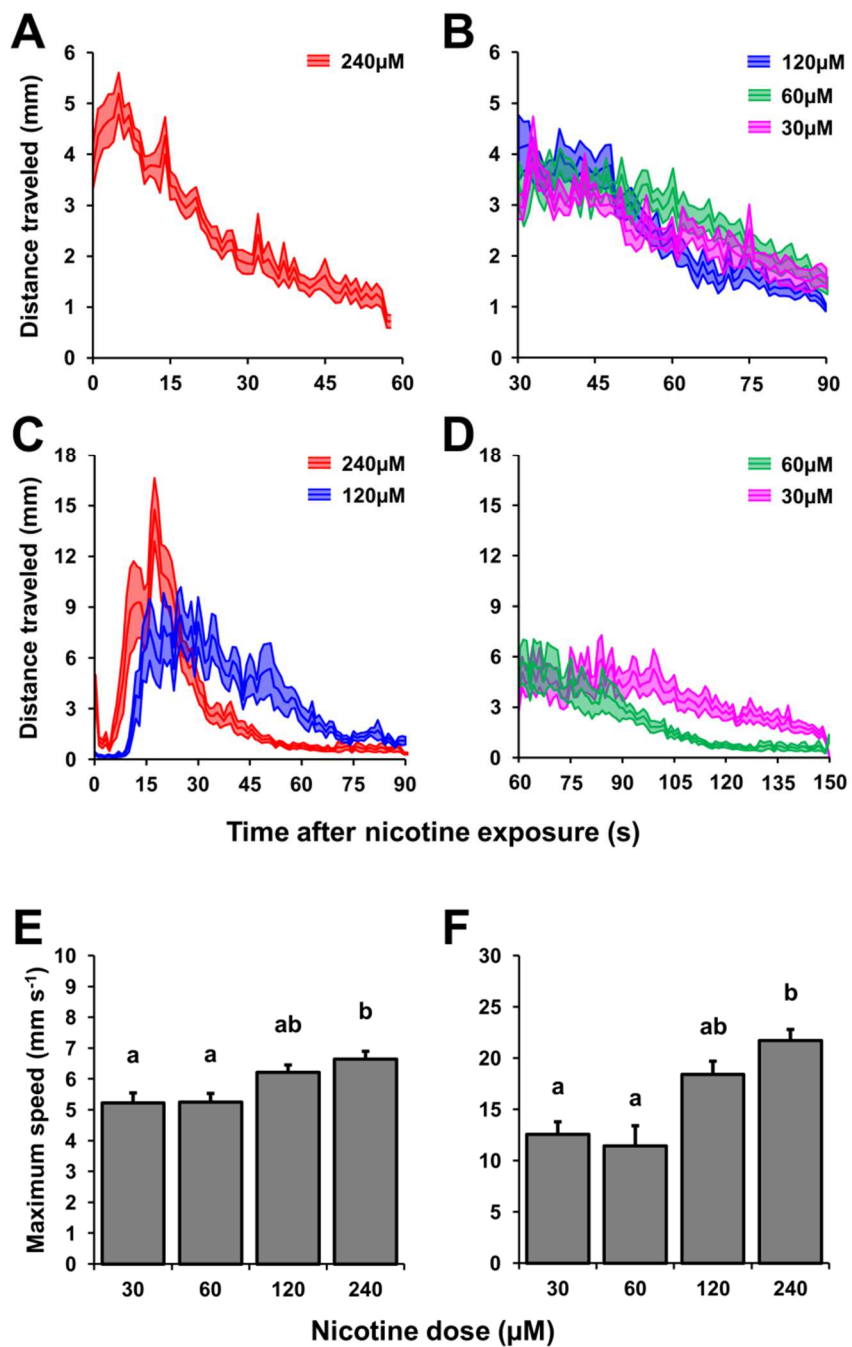


Figure 2.3: Nicotine-evoked locomotion dose response curves in 36 and 48 hpf zebrafish embryos

Figure 2.3: Nicotine-evoked locomotion dose response curves in 36 and 48 hpf zebrafish embryos

Nicotine dose response curves in 36 hpf (A and B) and 48 hpf (C and D) zebrafish embryos during the NLR. (C) The NLR of 36 hpf embryos triggered by 240 μ M of nicotine was characterized by a significantly higher maximum speed than the observed in the rest of the doses tested. (D) Similarly, 240 μ M of nicotine triggered a significantly higher maximum velocity in 48 hpf embryos (one-way ANOVA).

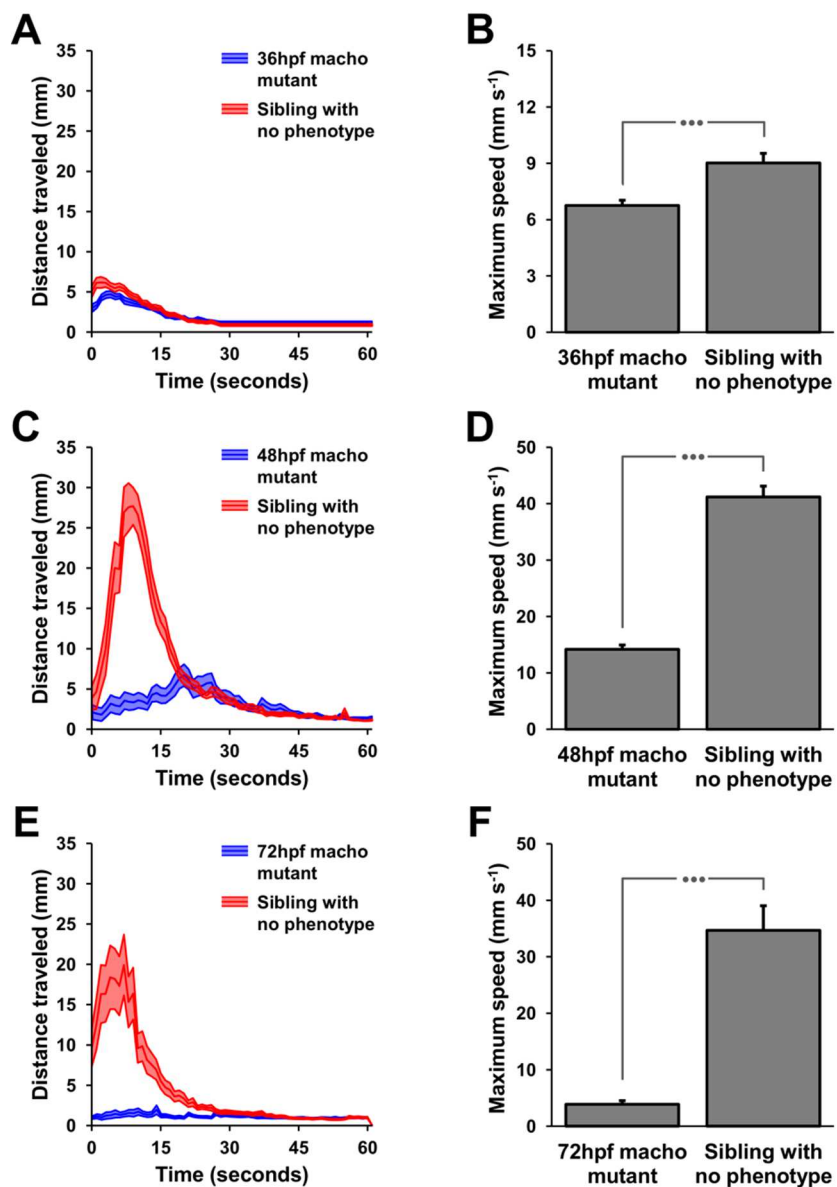


Figure 2.4: Validation of the nicotine-evoked locomotor response assay by testing it in the non-touch-responsive “macho” mutant zebrafish strain

Figure 2.4: validation of the nicotine-evoked locomotor response assay by testing it in the non-touch-responsive “macho” mutant zebrafish strain

The NLR assay was successful at discriminating mutant embryos from their non-mutant siblings. (A) The locomotor activity of 36 hpf embryos triggered by 120 μ M of nicotine was significantly different between mutants and non-mutant embryos as demonstrated by the comparison of the average maximum speed of mutant and non-mutant embryos (B). The difference between mutants and non-mutants became progressively more apparent in 48 hpf (C and D) and 72 hpf (E and F) embryos.

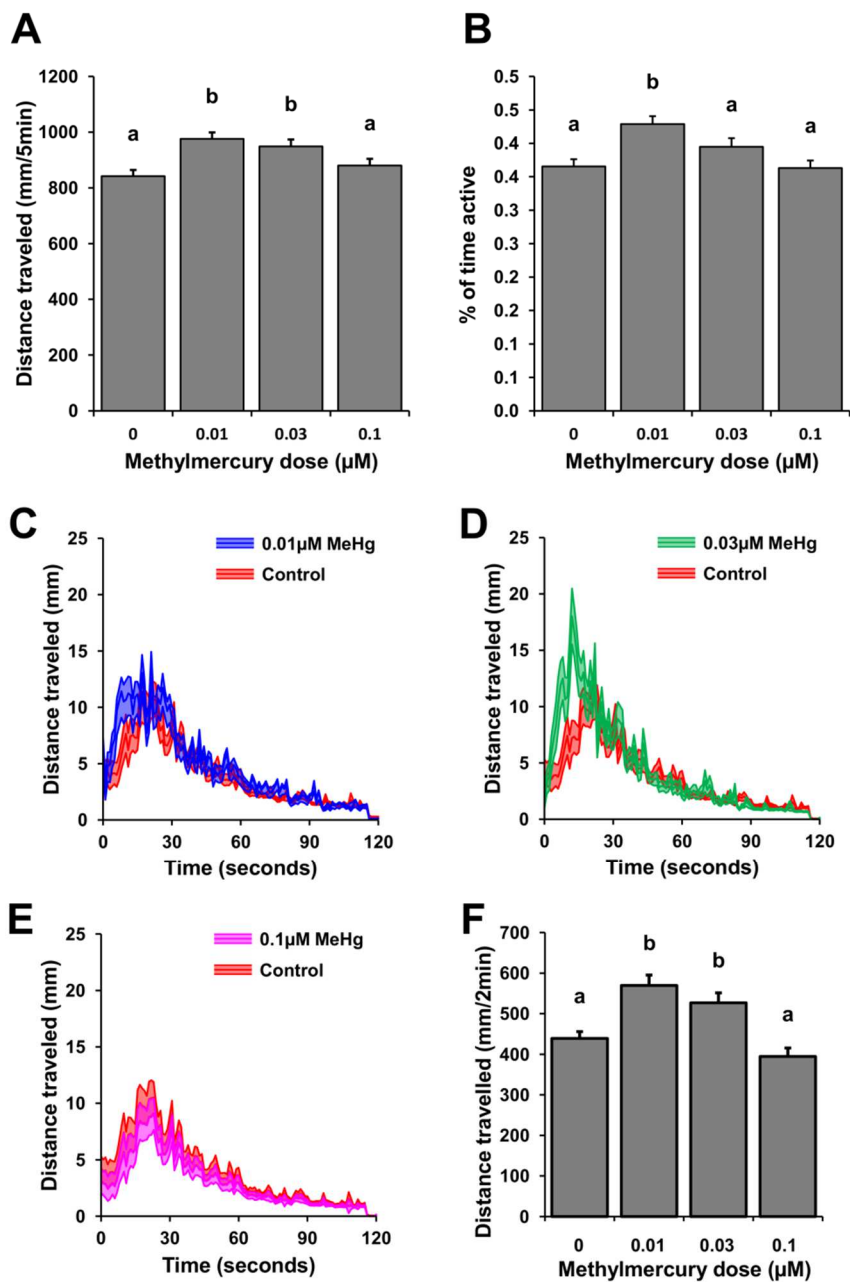


Figure 2.5: Spontaneous swimming of 6 dpf MeHg-exposed zebrafish eleutheroembryos and the NLR of MeHg-exposed 48 hpf embryos

Figure 2.5: spontaneous swimming of 6 dpf MeHg-exposed zebrafish eleutheroembryos and the NLR of MeHg-exposed 48 hpf embryos

(A) The spontaneous-swimming assay elucidated subtle yet significant ($P < 0.001$) increases in the total distance travelled (mm in 5 minutes) of free swimming 6 dpf zebrafish exposed to 0.01 and 0.03 μM of MeHg (B) Eleutheroembryos exposed to 0.01 μM MeHg as embryos also had an increased activity (% of time active) relative to all other doses. The NLR assay was conducted in 48 hpf embryos exposed to 0 μM (control), 0.01 μM , 0.03 μM and 0.1 μM ; the activity curves of all MeHg-exposed embryos were compared to the control (C through E). (F) As observed in 6 dpf eleutheroembryos, 48 hpf zebrafish embryos exposed to 0.01 and 0.03 μM of MeHg exhibited an increase in distance traveled during the analysis period.

Tables

Table 2.1: NLR dose response in 36 and 48 hpf zebrafish embryos

Nicotine dose (μM)	36 hpf zebrafish embryos		48 hpf zebrafish embryos	
	Maximum speed (mm s^{-1})	Latency of response(s)	Maximum speed (mm s^{-1})	Latency of response (s)
30	5.29 \pm 0.37 ^a	43.08 \pm 13.62 ^a	12.55 \pm 1.24 ^a	83.50 \pm 4.76 ^a
60	5.25 \pm 0.28 ^a	48.92 \pm 11.72 ^a	11.42 \pm 1.99 ^a	69.58 \pm 2.54 ^a
120	6.21 \pm 0.24 ^{ab}	38.17 \pm 7.33 ^a	18.43 \pm 1.27 ^{ab}	29.50 \pm 4.13 ^b
240	6.64 \pm 0.26 ^b	6.92 \pm 4.50 ^b	21.72 \pm 1.08 ^b	17.92 \pm 1.95 ^b
ANOVA on ranks (Klustral-Wallis test)				
<i>H</i>	13.4	29.9	22.5	38.1
<i>P</i>	0.004	<0.001	<0.001	<0.001

Note: Values are given as the mean \pm SE

Table 2.2: Modulation of the NLR in 48 hpf zebrafish embryos by chronic, low-dose exposure to nicotine during development

Embryonic nicotine exposure dose (μM)	Maximum speed (mm s^{-1})	Latency of response (s)	Distance traveled ($\text{mm } 90\text{s}^{-1}$)
0.0	21.72 \pm 1.08 ^a	17.92 \pm 1.95 ^a	299.63 \pm 16.08 ^a
0.5	25.69 \pm 1.53 ^a	6.17 \pm 0.89 ^b	257.31 \pm 18.30 ^a
1.0	16.58 \pm 1.10 ^b	37.25 \pm 6.18 ^a	310.66 \pm 26.19 ^a
ANOVA on ranks (Klusal-Wallis test)			
<i>H</i>	17.41	23.56	3.36
<i>P</i>	<0.001	<0.001	0.187

Note: Values are given as the mean \pm SE

Table 2.3: Effect of methylmercury on the NLR of 48 hpf zebrafish embryos

Embryonic methylmercury exposure dose (μM)	Maximum speed (mm s^{-1})	Latency of response (s)	Distance traveled (mm 2min^{-1})
0.00	33.06 \pm 1.47 ^a	19.26 \pm 1.70	439.01 \pm 16.77 ^a
0.01	41.06 \pm 1.48 ^b	18.92 \pm 1.65	569.29 \pm 25.84 ^b
0.03	43.27 \pm 1.90 ^b	17.94 \pm 1.74	526.67 \pm 24.57 ^b
0.10	31.64 \pm 1.80 ^a	14.50 \pm 1.45	394.46 \pm 20.90 ^a
ANOVA			
<i>F</i>	11.92	1.76	12.82
<i>P</i>	<0.001	0.156	<0.001

Note: Values are given as the mean \pm SE

CHAPTER 3: PARENTAL WHOLE-LIFE-CYCLE EXPOSURE TO DIETARY METHYLMERCURY IN ZEBRAFISH (*Danio rerio*) AFFECTS THE VISUALMOTOR RESPONSE, LOCOMOTION AND FORAGING OF OFFSPRING

Abstract

MeHg has been widely recognized as a neurotoxin in all vertebrates at concentrations considerably below lethal toxicity. However, compared with humans, other mammals and even birds, relatively little is known about the effects of chronic, environmentally realistic MeHg exposures in fish. Here we have evaluated the behavioral effects of prenatal MeHg by exposing a parental generation of zebrafish with environmentally relevant MeHg diets (0, 1, 3 and 10ppm) throughout its whole life cycle and running the offspring through a battery of behavioral tests, including the visual-motor response assay, evaluation of spontaneous swimming and prey capture. All MeHg treatments resulted in increased locomotor activity and prey capture efficiency.

Introduction

Mercury is a neurotoxic heavy metal that is released into the atmosphere by anthropogenic and natural sources, coal combustion being the primary anthropogenic source of this contaminant (Monson, 2009b). Atmospheric deposition causes the elemental Hg to be incorporated into aquatic ecosystems around the world (Risch et al., 2012b), after which bacteria transform this mercury into methylmercury (MeHg) (Bloom, 1992), a pervasive and persistent organic form of mercury.

The neurotoxicity of MeHg became notorious in the early 1970's when reports originating from Iraq and Japan linked this contaminant with cases of acute poisoning. Individuals exposed to high levels of MeHg in contaminated bread and seafood suffered parathesia, ataxia and constriction of the visual field (Grandjean et al., 2010). Presently, despite the efforts to circumvent another large scale acute MeHg poisoning, chronic low-dose exposure to MeHg has recently been implicated in neurobehavioral effects such as impaired motor function (Montgomery et al., 2008), learning disabilities (Smith et al., 2010) and attention deficit hyperactivity disorder (ADHD; Boucher et al., 2012).

Since the early reports on the acute poisoning tragedies, MeHg has been widely recognized as a neurotoxin in all vertebrates at concentrations considerably below those that cause lethal toxicity (Louis, 1977). However, compared with humans, other mammals and even birds, relatively little is known

about the effects of chronic, environmentally realistic MeHg exposures in fish (Scheuhammer et al., 2007b).

MeHg uptake by fish occurs primarily through dietary exposure (Depew et al., 2012) which subsequently leads to bioaccumulation and biomagnification (Alvarez et al., 2006b). More than 90% of total Hg (THg) in fish muscle tissue is in the form of MeHg (Drevnick and Sandheinrich, 2003; Scheuhammer et al., 2007a) and maternal burdens of this pollutant can be transferred to the eggs during oogenesis (Hammerschmidt and Sandheinrich, 2005). Maternal transfer of MeHg is particularly threatening to the offspring, due to the high susceptibility developing embryos to environmental contaminants (Mohammed, 2013).

Fish are especially relevant models for behavioral toxicology of aquatic pollutants, due to their direct relationship with the aquatic ecosystem in which the exposure occurs, as well as a long history of use of fish models in behavioral toxicology (Kane et al., 2005).

In particular, zebrafish larvae are particularly well suited for large-scale behavioral toxicology due to their small size, fast development and the capacity to obtain 200-300 eggs from a single adult zebrafish breeding pair (Hill et al., 2005). In addition to the advantages of the zebrafish as a model for ecotoxicology, it is also an increasingly recognized aquatic animal model for human disease (Lieschke and Currie, 2007).

In order to interact with its environment and survive, zebrafish larvae exhibit an ample behavioral repertoire. Spontaneous swimming is the most

fundamental behavioral paradigm in zebrafish larvae, however, they also exhibit more complex behaviors like a variety of startle responses and prey tracking (Budick and O'Malley, 2000; Burgess and Granato, 2007) all of which can be potentially compromised by exposure to a neurotoxicant.

A number of methods have been proposed to assess neurotoxicity in zebrafish, and they include, among others, the analysis of the response to abrupt light changes referred to as the visuomotor response (VMR) (Emran et al., 2008; MacPhail et al., 2009), as well as the analysis of free swimming with computer vision algorithms (Kane et al., 2005). Prey capture, on the other hand, is a lesser studied behavioral endpoint and assays in zebrafish larvae have mainly focused on larvae preying on paramecia (Bianco et al., 2011a; Budick and O'Malley, 2000; Gahtan et al., 2005). To the author's knowledge, no efforts have been made to analyze the effects of neurotoxicants on the prey capture ontology of zebrafish larvae.

Here, we have mimicked a whole life cycle exposure to an environmentally relevant dose of MeHg [1ppm (low dose)] (Hammerschmidt et al., 2002), as well as two higher doses [3ppm (medium dose) and 10ppm (high dose)] in zebrafish to elucidate their effects on fundamental behavioral paradigms of the offspring, namely the VMR and the early ontology of spontaneous swimming and prey capture ability.

Materials and methods

Fish husbandry

All of the animal protocols described hereafter were approved by the Institutional Animal Care and Use Committee (IACUC) of the University of Wisconsin - Milwaukee. Wildtype zebrafish (*Danio rerio*) larvae used in this study were from the EK strain [originally obtained from EkkWill Waterlife Resources (Ruskin, Florida, USA) and maintained in laboratory for well over 15 generations] and were raised in the NIEHS Children's Environmental Health Core Center (Milwaukee WI, USA).

All zebrafish embryos were raised at 28°C on a 14h:10h light:dark cycle. For the first 7 days post-fertilization (dpf) the embryos were reared in 86mm diameter Petri dishes in E2 embryo medium (15mM NaCl, 0.5mM KCl, 1mM MgSO₄, 150µM KH₂PO₄, 50µM Na₂HPO₄, 1mM CaCl₂, 0.7mM NaHCO₃) at a density of 200 embryos per dish; the E2 embryo medium was exchanged daily. After 7 dpf the larvae were transferred to 2L static tanks, at a density of 60 larvae per tank. After 21 dpf, the fish were transferred to 2L flow-through systems.

Once the fish developed sexual maturity (3- 4 months post fertilization), they were sorted by sex. Fish were kept in 2L (males) and 3L (females) polycarbonate flow-through tanks (Cambro manufacturing Co., Huntington Beach CA, USA) at a density of no higher than 4 fish per liter.

MeHg food preparation

An initial 3mM stock solution (in ethanol) of MeHg chloride (Sigma-Aldrich Co., St. Louis MO, USA) was used to make all of the required dilutions to obtain the desired final mercury concentrations in the diets. Adult zebrafish flake diets were treated with MeHg in batches of 500g of food; after weighing the food, the calculated amount of MeHg stock solution was mixed into 950mL of ethanol, subsequently this solution was mixed into the food; adult vehicle control diets (which we will hereon refer to as “0ppm” diets) were prepared by mixing 950mL of ethanol into 500g of food. The preparations were stirred three times daily under a hood for 4 days until all the ethanol had evaporated completely.

Similarly, larval micropellet diets were prepared in batches of 50g; 250mL of ethanol were used to mix in the MeHg into the food; larval vehicle control diets were prepared by mixing 250mL of ethanol into 50g of food. As with the adult flakes, the larval food was stirred three times daily under a hood until the ethanol evaporated completely.

Dietary MeHg exposure regimes

In order to mimic whole-life-cycle exposure in the wild, a parental generation (G_1) of fish was exposed to dietary MeHg throughout its whole life span (*i.e.* G_1 was born with a maternally transferred MeHg burden and it was raised with a MeHg diet until adulthood), so as to investigate the effects of this life-long MeHg exposure on its offspring (G_2) (Figure 3.1).

G₁ embryos were collected from 8 month old females [average weight 0.577g, (0.139 SD)] previously fed for 9 weeks with a prepared diet (Biodiet starter, Bio-Oregon, 4% body weight per day) containing nominal MeHg concentrations of 0, 0.5, 5 and 50ppm (Table 3.1). At the moment of collection, the G₁ embryos MeHg had reached burdens MeHg burdens of 0.005, 0.02, 0.2 and 1ppm (wet weight), respectively.

The G₁ embryos were raised to 7 dpf and transferred to 2L tanks, at a density of 60 larvae per tank (one tank per exposure group, in triplicate). Upon this moment, the G₁ larvae were fed *ad libitum* with an MeHg micropellet diet (Brine Shrimp Direct, Golden Pearls, Ogden, UT, USA) with nominal concentrations of 0, 1, 3, and 10ppm (Table 3.2). The size of the food pellets was adjusted throughout the development of the fish from 50-100µm sized pellets (7-14 dpf), to a mixture of 50-100µm and 100-200µm sized pellets (15-30 dpf); to exclusively 100-200µm sized pellets (31-120 dpf).

From 4 months of age onwards, the fish were fed with a crushed flake diet (Pentair Aquatic Eco-Systems Aquatox food, Apopka FL, USA), also containing 0, 1, 3, and 10ppm of MeHg. Platinum grade "Argentemia" brine shrimp nauplii (ARGENT laboratories, Redmond WA, USA) were introduced to the diet once the juveniles reached 40 dpf.

Upon the development of sexual characteristics, the fish were sorted by sex. Female zebrafish were housed in 3L polycarbonate flowthrough tanks (Cambro manufacturing Co., Huntington Beach, CA) at a density of 12 fish per tank (one tank per exposure group, in triplicate). Male fish were housed in 2L

polycarbonate flowthrough tanks at a density of 6 males per tank (one tank per exposure group, in triplicate). The fish were bred at 8 months of age in a ratio of 12 females to 6 males.

A total of 3 clutches of embryos were obtained from each exposure group of G₁ parents. All zebrafish breeding tanks were allowed to spawn for 3 hours, from 9:00am to 12:00am. Since this study was concerned with the effects of whole life cycle parental MeHg burdens, the newly spawned offspring (G₂) were no longer raised on MeHg diets.

Assessment of embryo mortality and early life stage (ELS) toxicity

In order to evaluate embryo mortality due to MeHg exposure, all eggs were collected and counted for each of all three replicates and exposure groups; after 24 hpf, all dead and unviable eggs were counted and discarded.

Additionally, ELS toxicity scoring (Heiden et al., 2005) was carried out to assess observable teratogenic effects of MeHg. Zebrafish embryos from each exposure group were transferred to 12-well plates (10 embryos per well), and the larvae were observed at 24, 72 and 144 hpf using an Olympus SZX12 stereomicroscope. The embryos were monitored in triplicate for each of the exposure groups and time points. Each individual was given an ELS toxicity score ranging from 0 to 4 based on the severity of defects and the presence of specific endpoints of MeHg toxicity (0 = normal; 1 = slight, generally one morphologic anomaly; 2 = moderate, generally two morphologic anomalies, 3 = severe, generally more than two morphologic anomalies, and 4 = dead).

Analysis of Hg contents in diets and tissues

THg content in tissues and MeHg diets were directly analyzed using a Direct Mercury Analyzer 80 (DMA-80, Milestone Inc, Shelton CT) as described by Basu and collaborators (2009). Both G₁ and G₂ maternal transferred embryonic Hg burdens were analyzed from pools of two hundred 4 hpf embryos for each exposure group, in triplicate. The morning after the spawning, the ovaries were excised from three G₂ females per dose, in triplicate, to assess THg in the ovary. G₁ and G₂ MeHg diets were also analyzed for THg content, in triplicate.

VMR assay

The VMR assay has been suggested as a screening paradigm to be used as an integral part of a behavioral test battery (MacPhail et al., 2009). The experiment consists of quantifying the response of multiple zebrafish larvae reacting to sudden changes in light intensity. Immediately at the onset of an abrupt change in light intensity zebrafish larvae exhibit a startle response (Colwill and Creton, 2011) which is followed by above-basal locomotion ("bursting") if lights were turned off, or below-basal locomotion ("freezing") if the lights were turned on. In both cases, zebrafish larvae gradually return to basal locomotion in the course of several minutes.

Here we carried out a modified version of this assay, originally published by Emran and collaborators (2008). After 10 minutes of acclimation in the dark, the larvae underwent two cycles of alternating 10 minute light and dark periods (for a total of 50 min).

The locomotor activity of the fish was monitored with a DanioVision system (Noldus Information Technology, Leesburg, VA), which consists of an enclosed chamber designed to hold a multiple-well plate in which fish larvae are imaged. The multiple-well plate is illuminated from underneath with a light box capable of emitting infrared (800–950 nm with a peak at 860 nm) and visible (430–700 nm) light. The light intensity in all light periods of the VMR assay were measured as 221.75 lux (Fisher Scientific Traceable Dual-Range Light Meter, Pittsburgh PA, USA). All VMR experiments were carried out from 12:00pm to 6:00pm to limit the effects of circadian rhythms.

The total distance traveled of each fish was analyzed using Ethovision software version 8.0; individual 6 dpf fish were observed in 24-well plates and tracked at a frame rate of 25 frames per second. A total of 126 larvae per exposure group were analyzed.

Analysis of 7 dpf larval zebrafish swimming behavior

A custom-made behavior observation chamber was designed for the purpose of this experiment. The apparatus consisted of a manifold holding four Logitech C920 web cameras pointing downwards into a Plexiglas tray that holds four 100mL 89mm x 89mm x 25mm white semitransparent rubberized polystyrene weigh boats (Cole-Parmer, Vernon Hills IL, USA). Underneath the apparatus, a flat 22" Acer P221W computer monitor is used as a light source, which provides 58 lux of constant illumination; a sheet of velum paper is used as a diffusing filter. In order to block extraneous light and visual stimuli, the whole

apparatus is surrounded by a custom made black polyethylene enclosure. All video recordings were streamed to a remote computer at a resolution of 960x720 and a frame rate of 30 fps using the MATLAB image acquisition toolbox. The weigh boats were filled with 25mL of 28°C E2 embryo medium; ten 7 dpf zebrafish larvae were placed in each boat and allowed to acclimate in the recording chamber for 5 minutes. After acclimation, the groups of free swimming larvae were recorded for 5 minutes. The locomotor activity of the larvae was analyzed using a free and open-source machine vision algorithm [python-ctrax (Branson et al., 2009), (www.ctrax.sourceforge.net)]; tracking errors were corrected using the “fixerrors” MATLAB toolbox provided by the ctrax developers. All raw trajectory data was imported to a custom Microsoft Excel macro (Microsoft, Redmond, WA, USA) to calculate rate of travel ($\text{mm}5\text{min}^{-1}$), swimming speed (mm s^{-1}), activity (% of time active), minimum speed (mm s^{-1}) net-to-gross displacement ratio (NGDR)⁴, maximum speed (mm s^{-1}), and scoot frequency (Hz). A total of 180 fish tracks were analyzed for each of the four exposure groups.

Routine swimming and prey capture at 8, 12 and 16 dpf

The swimming performance of the larval zebrafish was further monitored at 8, 12 and 16 dpf; immediately after each assay, the foraging efficiency of the

⁴ Net-to-gross displacement ratio (NGDR) is a measure of the linearity of the trajectory of an organism. Ratios closer to 1 indicate straighter trajectories; lower ratios suggest that an organism could be swimming in circles or meandering.

larvae was also monitored. At 9:00am, on the day of the analysis, 25 larvae were transferred to 10cm diameter glass Petri dishes containing 50mL of 28°C E2 embryo medium. The dish was then transferred to the recording chamber and the fish were allowed to acclimate for 5 minutes, after which they were recorded for 10 minutes. All recordings were carried out from 12:00pm to 6:00pm. A 30 second fragment was randomly selected from the 10 minute clips to analyze the spontaneous swimming of the larvae. The behavioral parameters analyzed included activity (% of time active) and NGDR.

Immediately after the recording of routine swimming, foraging efficiency was measured by introducing 6 *Artemia* nauplii per fish (*i.e.* 25 fish per dish foraging on 150 nauplii) into the Petri dish. The larvae were allowed to feed for 10 minutes, after which the remaining nauplii were counted. At the end of each experiment, the fish were returned to 2L tanks to be housed until the next experimental time point; the same fish were observed at 8, 12 and 16 dpf. A total of 150 fish tracks were analyzed per exposure group.

Data processing and statistical analysis

All behavioral data obtained from ctrax was processed with a custom Microsoft Excel macro to calculate rate of travel ($\text{mm } 5\text{min}^{-1}$), swimming speed (mm s^{-1}), % activity (% of time active), minimum speed (mm s^{-1}), NGDR, maximum speed (mm s^{-1}), and scoot frequency (Hz).

Statistical analyses were conducted with SigmaPlot software version 11.0 [Systat Software, San Jose CA, USA, (www.sigmaplot.com)]. All data was tested

for normality; multiple pair-wise comparisons were carried out with the Holm-Sidak method whenever the data passed the normality test, if not, the data was ranked and pair-wise comparisons were done with Dunn's method.

Measured concentrations of THg in the embryos were log transformed prior to statistical analysis with one-way ANOVA due to the 3 to 12 fold differences between exposure groups.

VMR, routine swimming and prey capture data were analyzed with repeated measures two-way ANOVA. Mortality, ELS toxicity scores and 7 dpf larval swimming behavior were analyzed with one-way ANOVA. Gaussian curves and regression analyses were fitted using the dynamic fitting function in SigmaPlot.

Results

Embryo mortality and early life stage (ELS) toxicity scoring

None of the MeHg exposures in this study caused any overt effects on fecundity of the adult females, embryo mortality or development at any of the developmental stages monitored (n=36 embryos; $P=0.116$). All fish used in subsequent behavioral experiments appeared healthy and had no morphological abnormalities (Appendices 2 and 3).

Mercury analyses

All THg burdens in embryos (both G₁ and G₂) were statistically different from each other (n=3 samples; $P<0.001$); the accuracy of the measured THg in diets versus its nominal concentration were between 90% and 122% (Tables 3.1 and 3.2).

THg burdens in embryos had a strong correlation with that of the maternal ovaries [Embryo THg = $0.0150 + (0.0797 \times \text{Ovary THg})$, $R^2=0.954$] (Figure 3.2); $8.76\% \pm 0.38$ (SE) of the THg in the ovaries was present in the embryos.

VMR assay

Zebrafish embryos monitored in this assay exhibited a characteristic pattern of high and low locomotor output in response to sudden transitions from dark to light. The locomotor activity of control 6 dpf zebrafish remained unchanged throughout the full duration of the first 20 minute dark period of this assay (Figure 3.3). In contrast, all MeHg exposed fish tested had a significantly

lower locomotor activity from the beginning of the initial 20 minute dark period to its conclusion (n=126 embryos; $P<0.001$). Furthermore, larvae from the 3ppm and 10ppm exposure groups had significantly lower locomotor activity towards the second half of both dark periods (n=126 embryos; $P<0.001$) (Figure 3.3, A). Similarly, the startle response was not affected in the first two sudden light transitions (dark to light and light to dark) but in the third light transition (dark to light) fish from the 3 and 10ppm exposure groups exhibited a significantly lower startle response (Figure 3.3, B).

Analysis of 7 dpf larval zebrafish swimming behavior

The behavior of 7 dpf zebrafish was characterized by an increase in distance travelled, percentage of time active and minimum speed (n=180 embryos; $P<0.001$) (Figure 3.4, A C and D), as well as a decreased NGDR (n=180 embryos; $P<0.001$). Maximum speed was significantly decreased in the 3 and 10ppm exposure groups ($P<0.001$) (Figure 3.4, F; note the dramatic decrease in 95th percentile of maximum speed of 3 and 10ppm exposure groups). Active swimming speed was only increased in the 1ppm MeHg treated group (n=180 embryos; $P<0.001$) (Figure 3.4, B).

Further analysis of the swimming kinematics of the larvae revealed that the observed increase in minimum speed was attributable to an increase of up to 26% in the frequency of slow swimming scoots (Figure 3.5).

Routine swimming and prey capture at 8, 12 and 16 dpf

As observed in 7 dpf fish, the behavior of 8, 12 and 16 dpf zebrafish was characterized by increases in % activity (Figure 3.6, A), coupled with decreases in NGDR (150 embryos; $P < 0.001$) (Figure 3.6, B). The occurrence of increases in activity was particularly noticeable in 16 dpf fish; subtle non-significant decreases in NGDR were observed in 8 dpf, however this decrease became much more prominent in 12 and 16 dpf fish.

No brine shrimp nauplii were consumed by 8 dpf zebrafish of any exposure group. Some foraging could be observed in 12 dpf fish, though no statistical differences between exposure groups were observed in this time point ($n=6$ dishes; $P=0.503$). Foraging was significantly increased in all MeHg treated 16 dpf Zebrafish (relative to 12 dpf) but not in the control fish. Not surprisingly, prey capture in all MeHg exposed 16 dpf zebrafish was significantly higher than the control group ($n=6$ dishes; $P < 0.001$) (Figure 3.7).

Discussion

MeHg accumulation in tissue

All of the dietary exposure regimes for G₁ fish were within what other authors have established to be environmentally relevant (Cambier et al., 2009; Hammerschmidt et al., 2002). A dietary exposure of 1ppm of MeHg represents what a fish would be exposed to by foraging on benthic invertebrates in low alkalinity lakes (Hammerschmidt et al., 2002), while concentrations of 3 and 10ppm are more relevant to heavily polluted sites, such as those impacted by clandestine gold mining in the Amazon basin (Durrieu et al., 2005). It has been estimated to be maternal transfer of MeHg to the eggs accounts for 2 to 11% of the concentration in the muscle (Latif et al., 2001). Here, we observed a similar range of 5 to 10% of THg transfer from the ovaries to the embryos; although our study did not quantify THg in muscle tissue, studies in yellow perch (*Perca flavescens*) have demonstrated that THg levels in the muscle are nearly identical to those found in the ovary of MeHg exposed females (DeBofsky, unpublished work). It is estimated that MeHg causes adverse effects in the behavior of adult fish at a toxicological threshold of 0.20ppm (measured in whole body tissue) (Wiener et al., 2012).

VMR assay

Our experiments showed effects on the intensity of the of the medium and high exposure groups (3 and 10ppm MeHg) of 6 dpf zebrafish larvae. These fish

manifested lower rates of travel after the second half of both dark periods, as well as a lower startle response towards the end of the assay.

Our results are consistent with a previous experiment that analyzed the C-start response of developmentally MeHg exposed zebrafish larvae reacting to single and multiple mechanical stimuli (Weber, 2006). In this experiment, fish exposed to a low concentration of waterborne MeHg (25 μ g/mg) did not exhibit significantly different velocities in response to a single mechanical stimulus or several consecutive stimuli (1, 2 or 4 hits per second). However, fish exposed to higher doses of MeHg (50 and 75 μ g/mg) and subjected to repeated stimulation had dramatic decreases in maximum velocities by the second or third stimulus.

It is estimated that MeHg causes adverse effects in the behavior of adult fish at a toxicological threshold of 0.20ppm (measured in whole body tissue) (Wiener et al., 2012). In our study, the mercury burdens in exposed embryos were high enough that the behavioral abnormalities observed could be partly due to post-hatch residual MeHg interfering with neuronal ion channels, neurotransmitter dynamics or neuronal function, as noted by Weber (2006). However, teratogenic effects of prenatal MeHg on the development and function of the brain and muscle, are additional putative mechanisms of behavior alteration (Ekino et al., 2007).

Although there is evidence of non-associative learning (habituation) in zebrafish larvae (Best et al., 2008; Weber, 2006), it would be an unlikely explanation for the gradual reduction in locomotor activity and startle response observed in the VMR assay. In such case, our results would suggest that MeHg

improves learning, which has been refuted in several studies (Baraldi et al., 2002; Smith et al., 2010). Furthermore, our spontaneous swimming experiments carried out in 7 dpf zebrafish also demonstrated reductions in maximum velocity in the 3 and 10ppm MeHg exposure groups in the absence of any sudden visual cues (apart from other larvae swimming in the same dish), suggesting that the alterations in both assays are most likely attributable to neuromuscular anomalies, rather than cognitive.

The relevance and purpose of the VMR as a survival behavior remains debatable, as it has been interpreted as a reaction intended to avoid a looming predator (Easter Jr and Nicola, 1996) or, more possibly, a response that reorients a larva that has strayed into a shaded environment back into a well lit location (Burgess and Granato, 2007). Nevertheless, this assay delivers consistent and reproducible results. In addition, similar results were observed in free swimming larvae later in development, evidencing the value of the VMR assay as a preliminary predictor of how MeHg affects high velocity swimming episodes in zebrafish larvae.

Routine swimming behavior and prey capture (separate swimming from prey capture and narrate developmentally)

Further experiments in 7 dpf zebrafish showed increased rates of travel, as well as increases in activity. MeHg exposed larvae exhibited an increased frequency of slow scoots and decreased NGDR, both of which are indicative of increased activity and turning frequency, respectively. MeHg has been reported

to cause both hyperactivity or hypoactivity, depending on dosage as well as the developmental stage of exposure, history of previous exposure or synergy with other contaminants (Sandheinrich and Miller, 2006; Vitalone et al., 2008). Hyperactivity has been reported in mummichogs exposed to MeHg as embryos (Weis et al., 1999). Similarly, other studies report that prenatally MeHg exposed rat pups showed increased locomotor activity (Daré et al., 2003; Gimenez-Llort et al., 2001).

In contrast, MeHg decreased maximum velocities in free swimming 7 dpf zebrafish in the medium and high exposure groups (3 and 10ppm). During spontaneous swimming, high speeds are characteristic of a darting motion, which larvae typically exhibit as a response to other unexpectedly approaching larvae, as zebrafish larvae are known to avoid each other (Pelkowski et al., 2011). As with the VMR assay, the observed decreases in high velocities were consistent with studies that assessed the startle response of zebrafish and Atlantic croaker exposed to MeHg (Alvarez et al., 2006b; Weber, 2006).

Monitoring of the routine swimming and prey capture of the larvae also evidenced continued increases in activity and decreases in NGDR throughout early development, from 8 to 16 dpf. Prey capture was also significantly increased in MeHg exposed 16 dpf zebrafish larvae. These results are consistent with reports that mummichog larvae from polluted sites are initially more active and better at prey capture than larvae from clean sites (Weis et al., 1999).

Remarkably few studies have assessed the effect of specific contaminants on the prey capture ability of fish, but the vast majority of these studies have

focused on the effects of MeHg in mummichog (*Fundulus heteroclitus*) (Weis et al., 2001; Weis and Weis, 1995a).

In zebrafish, several researchers have assessed the prey capture efficiency of zebrafish eleutheroembryos feeding on paramecia (Bianco et al., 2011b; Budick and O'Malley, 2000). However, while this approach has established the possibility of using prey capture as a relevant endpoint, no significant efforts have been made to adopt this experimental paradigm in the field of environmental toxicology using the zebrafish as a model.

Relevance of observed behavioral endpoints in predator-prey dynamics

The notion of a positive relationship between locomotor output, prey capture and predator avoidance has been a common assumption when creating simulation models of predator-prey interaction (Alvarez et al., 2006b). This notion holds true for our observations of increased frequency of low velocity scoots coupled with increased prey capture in zebrafish larvae. Likewise, this increase in slow scoot frequency and a reduction in maximum velocities could increase the likeliness of attracting predator's attention and reduce the chances of the larva to perform a high velocity escape, respectively. It is also important to acknowledge that while increased locomotion was implicated in higher prey capture in our laboratory setup, this scenario would likely change in the wild, where prey is often times more scarce and more challenging to capture.

Figures

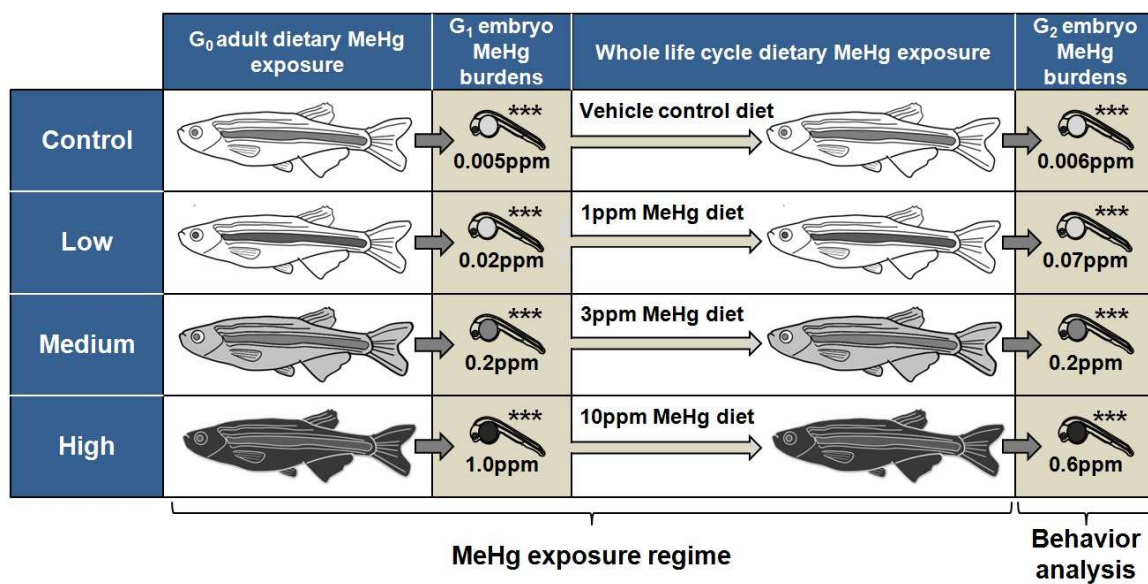


Figure 3.1: Whole life cycle MeHg exposure experimental design

Figure 3.1: Whole life cycle MeHg exposure experimental design

Adult zebrafish were fed with MeHg diets (vehicle control, low, medium and high) and the MeHg burdens of their offspring (G_1) were monitored for 9 weeks. Once the treated G_1 embryo MeHg burdens spanned levels between 0.01 and 1ppm and all pair wise comparisons of MeHg burdens were significantly different (One way ANOVA; $n=3$ samples; $P<0.001$) the embryos were raised with MeHg diets (0, 1, 3 and 10ppm MeHg). Once the fish reached adulthood, they were allowed to spawn, after which the MeHg burdens of the G_2 embryos were measured. All pair wise comparisons of MeHg burdens in the G_2 embryos were found to be significantly different to each other (One way ANOVA; $n=3$ samples; $P<0.001$). Since this study was concerned with the behavioral effects of parentally transmitted MeHg, the G_2 embryos were raised with regular diets (with no added MeHg) and monitored for behavioral abnormalities.

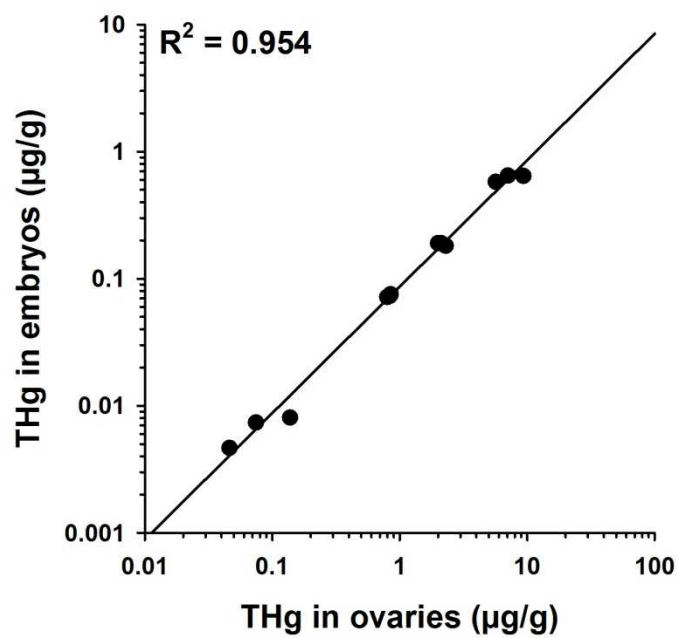


Figure 3.2: Regression analysis of THg in embryos as a function of THg in ovaries

Figure 3.2: Regression analysis of THg in embryos as a function of THg in ovaries

THg burdens in embryos had a strong correlation with that of the maternal ovaries [Embryo THg = 0.0150 + (0.0797 x Ovary THg), R²=0.954].

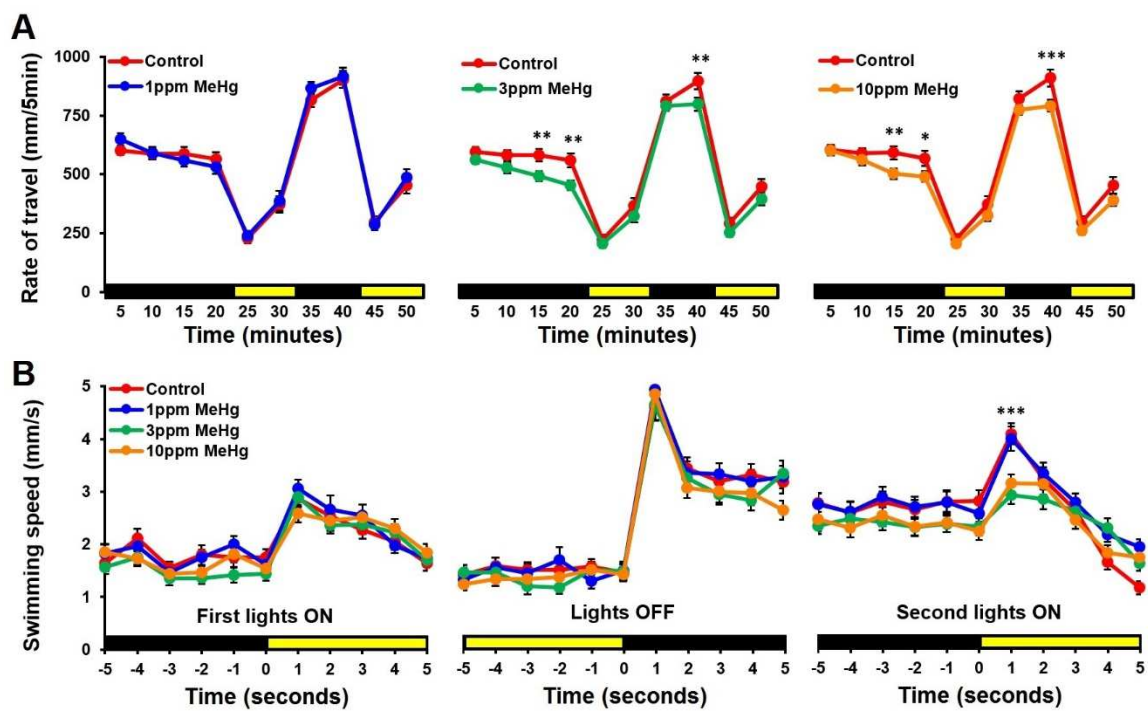


Figure 3.3: Parentally transmitted MeHg burdens affect the VMR of 6 dpf zebrafish offspring

Figure 3.3: Parentally transmitted MeHg burdens affect the VMR of 6 dpf zebrafish offspring

(A) Alternating dark and light cycles elicit a characteristic behavioral response in zebrafish embryos. There was a significant effect of light and dark conditions on the behavior of all exposures tested (Repeated measurements ANOVA; $P < 0.001$). The rate of travel (mm/5 minutes) was not affected in the 1ppm MeHg exposure group in any of the 5 minute time bins ($n=126$ fish, $P=0.67$). However, significant decreases in rate of travel could be observed in the second half of both dark periods of the VMR of the 3 and 10ppm MeHg exposure groups. (B) The startle response was not affected in the first two sudden light transitions (dark to light and light to dark) but in the third light transition (dark to light) fish from the 3 and 10ppm exposure groups exhibited a significantly lower startle response. Black and white bars along the X axis represent dark and light periods, respectively. Error bars represent the standard error of the mean (significance represented as $*p \leq 0.05$; $**p \leq 0.01$; $***p \leq 0.001$).

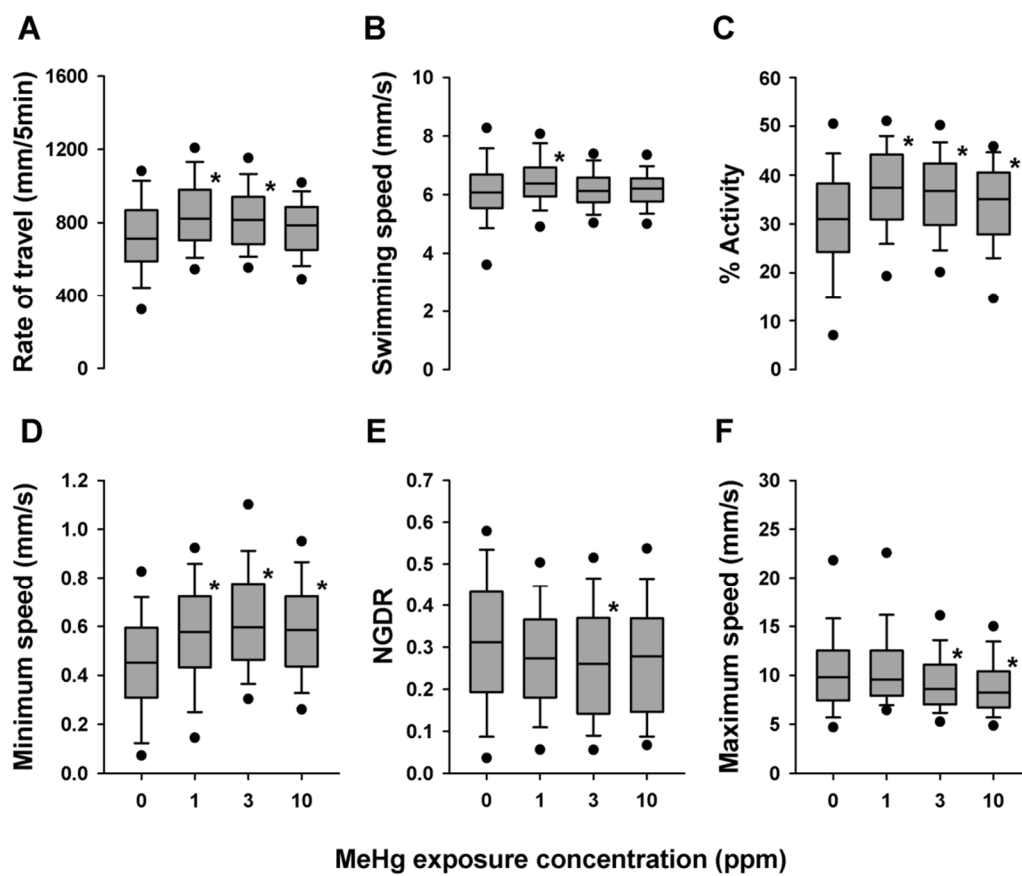


Figure 3.4: Effects of parental dietary MeHg on the spontaneous swimming of 7 dpf zebrafish offspring

Figure 3.4: Effects of parental dietary MeHg on the spontaneous swimming of 7 dpf zebrafish offspring

Multiple groups of ten 7 dpf zebrafish were recorded and their swimming activity was analyzed with a machine vision algorithm. The behavior of MeHg exposed 7 dpf zebrafish was characterized by increases in overall locomotor output reflected by higher rates of travel (A), swimming speed (B), % activity (C) and minimum speeds (D). Exposed fish also had less linear swimming trajectories exhibited by slight decreases in NGDR (E). Additionally, fish from the two higher dose groups had significantly lower maximum velocities (F) (* $p \leq 0.05$).

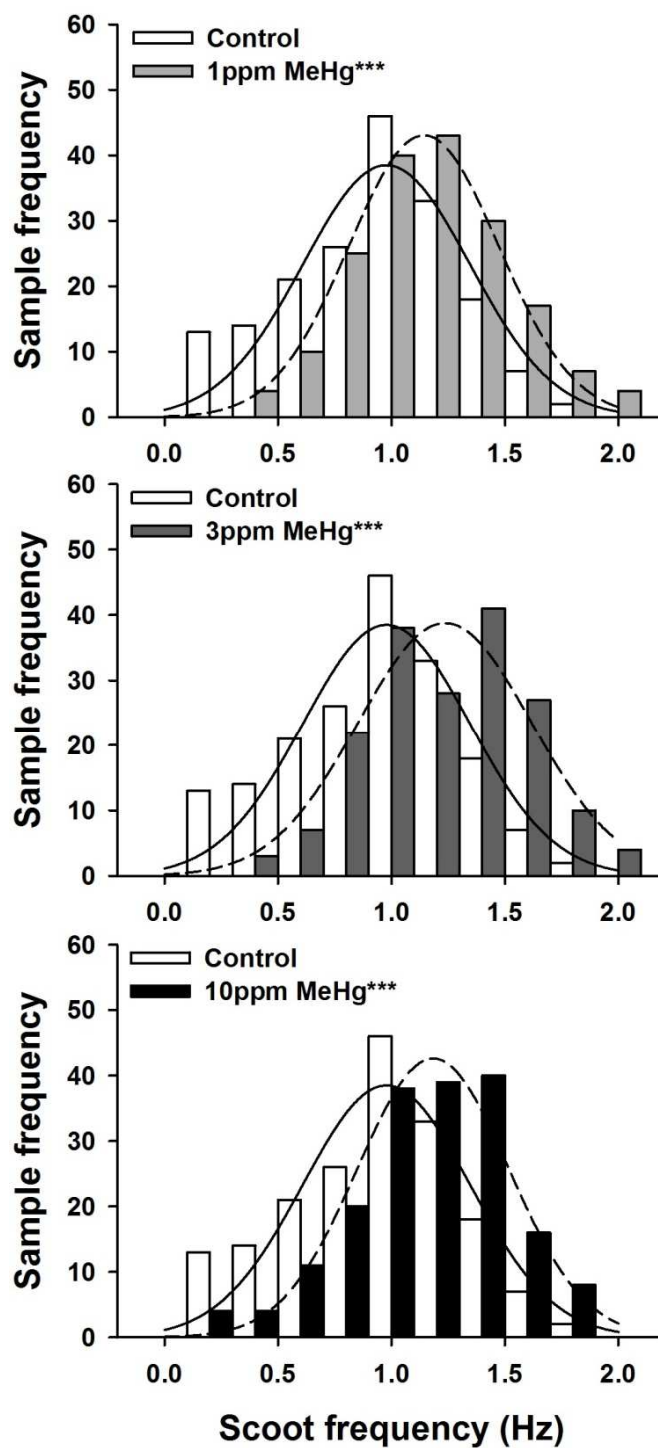


Figure 3.5: Maternal dietary MeHg burdens increase the swimming scoot frequency of the offspring

Figure 3.5: Paternal dietary MeHg burdens increase the swimming scoot frequency of the offspring

Zebrafish larvae swim in a series of low velocity “scoots” followed by a glide. Parental MeHg caused a significant increase in the scoot frequency of all MeHg exposed 7 dpf zebrafish (One way ANOVA; $n=180$ fish; $P<0.001$). Solid normal curves represent the sample frequency distribution of control fish; dotted curves represent MeHg exposed fish.



Figure 3.6: Monitoring of routine swimming of 8, 12 and 16 dpf and foraging efficiency assay

Figure 3.6: Monitoring of routine swimming of 8, 12 and 16 dpf and foraging efficiency assay

Zebrafish larvae were monitored throughout three time points to ascertain if increased locomotor output and reduced NGDR observed in 7 dpf fish would continue from 8 to 16 dpf. All experiments were done 5 minutes prior to a foraging efficiency assay. Increases in % activity were observed at 8 and 16 dpf (A); NGDR was also reduced at 12 and 16 dpf (B). Moreover, % activity at 16 dpf was significantly higher than measured at 8 and 12 dpf (Repeated measurements ANOVA, n=150 fish; $P < 0.001$).

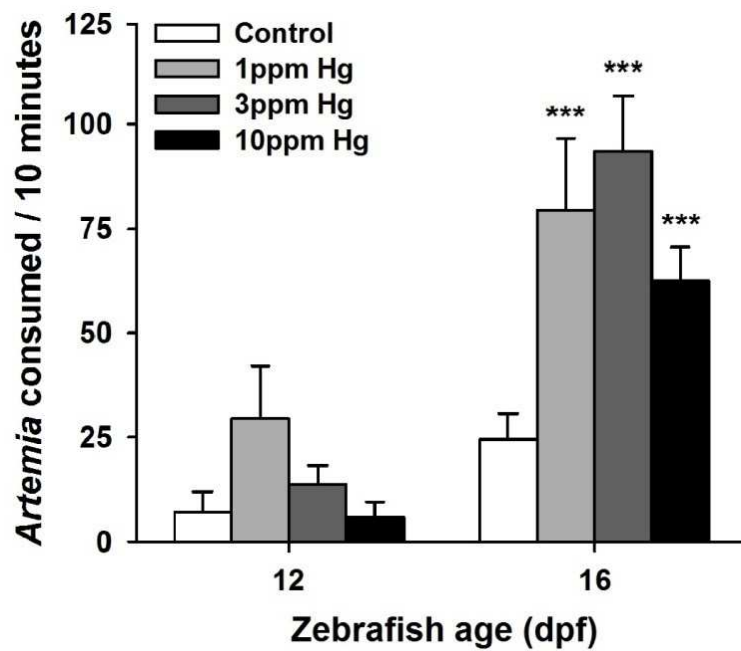


Figure 3.7: Prey capture is increased by MeHg exposure

Figure 3.7: Prey capture is increased by MeHg exposure

Foraging efficiency of larvae was assessed immediately after routine swimming monitoring. No foraging was observed in 8 dpf zebrafish (thus, the data is not represented in the graph); the first evidence of foraging was seen in 12 dpf fish. Foraging significantly increased in all MeHg treated 16 dpf Zebrafish (relative to 12 dpf) but not in the control fish. Correspondingly, prey capture in all MeHg exposed 16 dpf zebrafish was significantly higher than the control group. Error bars represent the standard error of the mean (n=6 dishes; $P < 0.001$).

Tables

Table 3.1: G₁ diet Hg concentrations and embryo burdens

Nominal Hg concentration in diet (ppm)	Measured Hg concentration in diet (ppm)	Embryo THg burden (ppm, wet weight)
0.0	0.12 ± 0.004	0.005 ± 0.001
0.5	0.61 ± 0.117	0.024 ± 0.002
5.0	4.48 ± 0.306	0.212 ± 0.031
50.0	47.35 ± 0.618	1.067 ± 0.052

Note: Values are given as the mean ± SE

Table 3.2: G₂ diet Hg concentrations and embryo burdens

Nominal diet Hg concentration in diet (ppm)	Measured Hg concentration in diet (ppm)	Embryo THg burden (ppm, wet weight)
0	0.05 ± 0.014	0.006 ± 0.001
1	1.11 ± 0.015	0.073 ± 0.001
3	3.62 ± 0.074	0.187 ± 0.004
10	11.16 ± 0.365	0.623 ± 0.039

Note: Values are given as the mean ± SE

CHAPTER 4: EFFECTS OF EARLY EMBRYONIC MeHg EXPOSURE IN THE LOCOMOTION, VISUALMOTOR RESPONSE AND FORAGING OF YELLOW PERCH (*Perca flavescens*) LARVAE

Abstract

Yellow perch (*Perca flavescens*) is a fish species of economical and ecological importance in the Great Lakes region. In Lake Michigan, this species has faced difficulties with successful recruitment. Low recruitment has been widely attributed to overfishing, however very few studies have linked the effect of neurotoxic contaminants, such as methylmercury (MeHg), on larval yellow perch. Methylmercury is environmentally present in the Great Lakes and its neurotoxicity has been shown to affect foraging behavior in exposed fish, as well as birds and mammals. Here, we investigated the effect of varying doses of MeHg (0, 0.03, 0.1 and 0.3 μ M) on the light/dark swimming activity, spontaneous locomotion and foraging of larval yellow perch. These experiments establish a knowledge-base of the effects of MeHg on the larval yellow perch's basal swimming behavior and its response to a fundamental environmental cue: light. Furthermore, since food limitation is thought to be one of the main causes of larval fish mortality, we also investigated the effects of MeHg on feeding behavior. In this study, we observed decreases in locomotor activity in all MeHg doses tested, coupled with a significant decrease in prey capture in one of the MeHg doses tested (0.1 μ M). These results suggest a link between MeHg exposure, locomotor activity and prey capture success, which in turn could have adverse implications for yellow perch population recruitment.

Introduction

Mercury is a widespread and pervasive neurotoxicant found in a variety of forms in freshwater and marine ecosystems around the world (Devlin, 2006). Among these ecosystems the Great Lakes Basin has been afflicted by a widespread mercury contamination that adversely affects the aquatic resources of the region (Monson, 2009a). Naturally occurring processes such as volcanic eruption can release inorganic mercury into the atmosphere, but it was the onset of the industrial revolution that introduced new sources of anthropogenic-derived mercury emissions such as fuel combustion, waste incinerators, mining, and manufacturing. Among all of the sources of mercury the most numerous and largest emitters are coal-fired power plants (Monson 2009). This contaminant enters the aquatic ecosystems primarily through atmospheric deposition (Risch et al., 2012a), after which microorganisms convert the elemental form of mercury into organic molecules. MeHg is reported to be the most abundant organic form of mercury and accounts for up to 99% of the total mercury fraction in analyzed tissues. Furthermore, the neurotoxicity of this contaminant has been shown to affect foraging behavior in exposed fish, as well as birds and mammals. Fish begin experiencing adverse effects from MeHg exposure at a tissue concentration of 0.2ppm in wet weight (ww) (Wiener, Sandheinrich et al. 2012); these effects include impaired swimming, abnormal startle response and reproductive effects.

The Wisconsin Department of Natural Resources (WIDNR) has monitored Hg in fish since the early 1970s, and although there are reports of a slow

reduction in MeHg in fish tissue, the prevalence of MeHg consumption advisories in almost every body of water in the Great Lakes region lingers on (Wiener, Sandheinrich et al. 2012).

Yellow perch (*Perca flavescens*) play an important role in the near-shore ecology of Lake Michigan (Clapp and Dettmers, 2004) and are extremely popular with commercial and recreational fishers around the lake (Summit, 2014). However, the populations of this important natural resource in Lake Michigan have experienced a considerable decrease since 1997. Wilber et al. (2005) estimates a decline of 92% of the stock of adult yellow perch in the state of Wisconsin, a species that before 1997 represented 85% of the recreational catch by number.

The decline of the yellow perch has been attributed mostly to overfishing, (Marsden and Robillard, 2004), introduction of invasive species (Shroyer and McComish, 2000) and only partly to poor recruitment, nonetheless little is known about the role of environmental neurotoxicants in the yellow perch population dynamics, or how contaminants can affect other species of the Great Lakes. A deeper understanding on this subject is required to allow fisheries and policy makers to consider the putative broader implications of environmental pollutants on the Great Lakes ecosystem.

Concentrations of mercury in yellow perch in the Great Lakes vary substantially, with the highest concentrations reported in fish from inland lakes (Harris and Bodaly, 1998; Wiener et al., 2012). A recent report by Wiener and collaborators (2012), compiled the analyzed MeHg concentrations from different

yellow perch tissues, obtained from 691 bodies of water scattered throughout the Great Lakes region. Mean whole-body concentrations of mercury in fish from 45 (6.5%) of these 691 waters equaled or exceeded 0.20 mg/g wet weight, the estimated threshold concentration for deleterious effects in fish. Furthermore, maximum whole-body concentrations in fish from 151 (22%) of these water bodies equaled or exceeded 0.2ppm, reaching up to 2.60ppm wet weight in muscle.

In light of the persistent deleterious concentrations of MeHg in yellow perch tissues, this study investigated the effects of MeHg exposure on the behavior of yellow perch larvae. Larval yellow perch – as opposed to adults – were selected as subject of this study due to the higher sensitivity of developing organisms to environmental insults, such as MeHg exposure (Samson and Shenker, 2000). Here, we have selected a suite of behavioral endpoints that encompass some of the most fundamental behaviors for the survival of fish larvae: swimming and capturing prey. Since food limitation is thought to be one of the main causes of larval fish mortality in nature (von Herbing and Gallager, 2000), this study has focused on elucidating a link between MeHg exposure, locomotor activity and ultimately prey capture success.

Materials and methods

Yellow perch broodstock and egg husbandry

All protocols for the care and handling of yellow perch were approved by the Institutional Animal Care and Use Committee (IACUC) of the University of Wisconsin – Milwaukee. Egg masses were obtained from sexually mature yellow perch kept as broodstock in the aquaculture facility of the School of Freshwater Sciences (University of Wisconsin-Milwaukee, USA). The eggs were collected from fifteen sexually mature yellow perch females (one egg mass per female) and then fertilized with the milt of one randomly selected male. The eggs were kept in a cooler at a temperature of approximately 10°C at all times. The fifteen fertilized egg masses were then divided into three biological replicates, each one pooling eggs from five different progenitor pairs (Figure 4.1); all experiments described hereafter were carried out with these three replicate sets of eggs.

When spawning, yellow perch females extrude up to 40,000 eggs into a long and continuous "accordion-folded" strand that is about 4-5cm thick and approximately a meter long (Mansueti, 1964). In order to plate these eggs in Petri dishes for incubation, the egg masses were cut into small ribbons containing roughly ten fertilized eggs each. A total of five ribbons (one from each spawning pair) were plated into each Petri dish containing 50mL of E2 embryo medium (Figure 4.1) (15mM NaCl, 0.5mM KCl, 1mM MgSO₄, 150μM KH₂PO₄, 50μM Na₂HPO₄, 1mM CaCl₂, 0.7mM NaHCO₃). The incubation of the eggs was initiated at 10°C and was progressively increased by 1°C every second day until

a final temperature of 20°C was reached. The E2 embryo medium was changed daily throughout the development of the yellow perch larvae.

Static waterborne MeHg exposure regimes

In order to mimic maternal MeHg transfer from the ovary to the egg, we carried out static waterborne MeHg exposures on newly spawned yellow perch eggs (Figure 4.1). Immediately after transferring the egg ribbons to Petri dishes, the developing embryos had reached the 128-cell stage (~12 dpf). At this point, all of the clean medium was suctioned out of the Petri dishes and quickly replaced with 50mL of one of five waterborne MeHg solutions: 0, 0.03, 0.1, 0.3 and 1µM MeHg (in 0.033% ethanol). Five dishes (each one containing roughly 50 eggs) were exposed to each solution. The embryos remained in the exposure solutions incubated at 10°C for 20 hours, after which all dishes were rinsed three times with fresh 10°C E2 medium. Once the eggs were thoroughly rinsed, they were kept in fresh E2 medium and returned to the incubator; E2 embryo medium was exchanged daily. At 14 dpf, the embryos were assisted to hatch by vigorously pipetting the eggs in and out of a 25mL pipette, thereafter, chorion debris and dead embryos were removed from the dishes and live embryos were immediately counted. Once yellow perch embryos initiated spontaneous swimming (17 dpf), pools of 10 randomly selected individuals per dose were flash frozen in liquid nitrogen (in triplicate) and stored for later analysis of total mercury (THg). THg contents in whole embryo tissues were directly analyzed using a Direct Mercury Analyzer 80 (DMA-80, Milestone Inc, Shelton CT) as described by Basu and collaborators (2009).

Analysis of 17 dpf larval yellow perch swimming behavior

Yellow perch larvae initiate swimming at approximately 17 dpf; at this point we initiated behavioral analyses. Commonly, the analysis of locomotor activity is carried out both in a dark and lit conditions to account for any possible effects of illumination on the behavioral responses of the experimental subjects (Ulhaq, Örn et al. 2013). Here, we analyzed the spontaneous swimming activity of 17 dpf yellow perch larvae in the dark and in the light for 15 minutes, after a 10 minute acclimation period.

The locomotor activity of the larvae was monitored with a DanioVision system (Noldus Information Technology, Leesburg, VA, USA), which consists of an enclosed chamber designed to hold a multiple-well plate in which fish larvae are imaged. The multiple-well plate is illuminated from underneath with a light box capable of emitting infrared (800–950 nm with a peak at 860 nm) and visible light (430–700 nm).

The total distance traveled of each fish was analyzed using Ethovision software version 8.0 (Noldus Information Technology, Leesburg, VA); individual fish were observed in 24-well plates and tracked at a frame rate of 25 frames per second (fps). A total of 36 larvae per exposure group were analyzed.

Visual-motor response assay

The visual-motor response (VMR) assay has been extensively described in the zebrafish as a complex behavioral paradigm that integrates both the visual perception and the locomotion of the fish (see chapter 3). The experiment

consists of tracking the activity of fish larvae while abruptly changing the light intensity in an enclosed observation chamber every 10 to 20 minutes. Zebrafish exhibit a robust increase in locomotion when the lights are suddenly turned off and, conversely, their locomotor activity decreases when the lights are turned on. Here we tested the VMR behavioral paradigm in the yellow perch to determine if this approach could prove useful in identifying behavioral alteration in this particular fish species.

For this assay, the yellow perch larvae were acclimated 10 minutes in the dark, after which they underwent two cycles of alternating 10 minute light and dark periods (for a total of 50 min). The monitoring of the activity of the yellow perch larvae was performed with a DanioVision system and the locomotor data was analyzed with Ethovision software version 8.0 (Noldus Information Technology, Leesburg, VA), as described previously.

Routine swimming and prey capture at 25 dpf larvae

The swimming performance of the larval yellow perch was once again monitored at 25 dpf prior to prey capture assessment. In order to do this, a custom-made behavior observation chamber was built. The apparatus consisted of a manifold holding two Logitech C920 web cameras pointing downwards into a Plexiglas tray, over which two Petri dishes could be placed. Underneath the apparatus, a flat 22" Acer P221W computer monitor was used as a light source, which provided 58 lux of constant illumination; a sheet of velum paper was used as a diffusing filter. In order to block extraneous light and visual stimuli, the whole

apparatus was surrounded by a custom made black polyethylene enclosure. All video recordings were streamed to a remote computer at a resolution of 960x720 and a frame rate of 30 fps using the MATLAB image acquisition toolbox.

At 9:00am, on the day of the analysis, 30 larvae were transferred to 10cm diameter glass Petri dishes containing 50mL of 20°C E2 embryo medium. Yellow perch larvae are extremely fragile and can be easily damaged even when handled with care; while 30 individuals were transferred to dishes, approximately 5 larvae were expected to die within the following 3 hours. At 12:00pm any dead larvae were removed and replaced. The dish was then transferred to the recording chamber and the fish were allowed to acclimate for 5 minutes, after which they were recorded for 10 minutes. All recordings were carried out from 12:00pm to 7:00pm.

A 30 second fragment was randomly selected from the 10 minute clips to analyze the spontaneous swimming of the larvae. The video clips were converted from 30 fps to 6 fps to facilitate manual frame-by-frame analysis of the footage. The analysis of locomotor of the larvae activity was performed with the Manual Tracking ImageJ plugin (Figure 4.2) (Fabrice Cordelières, Institut Curie, Orsay, France).

Immediately after the recording of routine swimming, foraging efficiency was measured by introducing 5 *Artemia* nauplii per fish (*i.e.* 30 fish per dish, foraging on 150 nauplii) into the Petri dish. The larvae were allowed to feed for 10 minutes, after which the remaining nauplii were counted.

Data processing and statistical analysis

Statistical analyses were conducted with SigmaPlot software version 11.0 [Systat Software, San Jose CA, USA, (www.sigmaplot.com)]. All data was tested for normality; multiple pair-wise comparisons were carried out with the Holm-Sidak method whenever the data passed the normality test, if not, the data was ranked and pair-wise comparisons were done with Dunn's method. Measured concentrations of THg in the embryos were log transformed prior to statistical analysis with one-way ANOVA due to the 3 to 12 fold differences between exposure groups.

Results

THg burdens in yellow perch embryos significantly increased as a function of MeHg exposure (0, 0.03, 0.10, 0.30 and 1.00 μ M). All THg burdens were statistically different from each other (n=3 samples; $P < 0.001$). From all the exposure regimes tested, only 1 μ M of acute waterborne MeHg exposure caused a significant decrease in post-hatch survival (n=15 dishes; $P < 0.001$). Since this study was concerned with sublethal effects of MeHg exposure, the surviving embryos from the 1 μ M MeHg exposure group was not utilized in further behavioral analyses (Table 4.1).

Yellow perch of all exposure groups tested in the light exhibited a strong increase in locomotor activity compared to the groups tested in the dark (n=92 fish, $P < 0.001$). All MeHg exposed larvae exhibited lower locomotor activity relative to control in the light (n=92 fish, $P < 0.001$), however no statistical differences were tested between exposure groups recorded in the dark (Figure 4.3).

Contrary to the behavioral responses observed in zebrafish eleutheroembryos subjected to the VMR assay (See chapter 3), yellow perch larvae respond to this assay with increased locomotion when the lights are turned on and decreased locomotion when the lights are turned off. Throughout the experiment, a slight increase in locomotor activity was observed in the 0.03 μ M MeHg exposure group relative to the controls; however, this trend was not significant. Similarly, there was also a non-significant decrease in locomotor

activity in the 0.10 μ M MeHg exposed larvae. During the last light period of the VMR assay the 0.03 μ M MeHg larvae swam statistically more than the 0.10 μ M MeHg group (Figure 4.4). When accounting for the total locomotor output throughout the whole experiment, the 0.03 μ M MeHg larvae were statistically more active than the 0.10 μ M MeHg group, but no MeHg exposure group was significantly different to the control (data not shown).

As observed in 17 dpf larvae, yellow perch larvae exposed to all MeHg concentrations tested continued having decreased locomotor activity (n=120 fish, $P < 0.05$); the lowest locomotor activity was observed in the 0.10 μ M MeHg exposure group, along with a higher NGDR (Figure 4.5). Similarly, the average prey capture was decreased in all exposure groups but only significantly in the 0.10 μ M MeHg exposure group (n=4 dishes, $P < 0.05$) (Figure 4.6).

Discussion

It is estimated that MeHg causes adverse effects in the behavior of adult fish at a toxicological threshold of 0.20ppm (measured in whole body tissue) (Wiener, Sandheinrich et al. 2012). In our study, the lowest dose of acute waterborne MeHg (0.03 μ M) resulted in an embryo body burden equal to this threshold, all other doses were well above this threshold, however they were comparable to other reported THg burdens in whole zebrafish embryos spawned by parents fed with a diet containing environmentally relevant concentrations of MeHg (Table 3.2).

To date, most behavioral work has been carried out in widely-utilized fish models such as the zebrafish, medaka, or goldfish, to name a few (Kalueff et al., 2013; Oshima et al., 2003; Saglio and Trijasse, 1998). However the application of novel methods to analyze behavior has allowed us to analyze behavior in the yellow perch, a non-model species.

When analyzing the VMR paradigm, the yellow perch exhibit a very different reaction to light intensity to that observed in zebrafish (MacPhail et al., 2009). Zebrafish are reported to exhibit lower locomotor activity in the light than in the dark; in the case of the yellow perch, their locomotion reaches a maximum in well-lit conditions. This response is presumably due to the strong phototactic behavior of this species early in development (Dr. Fred Binkowski, University of Wisconsin – Milwaukee, personal communication).

Yellow perch exhibited a characteristic increase/decrease of locomotion in response to abrupt light changes in the VMR assay; however the variation

between individuals was so great that it is difficult to draw conclusions about neurotoxic effects from this particular behavioral paradigm. Although this issue could be addressed by increasing the number of individuals per trial, the VMR assay requires roughly one hour to evaluate 24 individuals (one larva per well in a 24-well plate) which reduces the throughput of the experiment. This is particularly unpractical when dealing with a fish species that only spawns a once per year. Despite these drawbacks, a preliminary notion of lower locomotor activity in the 0.10 μ M MeHg exposure group could be inferred. This notion was confirmed later in 25 dpf fish in further locomotion and prey capture assays.

The swimming and prey capture experiments in 25 dpf larvae were done consecutively to assess if there was a relationship between locomotor output and prey capture, as it has observed previously in zebrafish (see chapter 3). All MeHg dosed individuals tested in the spontaneous swimming experiment exhibited lower locomotor output, as it had been observed at 17 dpf. Furthermore, prey capture was also significantly reduced in the 0.10 μ M MeHg exposed larvae; interestingly this same cohort performed poorly in the VSR assay, suggesting that this assay could have had good predictive value if the number of individuals tested would have been higher. Moreover, the notion of a positive relationship between locomotor output and prey capture is a common assumption when creating simulation models of predator-prey interaction (Alvarez, Murphy et al. 2006). This notion held true for our observations of hypoactivity coupled with decreased prey capture in yellow perch larvae.

Remarkably few studies have assessed the effect of specific contaminants on the prey capture ability of fish, all of these stemming from a single research group that has focused on the effects of MeHg in mummichog (*Fundulus heteroclitus*; Weis and Weis 1995; Weis, Smith et al. 2001). Our study contributes to the understanding of how MeHg affects fundamental survival skills in wild fish population. Overall, the observed concentrations of Hg in the tissue of yellow perch in this study were relatively high. It has been estimated that yellow perch eggs have mercury concentrations that are equivalent to roughly 2% of the mercury burdens in the maternal carcass (Hammerschmidt et al., 1999). This being said, if we consider a realistic concentration of 1-2ppm in yellow perch carcasses; one would expect concentrations of 0.02-0.04ppm in the eggs, which is one order of magnitude below our observed THg concentrations in the lowest MeHg dose of our assay (0.2ppm). In this context, the value of our study lies in the fact that it is the first to expose yellow perch eggs to MeHg in laboratory controlled conditions and measure Hg burdens in tissues of larvae as a function of MeHg exposure concentrations, thus establishing precedence for further studies to be carried out. This is not to discredit the observed behavioral effects in yellow perch; this study elucidated effects even at the lowest MeHg doses tested, therefore it is likely that effects would still be observed if the exposure concentrations are lowered.

Figures

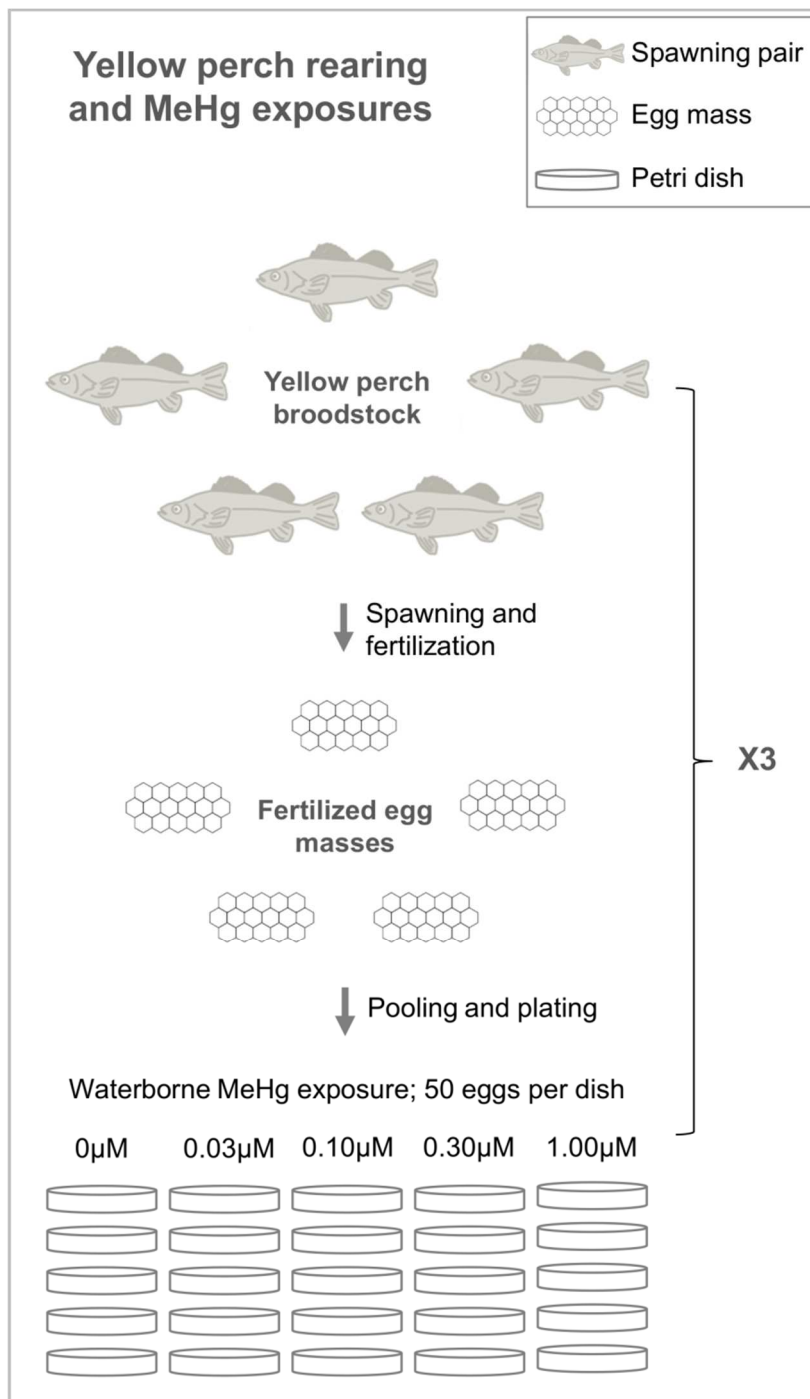


Figure 4.1: Yellow perch MeHg exposure assay

Figure 4.1: Yellow perch MeHg exposure assay

Five yellow perch spawning pairs were spawned; this rendered five egg masses which were then cut into ribbons, each ribbon containing roughly 10 eggs. The ribbons were then pooled and plated into Petri dishes, each dish containing 50 eggs (10 from each egg mass). Once inside of the Petri dishes, the eggs were exposed to five concentrations of waterborne MeHg (0, 0.03, 0.1, 0.3 and 1 μ M). This whole procedure was carried out in triplicate.

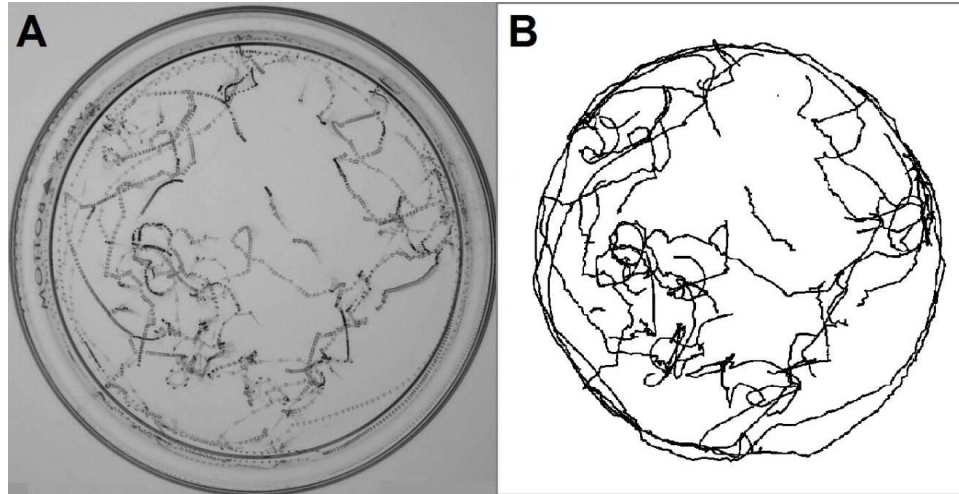


Figure 4.2: Individual trajectory traces from a group of free swimming 25 dpf yellow perch larvae

Figure 4.2: Individual trajectory traces from a group of free swimming 25 dpf yellow perch larvae

(A) Composite image of 30 seconds of yellow perch locomotion rendered with the ImageJ Z project, (B) individual traces from yellow perch embryos obtained with manual tracking. Notice the accuracy of the manual tracking as compared to the composite image.

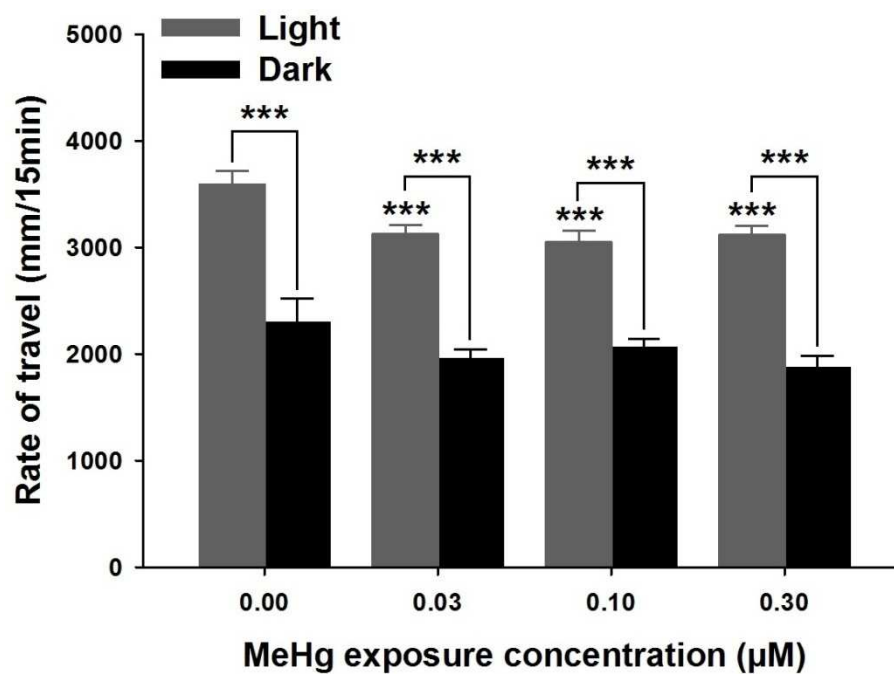


Figure 4.3: Comparison of locomotor activity in 17 dpf yellow perch exposed to MeHg and tested in two different lighting conditions

Figure 4.3: Comparison of locomotor activity in 17 dpf yellow perch exposed to MeHg and tested in two different lighting conditions

Yellow perch of all exposure groups tested in the light exhibited a strong increase in locomotor activity compared to the groups tested in the dark (n=92 fish, $P < 0.001$). All MeHg exposed larvae exhibited lower locomotor activity relative to control in the light (n=92 fish, $P < 0.001$), however no statistical differences were tested between exposure groups recorded in the dark.

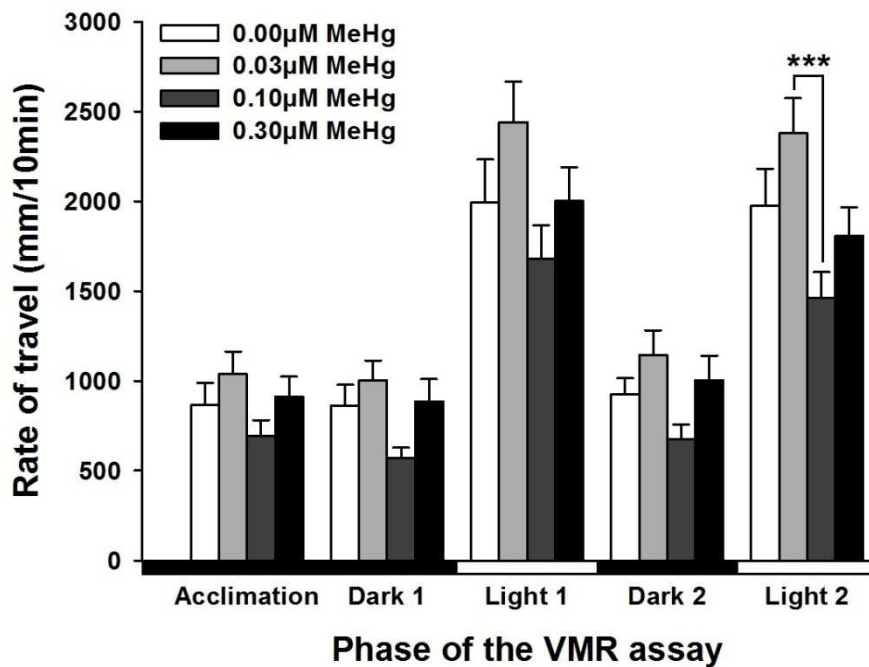


Figure 4.4: Locomotor output of 21 dpf yellow perch throughout the VMR assay

Figure 4.4: Locomotor output of 21 dpf yellow perch throughout the VMR assay

Throughout the experiment, a slight non-significant increase in locomotor activity was observed in the 0.03 μ M MeHg exposure group relative to the controls, but it was not significant. Similarly, there was also a non-significant decrease in locomotor activity in the 0.10 μ M MeHg exposed larvae. During the last light period of the VMR assay the 0.03 μ M MeHg larvae swam statistically more than the 0.10 μ M MeHg group.

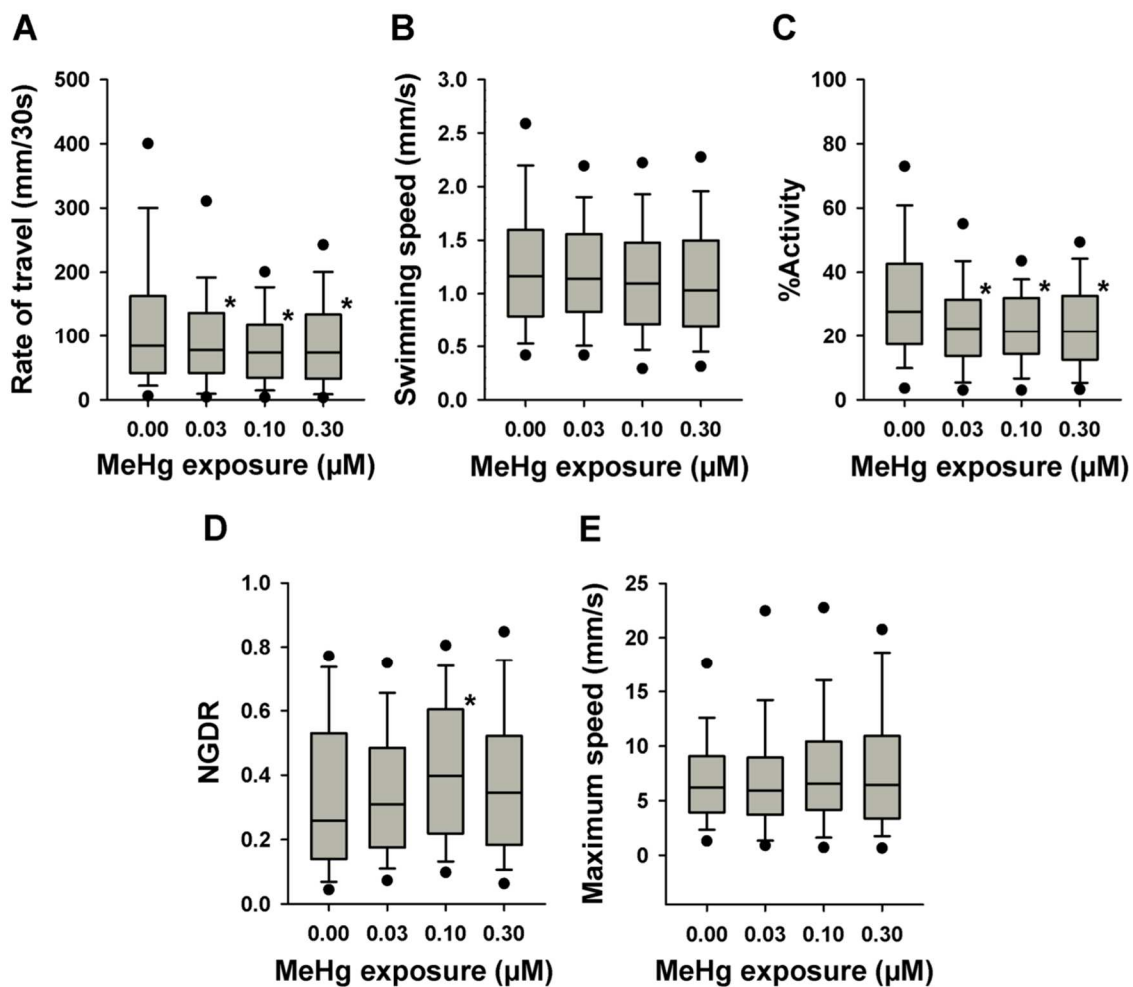


Figure 4.5: Locomotor output of 25 dpf yellow perch prior to prey capture assay

Figure 4.5: Locomotor output of 25 dpf yellow perch prior to prey capture assay

Multiple groups of 25 dpf yellow perch were recorded and their swimming activity was analyzed with a machine vision algorithm. The behavior of MeHg exposed 25 dpf yellow perch was characterized by decreases in overall locomotor output reflected by lower rates of travel (A). Swimming speed (B) was not significantly affected; however % activity (C) mirrored the rate of travel results. Exposed fish also had more linear swimming trajectories exhibited by increases in NGDR in 0.1 μ M MeHg exposed fish (D). Maximum speed (E) was not significantly affected.

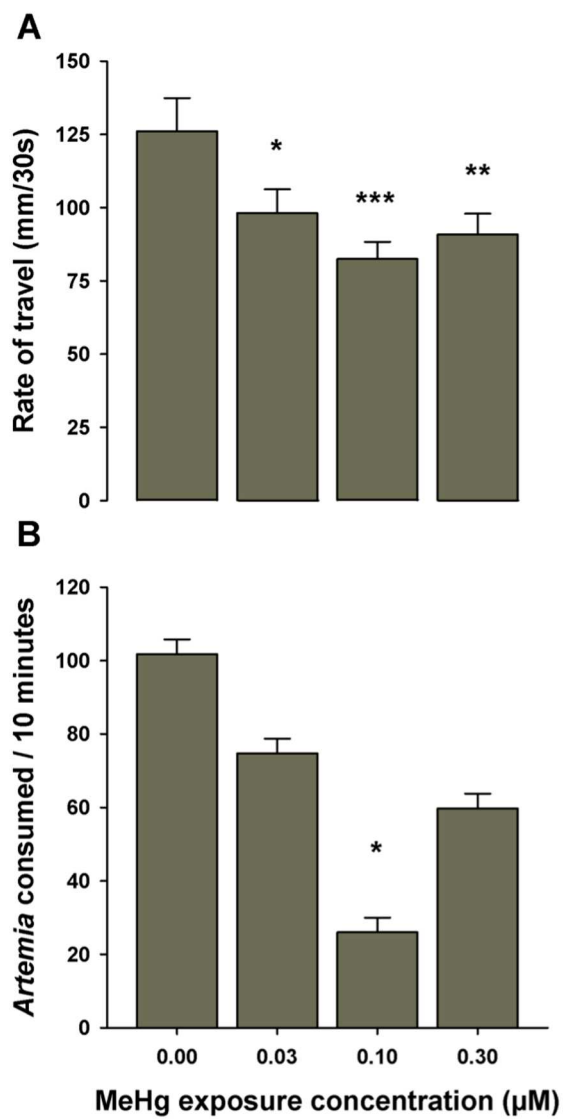


Figure 4.6: Locomotor activity and prey capture efficiency of 25 dpf yellow perch

Figure 4.6: Locomotor activity and prey capture efficiency of 25 dpf yellow perch

(A) Yellow perch larvae exposed to all MeHg exhibited decreased locomotor activity (n=120 fish, $P<0.05$); the lowest locomotor activity was observed in the 0.10 μ M MeHg exposure group. (B) Similarly, the average prey capture was decreased in all exposure groups but only significantly in the 0.10 μ M MeHg exposure group (n=4 dishes, $P<0.05$).

Tables

Table 4.1: THg concentrations and post-hatch mortality of 14 dpf yellow perch embryos

MeHg exposure concentration (μM)	THg in whole embryo tissue (ppm)	Post-hatch survival
0.00	0.02 ± 0.01^a	57.33 ± 3.48^a
0.03	0.21 ± 0.11^b	53.27 ± 1.94^a
0.10	0.95 ± 0.12^c	50.53 ± 2.94^a
0.30	3.14 ± 0.67^d	50.00 ± 3.32^a
1.00	14.93 ± 2.68^e	25.33 ± 3.36^b
ANOVA		
F	55.717	16.996
P	<0.001	<0.001

Note: Values are given as the mean \pm SE

CHAPTER 5: GENE EXPRESSION ALTERATION ASSOCIATED WITH EARLY EMBRYONIC MeHg EXPOSURE IN YELLOW PERCH (*Perca flavescens*) AND ZEBRAFISH (*Danio rerio*) LARVAE

Abstract

Methylmercury (MeHg) is an environmental neurotoxicant known to cause adverse effects in fish such as locomotor abnormalities, visual deficits or teratogenesis. Although there have been studies assessing the effects of MeHg in the gene expression of various fish species, little known about the molecular and physiological responses to MeHg in the yellow perch (*Perca flavescens*), a species of ecological and economical relevance to the North American Great Lakes that has faced population declines over the last 25 years.

The objective of this study was to carry out comparative gene expression analysis in yellow perch and zebrafish embryos to identify common biomarkers of MeHg exposure between the two species. In order to do this, we recreated environmentally realistic MeHg exposure assays in developing yellow perch and zebrafish embryos and then we quantified changes in gene expression. The power of the zebrafish model enabled us carry out high-throughput toxicogenomics to simultaneously identify multiple putative biomarkers of MeHg exposure that were later individually quantified in yellow perch by means of quantitative polymerase chain reaction (qPCR).

The high throughput analysis of gene expression in zebrafish revealed significant effects in pathways associated with neurodevelopment and behavior, such as circadian rhythm, response to light stimuli, photoperiodism, visual phototransduction, p53 signaling pathway, glutamate receptor activity, axon

guidance, brain development, transmission of nerve impulse, glutamate receptor activity, ataxia, autism and seizures.

Few MeHg exposure biomarker genes for yellow perch were evaluated here; however, two genes were significantly down regulated in both species, one involved in circadian rhythm (*per3*), the other in astrocytic glutamate uptake (*slc1a2a*). The parallelism of these results in two evolutionarily divergent species of fish suggests a robust effect of MeHg in the aforementioned pathways.

Introduction

Mercury is a neurotoxic heavy metal; it is incorporated into aquatic environments mainly by means of atmospheric deposition (Risch et al., 2012a) after which anaerobic bacteria metabolize mercury into methylmercury (MeHg; Bloom, 1992). This MeHg can undergo trophic transfer and it is progressively concentrated by each level of the food chain through the processes of bioaccumulation and biomagnification (Mason et al., 1995). Because of this, organisms that are high in the food chain (e.g. piscivorous fish, mammals and humans) are more susceptible to accumulate critical MeHg concentrations that can cause harmful effects such as locomotor abnormalities (Alvarez et al., 2006a), visual deficits (Weber et al., 2008) or teratogenesis (Samson and Shenker, 2000). The pervasiveness and persistence of this contaminant has resulted in being cataloged as one of the major contaminants causing consumption advisories in most of the freshwater systems in North America (Bhavsar et al., 2010), including the North American Great Lakes (Sandheinrich et al., 2011).

Although there is a precedence of studies that have assessed the effects of MeHg in the gene expression of zebrafish (Gonzalez et al., 2005; Ho et al., 2013), fathead minnow (Klaper et al., 2008); and rainbow trout (Liu et al., 2013), there is little known about the molecular responses to MeHg in the yellow perch (Pierron et al., 2009), a species of ecological and economical relevance to the North American Great Lakes that has faced population declines over the last 25 years (Marsden and Robillard, 2004).

Very few studies have addressed the issue of MeHg accumulation and adverse effects in yellow perch. However, there is a known linear relationship between maternal MeHg burdens and MeHg concentrations in the eggs of yellow perch (Hammerschmidt et al., 1999). Although small, this maternal MeHg transfer can adversely affect the offspring, due to the inherent sensitivity of developing embryos to environmental insults (Samson and Shenker, 2000).

The objective of this study was to carry out comparative gene expression analysis in yellow perch and zebrafish embryos to identify common biomarkers of MeHg exposure. The zebrafish was chosen as a surrogate model for yellow perch due to its ease of rearing, fully sequenced genome, and its status as an NIH supported model organism (Kalueff et al., 2014). The power of the zebrafish model enables us carry out high-throughput toxicogenomics to simultaneously identify multiple biomarkers of MeHg exposure that can later be individually quantified in yellow perch by means of quantitative polymerase chain reaction (qPCR).

Here, we mimicked environmental MeHg exposure to developing fish embryos in the laboratory. Yellow perch embryos were exposed to aqueous solutions of MeHg at roughly the 128-cell stage (~12 hpf), mimicking the early MeHg transfer from the maternal ovary to the eggs; zebrafish, on the other hand, were exposed to a full life-cycle MeHg dietary regime and then spawned, so as to quantify gene expression in their offspring.

The aforementioned approach does not only ensure environmentally realistic exposure regimes, but also ensures comparable exposure regimes and developmental stages while working with two very different fish species.

Materials and methods

Experimental organisms and tissue collection

All zebrafish and yellow perch were reared and experiments performed in the School of Freshwater Sciences in compliance with the Institutional Animal Care and Use Committee (IACUC) of the University of Wisconsin – Milwaukee. Embryos from each of the fish species were collected at the onset of spontaneous locomotor activity (5 dpf in zebrafish, 17 dpf in yellow perch). Since the husbandry and handling of the two fish species were performed as two independent experiments, the procedures for each will be discussed separately below.

Zebrafish: 5 dpf embryos were collected from four populations of parents that were subjected to a whole life-cycle exposure to dietary MeHg at nominal concentrations of 0, 1, 3 or 10ppm (see materials and methods section in chapter 3). For each of these MeHg-exposed parental populations, 5 embryos were pooled into 1.7-ml microcentrifuge tubes (MidSci, St. Louis, MO), each containing 200µl of RNA later (Qiagen, Hilden, Germany), flash frozen in liquid nitrogen and stored at -80°C until samples were needed. This was performed in triplicate for each of the MeHg doses tested.

Yellow perch: newly spawned eggs (128-cell stage; ~12 hpf) were reared for 24 hours in solutions prepared at nominal concentrations of 0, 0.03, 0.1 and 0.3µM of MeHg (all solutions prepared with E2 embryo medium; 0.033% ethanol as vehicle), after which the embryos were rinsed three times with E2 embryo

medium (see materials and methods section in chapter 4). Once the embryos reached 17 dpf, 8 embryos from each exposure group were individually transferred into 0.2ml PCR strip tubes, each containing 100µl of RNA later, flash frozen in liquid nitrogen and stored at -80°C , as described above. This procedure was performed in triplicate.

RNA Isolation and quality assurance

RNA was isolated from zebrafish embryo pools and from individual yellow perch whole-embryo tissue using the Direct-zol™ RNA MiniPrep kit (Zymo Research, Irving, CA), according to manufacturer's instructions. Tissues were homogenized on ice in 200µl of Direct-zol™ reagent (Zymo Research) in 1.7-ml microcentrifuge tubes, using a sterile micropestle (MidSci) and running the homogenate through a 27-gauge needle (BD Biosciences, Franklin Lakes, NJ). RNA quantity and quality were assessed using a NanoDrop ND1000 spectrophotometer (Thermo Fisher Scientific, Wilmington, DE), and a 2100 Agilent Bioanalyzer (Agilent Technologies, Santa Clara, CA) (Appendices 12 and 13).

Illumina TruSeq RNA Library Preparation and Sequencing of zebrafish RNA

Construction and sequencing of RNA libraries was completed by the University of Wisconsin-Madison Biotechnology Center; all zebrafish RNA samples submitted yielded an average of $2.04 \pm 0.19\mu\text{g}$ (average \pm standard error) of total RNA per pool of 5 embryos, with a RIN value of 9.19 ± 0.24 . Each RNA library was generated using a paired-end approach following the Illumina

“TruSeq RNA Sample Preparation Guide” and the Illumina TruSeq RNA Sample Preparation Kit (Illumina Inc., San Diego, CA).. Quality and quantity of finished libraries were assessed using an Agilent DNA1000 series chip assay and Invitrogen Qubit HS Kit (Invitrogen, Carlsbad, CA), respectively. Each library was standardized to 2 μ M. Cluster generation was performed using a TruSeq Single Read Cluster Kit (v3) and the Illumina cBot, with libraries multiplexed for paired end 100bp sequencing using the TruSeq 100bp SBS kit (v3) and HCS1.6 software, on an Illumina HiSeq2000.

RNA-Seq data analysis

All bioinformatics procedures and analyses were performed by the University of Wisconsin-Milwaukee Laboratory for Public Health Informatics and Genomics (LPHIG). Adapters and low quality bases were removed from the initial 2x101bp Illumina TruSeq and trimmed using Cutadapt (Martin, 2011). Illumina TruSeq Adapters were removed as prescribed by the Cutadapt manual, using an error rate of 10% and a minimum overlap between the read and the adapter of five nucleotide bases. To alleviate sequencing-related GC biases at the 5' end of each read, the first seven bases were removed from all forward and reverse strand reads. FastQC (Andrews, 2010) was used to ensure that cleaned reads were of higher quality than initial raw reads supplied by the sequencer; per-base GC% and over-represented sequence statistics also confirmed adapter contamination was minimized.

The cleaned reads for each sample were independently aligned to the reference zebrafish genome (Zv9, UCSC) using TopHat (v. 2.0.11) (Kim et al., 2013; Trapnell et al., 2009). The alignment output from TopHat was converted into a transcriptome using Cufflinks (v. 2.2.1), with the Zv9 Gene Transfer Format (GTF) as a guide; a mate-pair-distance of 0 and a maximum of 2 mismatches bases per alignment was used. Alignment data was confirmed using RNAseQC (DeLuca et al., 2012) against the Zv9 reference transcriptome. Using these alignments, an embryo-specific transcriptome was assembled using Cufflinks (Trapnell et al., 2012), with the Zv9 transcriptome as a reference to correct fragment biases by better identifying the start/end point of each exon (Roberts et al., 2011). The transcriptome from each sample was then merged together into a single embryo transcriptome using Cuffmerge. Differential expression was conducted with Cuffdiff using pooled dispersion, geometric normalization, and the merged embryo transcriptome; TopHat alignments were grouped using MeHg exposure levels. A summary of the steps employed to analyze the RNA-seq data are reviewed in Figure 5.1.

Gene ontology (GO) and KEGG enrichment analysis was performed using WEB-based GEne SeT AnaLysis Toolkit (WebGESTALT; (Zhang et al., 2005). In order to visualize differentially expressed genes, a heat map was generated using GenePattern (Reich et al., 2006), with hierarchical clustering of genes based on Pearson Correlations.

Gene Set Enrichment Analysis (GSEA) (Subramanian et al., 2005) was then performed to identify enrichment in gene sets specifically associated with

neuronal development, cognitive function, behavior and abnormal neurological phenotypes as described by Thomas and collaborators (2012). All dysregulated genes for each MeHg treatment were arranged into individual RNK files in descending order, according to their $\log_2(\text{fold change})$ as indicated by the official GSEA web page (www.broadinstitute.org). These RNK files were run against two custom gene set collections containing gene sets associated with neurological processes and phenotypes. The first collection was based the version 5.0 of the “c2: curated gene sets” and the “c5: gene ontology (GO) gene sets”, available for download in the GSEA official web page; the second collection was based on gene sets downloaded from the Human Phenotype Ontology web page (www.human-phenotype-ontology.org). Gene set enrichment analysis was performed with the GSEAPreranked algorithm included in the GenePattern suite.

Selection of biomarkers of MeHg exposure for yellow perch

Biomarkers of MeHg exposure for yellow perch were selected from the information gathered by differential gene expression analysis in zebrafish. A list of potential MeHg biomarkers of exposure was populated by selecting genes that gathered the following criteria: 1) the gene must have been differentially expressed ($q \text{ value} \leq 0.05$), preferably in at least two of the three MeHg exposure concentrations tested in zebrafish (1, 3 and 10ppm MeHg), 2) the differentially expressed genes must have a known involvement in biological pathways that is congruent with MeHg neurotoxicity (e.g. neurological processes and phenotypes), 3) the genes selected must preferably have an ortholog in yellow perch that has been sequenced and published, if not, the gene must have a

sufficient wealth of published ortholog sequences in other teleost fishes to allow for primer design from mRNA or protein alignment of conserved regions of the gene. Based on these criteria, the following genes were selected as potential biomarkers of MeHg exposure in our paradigm: *cry1a*, *per3*, *slc1a2a*, *prkacbb*, and *opn1lw*.

cry1a and *per3* are both involved in circadian rhythm, *cry1a* is also involved in the oxidative stress response (KEGG) and DNA repair; *slc1a2a* is associated with astrocytic glutamate uptake; *prkacbb* is required in the calcium and insulin signaling pathway and in the hedgehog signaling pathway (KEGG); *opn1lw* is associated with visual phototransduction. Additionally, three genes were selected as internal reference genes for quantitative reverse transcription PCR (RT-qPCR): *elongation factor 1a (ef1a)*, *elongation factor 2 (ef2)*, and *ribosomal protein L13a (l31a)*. These reference genes have been utilized successfully in RT-qPCR assays in yellow perch (Pierce et al., 2013), furthermore they were confirmed to not be significantly affected by MeHg exposure in our zebrafish assay.

RT-qPCR primer design for yellow perch

All primers described hereafter were synthesized by Integrated DNA Technologies, Inc., (IDT; Coralville, IA) and purified by standard desalting.

Primers for *cry1a* were designed from a yellow perch mRNA sequence retrieved from the NCBI database (accession number: HQ206616.1) using the

NCBI web-based PrimerBlast software (Integrated DNA Technologies Inc., Coralville, IA, USA).

Primers for *prkacbb* were designed from sequence alignments of mRNA from Atlantic salmon (*Salmo salar*; BT059675.1), rainbow trout (*Oncorhynchus mykiss*; NM_001124589.1) and zebrafish (NM_001034976.1); mRNA sequences were aligned with the CLC Sequence Viewer v7 software (Qiagen, Hilden, Germany), then the alignment file was then used as input for the PriFi primer design tool (Fredslund et al., 2005).

For *per3*, *slc1a2a* and *opn1lw*, degenerate primers were first designed by creating protein alignments from common carp (*Cyprinus carpio*), goldfish (*Carassius auratus*), guppy (*Poecilia reticulata*), medaka, (*Oryzias latipes*), Mexican tetra (*Astyanax mexicanus*), Senegalese sole (*Solea senegalensis*), three-spined stickleback (*Gasterosteus aculeatus*), torafugu (*Takifugu rubripes*) and zebrafish (Appendix 15). Conserved amino acid “blocks” in the protein alignment were identified with the Bookmaker software (www.blocks.fhcrc.org) and then utilized for degenerate primer design using the “COnsensus-DEgenerate Hybrid Oligonucleotide Primers” (CODEHOP) program (Rose et al., 2003). Standard PCR was then carried out with the degenerate primers (Appendix 16) along with control larval yellow perch cDNA, the amplicons were then sequenced at the Great Lakes Genomics Center (University of Wisconsin – Milwaukee) following standard Sanger sequencing in a 3730 Analyzer (Thermo Fisher Scientific, Waltham, MA). These amplicon sequences were then “blasted” with the NCBI nucleotide-BLAST algorithm to verify their identity. Upon

confirming that the sequences of the PCR amplicons were congruent with the sequences of the expected genes, nested RT-qPCR primers were designed from the newly obtained yellow perch sequences utilizing PrimerBlast.

Primer optimization for RT-qPCR

For each primer pair, a PCR reaction was performed at eight different annealing temperatures (53.0°C, 53.5°C, 54.3°C, 55.7°C, 57.3°C, 58.6°C, 59.5°C and 60°C), and products were run on a 1.5% agarose gel in order to confirm PCR product size and visualize any potential off-target results; this also allowed for confirmation of an optimal annealing temperature across all primer pairs.

The PCR efficiency for all selected primer pairs was evaluated using a standard dilution series. RNA extracted from 5 control samples (5 unexposed yellow perch larvae; 17 dpf) was pooled. Then, 1µg of RNA was converted to cDNA using the RTTM Master Mix (Lambda Biotech, St. Louis, MO, USA) per the manufacturer's protocol, to create a standard dilution series ranging from 0.12 to 30ng/µl. Thereafter, two-step RT-qPCR was completed using EvaGreen® qPCR Master Mix (MidSci, St. Louis, MO, USA), according to the manufacturer's instructions (8ng cDNA per reaction; 12µl reaction volumes) and a StepOne Plus real-time qPCR instrument (95°C [10 minutes]; 95°C [30 seconds], 57.3°C [40 seconds], 72°C [40 seconds] for 40 cycles; 95°C [15 seconds], 60°C [60 seconds], and 95°C [15 seconds]). An efficiency of 90-110% was considered satisfactory. All RT-qPCR reactions were carried out in triplicate. Melting-curve analysis was employed to confirm the amplification of a single product.

Yellow perch RT-qPCR

Each yellow perch whole-embryo tissue sample rendered $1.78 \pm 0.05\mu\text{g}$ of total RNA, with a RIN value of 9.0 ± 0.06 (Appendix 12). RNA samples (250-500ng) were treated with RQ1 RNase-Free DNase (Promega Corporation, Madison, WI) to eliminate possible contaminating DNA prior to downstream applications, and then converted to cDNA using the RTTM Master Mix.

Relative quantification of gene expression was measured in 8 yellow perch larvae per MeHg exposure group, with each sample run in triplicate and each plate containing all three normalizer genes (*elongation factor 1a* [*ef1a*], *elongation factor 2* [*ef2*], and *ribosomal protein L13a* [*l31a*]).

RT-qPCR was performed using the StepOne Plus real-time qPCR instrument (Life Technologies Corp., Carlsbad, CA; cycle conditions: 95°C [10 minutes]; 95°C [30 seconds], 57.3°C [40 seconds], 72°C [40 seconds] for 40 cycles; 95°C [15 seconds], 60°C [60 seconds], and 95°C [15 seconds]), using EvaGreen qPCR Master Mix and gene-specific primers (8ng RNA per reaction; 12 μl reaction volumes).

RT-qPCR data was analyzed using the qBase algorithm via StepOnePlusTM software (version 2.3). Each resultant normalized relative quantity (NRQ) was then calibrated to the individual sample with the lowest normalized quantity mean (*i.e.*, lowest level of target gene expression; NRQ =1) for each target gene. RT-qPCR fold changes were calculated as the ratio of average NRQ values among treatment and control groups [2]. Calibrated NRQ

values were analyzed via individual one-way analysis of variance (ANOVA) tests to evaluate the differences in target gene expression in treated *versus* control groups. Tukey's multiple-comparison tests were used if statistical significance was observed. All statistical analyses were conducted using SigmaPlot 11 (Systat Software, Inc., Chicago, IL, USA) with $P < 0.05$ considered to be statistically significant.

Results

Zebrafish whole-embryo RNA-Seq

Transcriptomic analysis by RNA-seq in the offspring of zebrafish exposed to dietary MeHg throughout their whole-life revealed a total of 345 unique genes that were significantly dysregulated in treated zebrafish embryos ($q \leq 0.05$), out of which, 65 genes were dysregulated in the 1ppm exposure group, 227 genes in the 3ppm exposure group, and 208 genes in the 10ppm exposure group (Figure 5.2, Appendices 4-9).

Among the top 15 significantly enriched ($p \leq 0.05$) gene ontology (GO) terms for biological processes (Table 5.1), several were associated with pathways that affect behavior and interaction with the environment such as response to abiotic stimulus, response to radiation, photoperiodism, circadian rhythm and rhythmic process; additionally, there was significant enrichment in pathways associated with response to oxidative stress ($p = 0.007$) and response to stress ($p = 0.0416$) (Appendix 10). KEGG enrichment analysis confirmed significant effects ($p \leq 0.05$) in pathways associated with circadian rhythm, as well as with ABC transporters, p53 signaling pathway and cell cycle (Table 5.2). Phenotype enrichment analysis elucidated significant effects in pathways involved in visual and behavioral phenotypes, such as photophobia, night blindness, and intermittent cerebellar ataxia ($p \leq 0.05$) (Table 5.3).

Further analysis performed with GSEA confirmed significant enrichment in pathways relevant to neurodevelopment and behavior, such as axon guidance,

brain development, transmission of nerve impulse, glutamate receptor activity, ataxia, autism and seizures (Tables 5.4 – 5.7, Appendix 11).

Yellow Perch RT-qPCR

RT-qPCR was used to compare effects of MeHg exposure on transcript abundance in yellow perch embryos. Target genes were selected as putative biomarkers of MeHg exposure, based on information gathered from RNA-seq performed in MeHg exposed zebrafish embryos. Five genes were analyzed (*cry1a*, *per3*, *slc1a2a*, *prkacbb* and *opn1lw*), targeting key pathways observed to have been dysregulated in the zebrafish, namely circadian rhythm, oxidative stress, astrocytic glutamate uptake and visual phototransduction (Appendix 14). Out of these target genes, *per3* and *slc1a2a* were significantly dysregulated ($p = 0.003$ and $p = 0.002$, respectively). Moreover, *cry1a* and *prkacbb* had a noteworthy yet not-significant ($p = 0.058$ and $p = 0.051$) reduction in relative expression, which was especially noticeable in the 0.1 μ M MeHg exposure group; the expression of *opn1lw* remained unaltered across all MeHg exposure concentrations ($P=0.63$) (Figure 5.3).

Discussion

Following whole-life-cycle MeHg dietary exposure of a parental generation of zebrafish, their offspring exhibited significant alteration in genes associated with pathways that mediate neuronal development and behavior. Interestingly, some of the most affected pathways were those involved with circadian rhythm and rhythmic processes. The disruption of pathways that regulate circadian rhythm would certainly explain the alteration in behavior that has been previously reported in MeHg-exposed zebrafish embryos (see chapter 3), however, only a few seminal studies have linked prenatal MeHg exposure with circadian rhythm alteration in rodents (Arito et al., 1984), therefore more studies are imperative to clarify the role of MeHg in the modulation of behavior *via* circadian rhythm alteration.

Another putative link between MeHg toxicity and circadian rhythm is the recently reported role of certain circadian rhythm genes in the molecular responses to oxidative stress and DNA damage response (Uchida et al., 2010), the latter being pathways that are commonly affected by MeHg exposure (Gonzalez et al., 2005). Among the genes that were observed to be dysregulated in our study, *cry1a* is reported to have a role in both circadian rhythm and response to oxidative stress and DNA repair. Moreover the knockout of this gene was reported to result in accelerated periodicity of locomotor activity in zebrafish embryos (Uchida et al., 2010). This phenotype is consistent with the one observed in the siblings of the embryos that we analyzed here for gene expression alteration (See chapter 3).

The main environmental stimulus that modulates circadian rhythm is light (Cahill, 1996); not surprisingly, a large number of pathways significantly affected by MeHg were involved in visual phototransduction and response to light stimuli. These findings are consistent with a wealth of literature that has associated MeHg with visual impairment (Burbacher et al., 2005; Ho et al., 2013; Weber et al., 2008), by affecting the visual cortex and various regions of the retina (Goto et al., 2001). More specifically, methylmercury has been found to affect photoreceptors in the retina of zebrafish embryos, especially in the ones located in the inner and outer nuclear layers (Korbass et al., 2010; Korbass et al., 2013). These results mirror the observations of Weber (2008), where zebrafish exposed to MeHg as embryos (≤ 4 hpf) developed adult onset of visual deficits; these findings have since been confirmed by Kalluvila and collaborators. (University of Wisconsin – Milwaukee; unpublished data).

MeHg is known to accumulate preferentially in astrocytes and inhibit glutamate uptake, leading to MeHg-induced excitotoxicity⁵ (Aschner et al., 2000). Our zebrafish RNA-seq results revealed that genes associated with the glutamate receptor activity pathway were significantly affected by MeHg, in particular, the expression levels of the solute carrier family 1 (*slc1a2a*; glial high affinity glutamate transporter) exhibited a MeHg dose-dependent decrease that reached a 3.2 fold down-regulation in the highest MeHg exposure group

⁵ Excitotoxicity refers to the process by which neurotransmitters such as glutamate cause excessive stimulation of nerve cells, leading to damage or death of the cell

(10ppm). These findings suggest that MeHg-induced neurotoxicity may partly be occurring through the aforementioned mechanism of excitotoxicity.

Other pathways found to be affected by MeHg exposure in our assay included the p53 signaling pathway and cell cycle (Table 5.2). MeHg has been previously implicated in p53-mediated cell cycle arrest leading to cell proliferation disruption (Gribble et al., 2005). Disruption of neuronal migration, a process intimately linked to cell proliferation, has also been reported to be affected by MeHg exposure (Burke et al., 2006; Kakita et al., 2000). Congruent with these observations, our analysis elucidated effects on axon guidance, axonogenesis and neuron projection.

Prospective biomarkers of MeHg exposure were selected from our zebrafish assay to be evaluated in yellow perch by means of RT-qPCR analysis (Table 5.8). This approach has been previously reported by Liu and collaborators (2013) who carried out parallel gene expression analysis in zebrafish and rainbow trout. Here we evaluated zebrafish and yellow perch, two species that last shared a common ancestor approximately 231.5 million years ago (www.timetree.org) (Hedges et al., 2006). In contrast with the approach of Liu and collaborators, the present study ensured that gene expression quantification of the two species of fish was carried out at comparable developmental stages to reduce biological variability; to achieve this, the onset of locomotor activity in both species was utilized as a common milestone at which to analyze gene expression (5 dpf in zebrafish 17 dpf in yellow perch).

Out of the five target genes that were selected as biomarkers of MeHg exposure for yellow perch, *per3* and *slc1a2a* were significantly down regulated; these genes associated with circadian rhythm and astrocytic glutamate uptake were similarly down regulated in the zebrafish. This parallelism between the results observed in two evolutionarily divergent species of fish suggests a robust role of the aforementioned pathways in MeHg-induced neurotoxicity.

Although *cry1a* – another circadian rhythm gene – was not significantly dysregulated, it did exhibit a notable reduction ($p = 0.058$) in expression, especially in yellow perch embryos exposed to $0.1\mu\text{M}$ MeHg. A similar observation was made with *prkacbb* ($p = 0.051$), a gene involved in the calcium and insulin signaling pathways, as well as the hedgehog signaling pathway. Out of the genes that exhibited no significant dysregulation, only the visual phototransduction opsin 1 gene (*opn1lw*) exhibited a “flat line” trend across all MeHg exposures, contrasting strongly with our observations in zebrafish and other similar studies gene expression quantification studies in zebrafish (Ho, et al, 2013).

Few MeHg exposure biomarker genes for yellow perch were evaluated here due to the difficulties of carrying out gene expression quantification in non-model organisms. However, our results do suggest common MeHg-induced molecular alterations in zebrafish and yellow perch, affecting genes associated with circadian rhythm and glutamate uptake pathways.

Figures

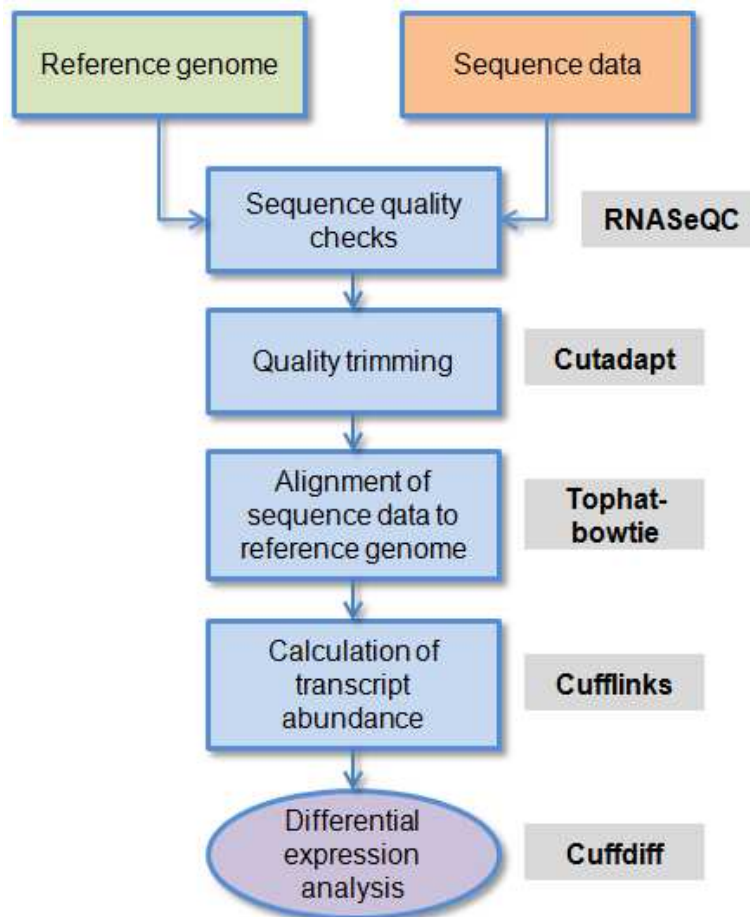


Figure 5.1: Schematic representation of the software packages used to create an RNA-seq analysis pipeline

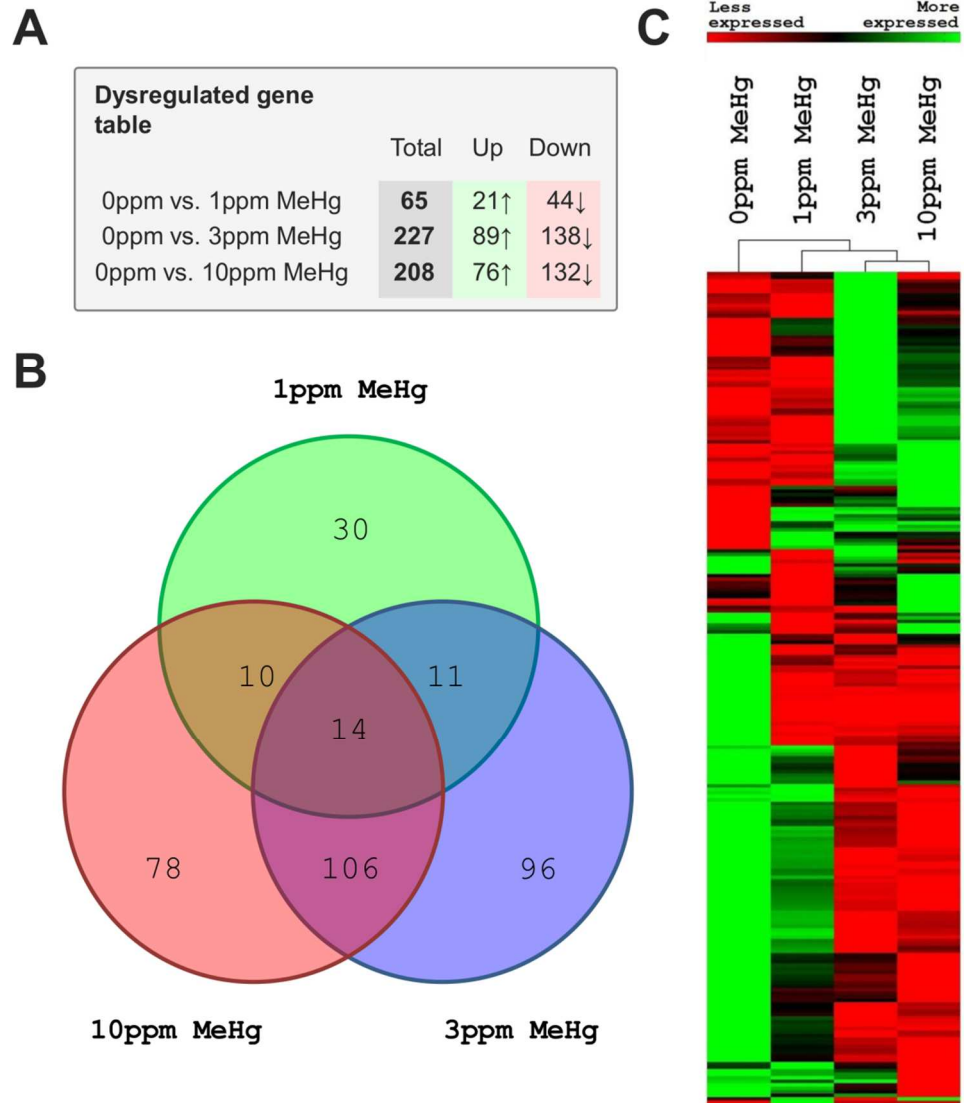


Figure 5.2: Transcriptomic analysis of dysregulated genes in MeHg-exposed 5 dpf zebrafish embryos

Figure 5.2: Transcriptomic analysis of dysregulated genes in MeHg-exposed 5 dpf zebrafish embryos

Zebrafish embryo transcriptomic analysis by RNA-seq; each exposure group was comprised of three samples of RNA from five pooled individual 5 dpf embryos. (A) The number of genes significantly dysregulated as a function of MeHg exposure (FDR < 0.05). (B) Overlap of significantly dysregulated genes among treatment groups is shown in the Venn diagram. (C) Hierarchical clustering analysis of Fragments Per Kilobase of exon per Million (FPKM) fragments. Green indicates the exposure group with the lowest FPKM value, and red signifies the exposure group with the highest FPKM value for each given gene.

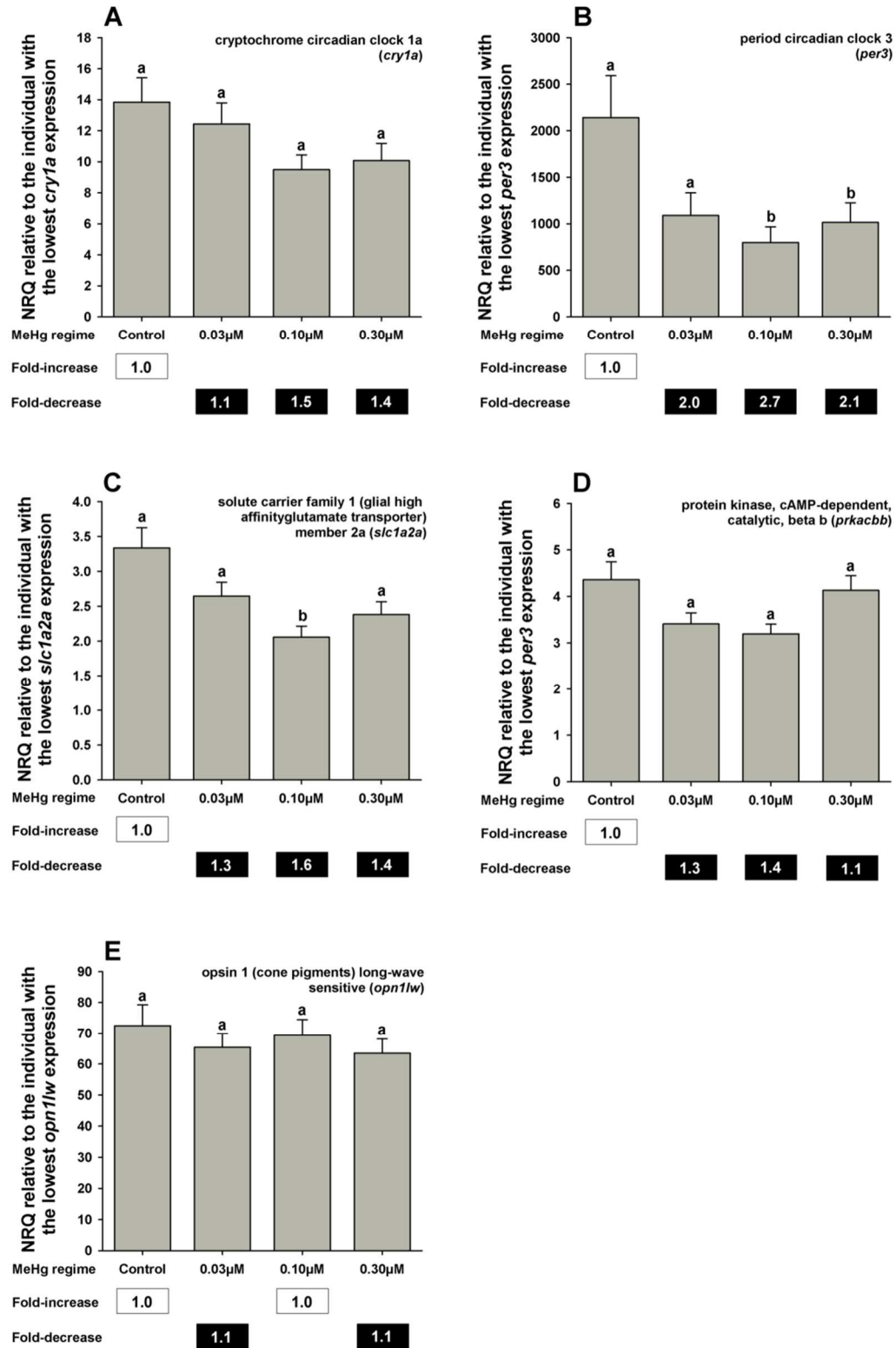


Figure 5.3: Expression analysis of selected genes in yellow perch

Figure 5.3: Expression analysis of selected genes in yellow perch

RT-qPCR was used to compare effects of MeHg exposure on transcript abundance in yellow perch embryos. Five genes were analyzed (*cry1a*, *per3*, *slc1a2a*, *prkacbb* and *opn1lw*), targeting key pathways observed to have been dysregulated in the zebrafish, namely circadian rhythm, oxidative stress, astrocytic glutamate uptake and visual phototransduction. Out of these target genes, *per3* and *slc1a2a* were significantly dysregulated ($p = 0.003$ and $p = 0.002$, respectively). Moreover, *cry1a* and *prkacbb* had a noteworthy yet not-significant ($p = 0.058$ and $p = 0.051$) reduction in relative expression, which was especially noticeable in the $0.1\mu\text{M}$ MeHg exposure group; the expression of *opn1lw* remained unaltered across all MeHg exposure concentrations ($P=0.63$)

Tables

Table 5.1: Gene ontology (GO) enrichment analysis of the top 20 biological functions affected by MeHg exposure in zebrafish embryos

Biological function	Source	Number of genes	Adjusted P
response to light stimulus	GO:0009416	17	5.87E-15
response to radiation	GO:0009314	18	1.44E-14
Photoperiodism	GO:0009648	9	7.09E-13
response to abiotic stimulus	GO:0009628	18	2.16E-09
circadian rhythm	GO:0007623	7	3.14E-07
rhythmic process	GO:0048511	7	1.07E-05
nucleic acid metabolic process	GO:0090304	57	7.53E-05
cellular biosynthetic process	GO:0044249	62	0.0002
cellular nitrogen compound metabolic process	GO:0034641	67	0.0002
nucleobase-containing compound metabolic process	GO:0006139	64	0.0003
biosynthetic process	GO:0009058	64	0.0003
cellular nitrogen compound biosynthetic process	GO:0044271	48	0.0004
heterocycle metabolic process	GO:0046483	65	0.0005
cellular aromatic compound metabolic process	GO:0006725	65	0.0005
organic cyclic compound metabolic process	GO:1901360	66	0.0005
nitrogen compound metabolic process	GO:0006807	68	0.0009
organic substance biosynthetic process	GO:1901576	61	0.001
organic cyclic compound biosynthetic process	GO:1901362	47	0.001
aromatic compound biosynthetic process	GO:0019438	46	0.0011
nucleobase-containing compound biosynthetic process	GO:0034654	45	0.0012

Table 5.2: KEGG enrichment analysis of genes affected by MeHg exposure in zebrafish embryos

KEGG pathway description	Source	Number of genes	Adjusted P
Circadian rhythm - mammal	4710	11	2.94E-14
ABC transporters	2010	4	0.0046
Metabolic pathways	1100	22	0.0092
p53 signaling pathway	4115	5	0.0092
DNA replication	3030	5	0.0138
Ribosome biogenesis in eukaryotes	3008	4	0.023
Cell cycle	4110	6	0.0368

Table 5.3: Phenotype enrichment analysis of dysregulated genes in MeHg exposed zebrafish

Description	Source	Number of genes	Adjusted P
Fundus atrophy	HP:0001099	2	0.0469
Night blindness	HP:0000662	9	0.0469
Intermittent cerebellar ataxia	HP:0006862	2	0.0469
Arthralgia of the hip	HP:0003365	2	0.0469
Photophobia	HP:0000613	10	0.0469
Eye poking	HP:0001483	2	0.0469

Table 5.4: Gene set enrichment analysis (GSEA) results for each MeHg exposure concentration tested in zebrafish embryos (Curated gene collection)

C2: Curated gene set collection

<i>Gene set description</i>	<i>Source</i>	<i>1ppm MeHg</i>	<i>3ppm MeHg</i>	<i>10ppm MeHg</i>
Axon guidance	KEGG		NES=1.642 P=0.033 q=0.305	NES=2.812 P=0.000 q=0.000
Axon guidance	REACTOME		NES=1.472 P=0.065 q=0.159	
Neuroactive ligand receptor interaction	KEGG		NES=-1.685 P=0.035 q=0.043	NES=1.560 P=0.035 q=0.292
Neurotransmitter receptor binding and downstream transmission in the postsynaptic cell	REACTOME		NES=-2.676 P=0.000 q=0.003	
Neurotransmitter release cycle	REACTOME	NES=-1.633 P=0.044 q=0.296	NES=-1.874 P=0.008 q=0.024	
Parkinson's disease	KEGG		NES=-3.047 P=0.000 q=0.000	NES=-2.867 P=0.000 q=0.000
Parkinson's disease	KEGG		NES=-3.047 P=0.000 q=0.000	NES=-2.867 P=0.000 q=0.000

Note: All gene sets described in tables 5.4 to 5.8 were significantly enriched. Each gene set includes the NES (Normalized Enrichment Score) p value and q value for each MeHg exposure concentration. Values in bold if $q \leq 0.25$.

Table 5.5: Gene set enrichment analysis (GSEA) results for each MeHg exposure concentration tested in zebrafish embryos (Biological process collection)

C5: GO Biological process collection

<i>Gene set description</i>	<i>Source</i>	<i>1ppm MeHg</i>	<i>3ppm MeHg</i>	<i>10ppm MeHg</i>
Axon guidance	GO:0007411		NES=-1.648 P=0.038 q=0.048	
Axonogenesis	GO:0007409		NES=-1.848 P=0.008 q=0.026	
Brain development	GO:0007420		NES=-1.323 P=0.154 q=0.186	
Central nervous system development	GO:0007417		NES=-1.295 P=0.171 q=0.198	
Generation of neurons	GO:0048699		NES=-2.138 P=0.006 q=0.007	
Nervous system development	GO:0007399		NES=-1.786 P=0.018 q=0.031	
Regulation of neurotransmitter levels	GO:0001505		NES=-1.736 P=0.026 q=0.035	
Transmission of nerve impulse	GO:0019226	NES=-2.532 P=0.000 q=0.002		

Table 5.6: Gene set enrichment analysis (GSEA) results for each MeHg exposure concentration tested in zebrafish embryos (Cellular component and molecular function collections)

C5: GO Cellular component collection

<i>Gene set description</i>	<i>Source</i>	<i>1ppm MeHg</i>	<i>3ppm MeHg</i>	<i>10ppm MeHg</i>
Neuron projection	GO:0043005		NES=-1.966 P=0.006 q=0.015	

C5: GO Molecular function collection

<i>Gene set description</i>	<i>Source</i>	<i>1ppm MeHg</i>	<i>3ppm MeHg</i>	<i>10ppm MeHg</i>
Glutamate receptor activity	GO:0008066		NES=-1.780 P=0.020 q=0.029	

Table 5.7: Gene set enrichment analysis (GSEA) results for each MeHg exposure concentration tested in zebrafish embryos (Human phenotype ontology collection)

HPO: Human phenotype ontology collection

<i>Gene set description</i>	<i>Source</i>	<i>1ppm MeHg</i>	<i>3ppm MeHg</i>	<i>10ppm MeHg</i>
Abnormal neuron morphology	HP:0012757		NES=-1.760 P=0.017 q=0.077	
Abnormality of vision	HP:0000504			NES=-1.680 P=0.029 q=0.182
Ataxia	HP:0001251		NES=-2.079 P=0.000 q=0.020	
Attention deficit hyperactivity disorder	HP:0007018	NES=1.838 P=0.011 q=0.167		
Autism	Wall, et al. (2008)		NES=-2.094 P=0.000 q=0.040	NES=1.535 P=0.065 q=0.242
Epileptic encephalopathy	HP:0200134		NES=-1.802 P=0.024 q=0.083	
Epileptiform EEG discharges	HP:0011182		NES=-1.451 P=0.097 q=0.209	
Motor neuron atrophy	HP:0007373		NES=-1.650 P=0.030 q=0.102	
Neurodevelopmental delay	HP:0012758			NES=-2.246 P=0.000 q=0.012
Peripheral axonal degeneration	HP:0000764	NES=-1.576 P=0.039 q=0.443		
Seizures	HP:0001250			NES=-2.500 P=0.000 q=0.003

Table 5.8: Dysregulated genes in zebrafish and yellow perch

Gene symbol	Organism	Gene expression alteration (Fold change)		
		Low MeHg dose	Medium MeHg dose	High MeHg dose
<i>cry1a</i>	Zebrafish	- 1.1	- 1.5	- 1.4
	Yellow perch	- 1.1	- 1.5	- 1.4
<i>per3</i>	Zebrafish	-1.2	- 4.4	- 6.4
	Yellow perch	- 2.0	- 2.7	- 2.1
<i>slc1a2a</i>	Zebrafish	- 1.4	- 2.2	- 3.2
	Yellow perch	- 1.3	- 1.6	- 1.4
<i>prkacbb</i>	Zebrafish	- 1.6	- 4.1	- 2.6
	Yellow perch	- 1.3	- 1.4	- 1.1
<i>opn1lw1</i>	Zebrafish	1.4	3.4	4.4
	Yellow perch	-1.1	1.0	-1.1

Note: Numbers in bold are significantly different to control (P<0.05)

CHAPTER 6: SUMMARY OF THE DISSERTATION

The objectives of this dissertation were to identify MeHg-induced alterations in the behavior of yellow perch and zebrafish, and to uncover common molecular biomarkers of MeHg exposure in both species. Behavioral and gene expression phenotypes in both yellow perch and zebrafish were successfully elucidated, however each chapter of this document addresses a discrete portion of a larger research question – How does MeHg affect the behavior and gene expression of yellow perch and zebrafish?

In this final chapter, significant conclusive remarks integrating the entire dissertation will be discussed.

Significance 1: Comparative behavioral effects of waterborne or whole life cycle dietary MeHg exposure in zebrafish embryos

We tested two different methods of delivering MeHg to developing zebrafish embryos. The first method was to expose newly spawned embryos (≤ 2 hpf) to an aqueous MeHg solution, mimicking maternal MeHg transfer from the ovary to the egg. The second method was a whole-life-cycle dietary exposure which was carried out in zebrafish from their embryonic stages until the onset of sexual maturity, so as to collect newly spawned embryos from parents that had been exposed to MeHg throughout their whole life.

Administration of MeHg to fish embryos via waterborne exposure is a quick, simple, and reasonably realistic approach for toxicity screening (Weber et

al., 2008). However, this study posed the question of whether a more environmentally realistic exposure route would deliver a more accurate representation of the effects of MeHg in nature. A whole-life-cycle dietary MeHg exposure assay was chosen because it integrated not only the most realistic route of MeHg exposure, – the diet – but it also the notion that organisms that inhabit contaminated ecosystems are in constant contact with the contaminants throughout their whole life.

To the author's knowledge, this study is the first to carry out a dietary MeHg exposure assay throughout the whole life cycle of zebrafish in laboratory controlled conditions. Although notable mentions of similar studies include the reported partial life cycle dietary exposures of zebrafish and rainbow trout to MeHg (Liu, et al, 2013).

Similar effects of MeHg were observed in zebrafish embryos raised from a waterborne exposure assay and from parents exposed to dietary MeHg throughout their whole life. In both cases, we observed a significant increase in locomotor activity that followed an inverted "U" shaped dose-response curve. In other words, low and medium concentrations of MeHg would elicit hyperactivity but, at a higher dose, fish did not behave any different than the controls. The fact that both assays rendered hyperactivity following a hormetic trend would suggest that similar mechanisms of MeHg-induced neurotoxicity are involved in both.

Our results suggest that MeHg waterborne exposures are an effective and simple alternative to dietary exposures. This is not to say that both approaches should be used interchangeably, but it highlights the fact that waterborne MeHg

exposures are an excellent approach to carry out preliminary MeHg toxicity studies quickly, which can then be recreated through the more realistic dietary exposures.

Significance 2: Zebrafish and yellow perch exhibit distinct behaviors and different behavioral responses to MeHg exposure

This study elucidated important differences between the behaviors of zebrafish and yellow perch free-swimming embryos. Perhaps the most staggering difference between the behaviors of these two species is the one illustrated by the visual-motor assay. In this assay, fish larvae inside of an enclosed chamber were subjected to a series of alternating and abrupt changes in the lighting conditions every 10 minutes. In this well-documented behavioral paradigm zebrafish embryos react with reduced locomotor activity during the light periods and an increased locomotor activity during the dark periods. In contrast to the responses in zebrafish, yellow perch larvae exhibit a higher locomotor activity in light periods and a reduced locomotor activity during dark periods. These observations are likely to be rooted in the ecological and evolutionary context of these two species. Burgess and Granato (2007) interpret the response of the zebrafish as a response that reorients a larva that has strayed into a shaded environment back into a well-lit location; conversely, the response of the yellow perch is likely related to the strong phototaxis that this species exhibits during its early development.

More subtle differences between the basal locomotor behaviors of the zebrafish and yellow perch arise from observing their spontaneous swimming kinematics. In this study, we observed that zebrafish free-swimming embryos exhibit a constant scoot-and-glide locomotion, while the yellow perch exhibit a continuous glide that lasts for a few seconds, followed by long resting periods, this characteristic locomotion pattern has been referred to as “saltatory behavior” (O’Brien et al., 1990). The baseline swimming behaviors of both fish are rooted in their prey searching strategies; zebrafish larvae continuously scoot-and-glide until they encounter a nearby prey item, which they capture by a powerful suction (Budick and O'Malley, 2000); on the other hand, yellow perch larvae exhibit the aforementioned saltatory behavior, and once they have encountered prey, they capture it by energetically ramming towards it.

The behavioral responses to MeHg in zebrafish and yellow perch were also dissimilar. At comparable MeHg exposure regimes, zebrafish exhibited hyperactivity and yellow perch exhibited hypoactivity. This trend was also observed in prey capture assays; the hyperactive MeHg-exposed zebrafish caught more prey items than the control organisms, while the hypoactive MeHg-exposed yellow perch caught less prey items.

One might argue that the differences in the behavioral responses to MeHg between the two species could be attributed to the differences in MeHg exposure regimes. MeHg exposure in zebrafish occurred in the maternal ovary, making for an immediate MeHg delivery to the egg. In the case of yellow perch embryos, MeHg exposure occurred outside of the ovary via waterborne exposure, with a

lag of approximately 12 hours after being spawned. However, this notion is unlikely to be the cause of differential behavioral responses between species, given the fact that zebrafish embryos still exhibited hyperactivity when exposed to the same concentrations of waterborne MeHg that elicited hypoactivity in yellow perch. Furthermore, the THg body burdens in hyperactive zebrafish embryos from medium and high dietary exposure regimes (0.19 ± 0.004 ppm and 0.62 ± 0.039 ppm) were comparable with those of hypoactive yellow perch raised from low and medium waterborne exposure regimes (0.21 ± 0.11 ppm and 0.95 ± 0.12 ppm). This notion discards the possibility of overtly dissimilar THg burdens as a factor contributing to the observed differences in behavioral responses.

It is plausible that the observed species-dependent discrepancy between MeHg-induced behavior alterations is attributable to the rate at which these species metabolize MeHg. Slower metabolism and excretion would mean that MeHg remains in the tissues on fish larvae for a longer time, and *vice versa*. Since the yolk is the primary focal source of MeHg in developing fish embryos, perhaps the zebrafish with its complete yolk sac depletion in 6-7 days post-fertilization is subject to a shorter MeHg exposure window than the slower developing yellow perch, which does not deplete its yolk sac until it reaches 18-20 dpf (Mansueti, 1964). Furthermore, the slow development and considerably lower rearing temperatures of the yellow perch could both be contributing factors to a slower MeHg metabolism (Harris and Bodaly, 1998) and thus a presumably more prolonged MeHg exposure. This, in turn, could produce unique behavioral

effects, as illustrated by the fact that MeHg exposure at different stages of development can result in hyperactivity or hypoactivity in fish, depending on the developmental window of exposure (Weis and Weis, 1995b). Moreover, an even simpler yet-valid reasoning is that the difference between MeHg-induced behavioral alterations in these species is due to the sheer inherent differences between the baseline-swimming behaviors of zebrafish and yellow perch. In other words, MeHg may have affected behavior differently because both fish species are genetically predisposed to exhibit distinct locomotor patterns.

One aspect of MeHg-induced behavioral alteration that was common between the two species was a clear hormetic MeHg dose response; while zebrafish exhibited hyperactivity in low and medium concentrations of MeHg, but not high concentrations, the yellow perch exhibited a stronger hypoactivity in a medium MeHg dose. Also, only yellow perch exposed to a medium MeHg concentration exhibited significant difficulty while capturing prey; low and high concentrations of MeHg did not affect yellow perch prey capture significantly.

Quantitatively, the behaviors in zebrafish and yellow were very contrasting (*i.e.* if the species are to be compared in function of how *much* they swam or how *many* prey items they captured). However, one could argue that qualitatively the responses are both equally abnormal. This raises the question of whether the seemingly dissimilar behavioral outputs of MeHg exposure in both species could have similar molecular mechanisms in common. This notion will be discussed next.

Significance 3: Significantly dysregulated genes in both zebrafish and yellow perch were congruent with their observed behavioral alterations

As it has been extensively discussed in previous chapters, MeHg is known to cause a large gamut of behavioral alterations; similarly, MeHg also affects a large gamut of physiological and molecular processes. However, it can be challenging to link observed behavioral phenotypes to physiological and molecular processes (Guo, 2004). Our approach was to utilize the zebrafish model to elucidate MeHg-induced behavioral alterations. After behavioral alterations were confirmed, we proceeded to carry out high-throughput gene expression analysis in the siblings of the fish that were screened in the behavior assays.

In this study, MeHg exposure in zebrafish embryos was linked to significant enrichment in gene sets associated with human neurological phenotypes such as impaired vision, motor neuron atrophy, intermittent cerebellar ataxia, seizures, autism and attention-deficit/hyperactivity-disorder (ADHD). Remarkably, all of these phenotypes have been reported to be associated with MeHg exposure in humans and they are consistent with the behavioral phenotypes observed in our zebrafish assays and in other studies in fish and wildlife.

The most notably dysregulated pathways in MeHg exposed zebrafish were those involved with circadian rhythm and visual phototransduction. Circadian rhythm genes have a central role in synchronizing the behavior of an

organism with the rhythms of its environment (Cahill, 1996), Moreover, these genes have also been implicated in the response to oxidative stress and DNA repair (Uchida et al., 2010), and even in the occurrence of ADHD (Whalley, 2015), all of which are reportedly congruent with MeHg exposure. In particular, the circadian rhythm genes *cry1a* and *per1b* have been implicated in hyperactivity in zebrafish. The knock-out of *cry1a* has been shown to accelerate the periodicity of locomotor activity in zebrafish larvae (Uchida et al., 2010), while the knock-out of *per1b* is reported to cause a three-fold increase in locomotor activity, along with a number of ADHD-like phenotypes, such as learning impairment and impulsivity (Whalley, 2015). Both of the aforementioned genes were significantly down regulated in our zebrafish assay, which would explain the observed hyperactivity of the MeHg treated eleutheroembryos. Moreover, only a handful of studies have investigated the effects of MeHg in circadian rhythm and all of these have been performed in rodents (Arito et al., 1983; Arito et al., 1982). Nonetheless, these studies have observed MeHg-induced effects in the circadian rhythm of rats. This study did not contemplate a full circadian rhythm experiment, however the data compiled from gene expression analysis strongly suggests that MeHg exposed zebrafish may exhibit disrupted circadian rhythms. This being said, further experiments are required to assess the effects of MeHg in the circadian rhythm of zebrafish.

Due to the wealth of literature associating MeHg with visual impairment, this study attempted to quantify visual acuity, although without success (see chapter 6, significance 4). Nevertheless, the gene expression data revealed

strong effects of MeHg in pathways associated with visual phototransduction in the zebrafish. Moreover, phenotype enrichment analysis elucidated enrichment in genes associated with visual impairment, such as fundus atrophy and night blindness. These results are consistent with vision tests performed by Weber (2008) and Kalluvila (unpublished data).

The search for biomarkers of MeHg exposure in yellow perch rendered few candidates, due to the limited number of transcript sequences reported in this species, along with the challenges of developing efficient primer sets from mRNA and protein alignments from other teleost fish species. However, the analysis of gene expression gave some indication that circadian rhythm could be affected by MeHg in yellow perch, as suggested by the significant down regulation of the *per3* gene. In addition, the effects of MeHg in the locomotor output and prey capture of yellow perch mirrored each other (Figures 4.3 and 4.4); intriguingly, the trends in the expression levels of *cry1a*, *per3* and *slc1a2a* are remarkably similar to the aforementioned data (Figure 5.3; A-C). The implications of this observation are highly relevant, as it suggests a link between three very distinct levels of MeHg-induced effects: molecular (gene expression), organismal (behavior) and ecological (prey capture).

To evaluate pathways associated with vision in the yellow perch, the *opn1lw* gene was quantified, however no significant effects on the expression of this gene was observed. Contrary to the data obtained from our zebrafish study and other reports (Ho et al., 2013), opsin gene *opn1lw* was not a robust indicator of MeHg exposure. Since this gene is exclusively expressed in the retina, a

failure to observe significant effects of MeHg in the expression of this gene could be due to the fact that our gene expression analysis was not tissue-specific.

Significance 4: MeHg affects genes associated with vision; however assays to quantify visual acuity in non-model fish need to be further developed

Quantification of visual acuity is an inherently challenging task in animal models and even more so in fish larvae due to the sheer technical difficulties of determining whether a larva is seeing a visual stimulus or not. Despite this notion, two well-acknowledged methods have been previously utilized to objectively analyze vision in zebrafish embryos; these are the optokinetic response (OKR) and the optomotor response (OMR) (Neuhauss, 2003). Both of these assays employ similar principles to elicit a measurable reaction in zebrafish embryos in response to a visual stimulus; for the OKR, a rotating grating of high-contrast bars (usually black and white) is utilized to elicit saccadic movements in the eyes of immobilized embryos; for the OMR a similar grating is used to elicit a locomotor response in embryos swimming within individual raceways. Here, we attempted to replicate these methods in the zebrafish, only to later observe that yellow perch embryos are too fragile to be safely manipulated and immobilized to carry out an OKR assay. Moreover, when attempting to elicit the OMR in yellow perch larvae, they surprisingly did not respond to the grating motion to which the zebrafish did. These observations underline the strong differences between species, not only behavioral, but also in terms of the technical aspects of the handling of these species to successfully perform experiments.

The aforementioned observations ascertain the need to develop assays for visual acuity that can easily be transferred from one fish species to another. More importantly, it is critical that such an assay delivers information that can be translated to environmentally relevant endpoints such as prey capture and predator avoidance.

REFERENCES

- Alvarez, M.d.C., Murphy, C.A., Rose, K.A., McCarthy, I.D., and Fuiman, L.A. (2006a). Maternal body burdens of methylmercury impair survival skills of offspring in Atlantic croaker (*Micropogonias undulatus*). *Aquat Toxicol* 80, 329-337.
- Alvarez, M.d.C., Murphy, C.A., Rose, K.A., McCarthy, I.D., and Fuiman, L.A. (2006b). Maternal body burdens of methylmercury impair survival skills of offspring in Atlantic croaker (*Micropogonias undulatus*). *Aquatic Toxicology* 80, 329-337.
- Andrews, S. (2010). FastQC: A quality control tool for high throughput sequence data. Reference Source.
- Arito, H., Hara, N., and Torii, S. (1983). Effect of methylmercury chloride on sleep-waking rhythms in rats. *Toxicology* 28, 335-345.
- Arito, H., Sudo, A., Hara, N., Nakagaki, K., and Torii, S. (1982). Changes in circadian sleep-waking rhythms of rats following administration of methylmercury chloride. *Industrial health* 20, 55-65.
- Arito, H., Tsuruta, H., and Nakagaki, K. (1984). Acute effects of toluene on circadian rhythms of sleep-wakefulness and brain monoamine metabolism in rats. *Toxicology* 33, 291-301.
- Aschner, M., Yao, C.P., Allen, J.W., and Tan, K.H. (2000). Methylmercury alters glutamate transport in astrocytes. *Neurochemistry international* 37, 199-206.
- Baraldi, M., Zanolli, P., Tascetta, F., Blom, J.M., and Brunello, N. (2002). Cognitive deficits and changes in gene expression of NMDA receptors after prenatal methylmercury exposure. *Environmental Health Perspectives* 110, 855.
- Best, J.D., Berghmans, S., Hunt, J.J., Clarke, S.C., Fleming, A., Goldsmith, P., and Roach, A.G. (2008). Non-associative learning in larval zebrafish. *Neuropsychopharmacology* 33, 1206-1215.
- Bhavsar, S.P., Gewurtz, S.B., McGoldrick, D.J., Keir, M.J., and Backus, S.M. (2010). Changes in mercury levels in Great Lakes fish between 1970s and 2007. *Environmental Science & Technology* 44, 3273-3279.
- Bianco, I.H., Kampff, A.R., and Engert, F. (2011a). Prey Capture Behavior Evoked by Simple Visual Stimuli in Larval Zebrafish. *Frontiers in Systems Neuroscience* 5, 101.
- Bianco, I.H., Kampff, A.R., and Engert, F. (2011b). Prey capture behavior evoked by simple visual stimuli in larval zebrafish. *Frontiers in systems neuroscience* 5.

Bloom, N. (1992). Mercury and methylmercury in individual zooplankton: implications for bioaccumulation. *Limnology and Oceanography* 37, 1313-1318.

Boucher, O., Jacobson, S.W., Plusquellec, P., Dewailly, É., Ayotte, P., Forget-Dubois, N., Jacobson, J.L., and Muckle, G. (2012). Prenatal methylmercury, postnatal lead exposure, and evidence of attention deficit/hyperactivity disorder among Inuit children in Arctic Québec. *Environmental Health Perspectives* 120, 1456-1461.

Branson, K., Robie, A.A., Bender, J., Perona, P., and Dickinson, M.H. (2009). High-throughput ethomics in large groups of *Drosophila*. *Nat Meth* 6, 451-457.

Budick, S.A., and O'Malley, D.M. (2000). Locomotor repertoire of the larval zebrafish: swimming, turning and prey capture. *Journal of Experimental Biology* 203, 2565-2579.

Burbacher, T.M., Grant, K.S., Mayfield, D.B., Gilbert, S.G., and Rice, D.C. (2005). Prenatal methylmercury exposure affects spatial vision in adult monkeys. *Toxicology and applied pharmacology* 208, 21-28.

Burgess, H.A., and Granato, M. (2007). Modulation of locomotor activity in larval zebrafish during light adaptation. *Journal of Experimental Biology* 210, 2526-2539.

Burke, K., Cheng, Y., Li, B., Petrov, A., Joshi, P., Berman, R.F., Reuhl, K.R., and DiCicco-Bloom, E. (2006). Methylmercury elicits rapid inhibition of cell proliferation in the developing brain and decreases cell cycle regulator, cyclin E. *Neurotoxicology* 27, 970-981.

Cahill, G.M. (1996). Circadian regulation of melatonin production in cultured zebrafish pineal and retina. *Brain research* 708, 177-181.

Cambier, S., Benard, G., Mesmer-Dudons, N., Gonzalez, P., Rossignol, R., Brethes, D., and Bourdineaud, J.-P. (2009). At environmental doses, dietary methylmercury inhibits mitochondrial energy metabolism in skeletal muscles of the zebra fish (*Danio rerio*). *The international journal of biochemistry & cell biology* 41, 791-799.

Clapp, D.F., and Dettmers, J.M. (2004). Yellow Perch Research and Management in Lake Michigan. *Fisheries* 29, 11-19.

Colwill, R.M., and Creton, R. (2011). Imaging escape and avoidance behavior in zebrafish larvae. *Reviews in the neurosciences* 22, 63-73.

Daré, E., Fetissov, S., Hökfelt, T., Hall, H., Ögren, S.O., and Ceccatelli, S. (2003). Effects of prenatal exposure to methylmercury on dopamine-mediated locomotor activity and dopamine D2 receptor binding. *Naunyn-Schmiedeberg's archives of pharmacology* 367, 500-508.

DeLuca, D.S., Levin, J.Z., Sivachenko, A., Fennell, T., Nazaire, M.-D., Williams, C., Reich, M., Winckler, W., and Getz, G. (2012). RNA-SeQC: RNA-seq metrics for quality control and process optimization. *Bioinformatics* 28, 1530-1532.

Depew, D.C., Basu, N., Burgess, N.M., Campbell, L.M., Devlin, E.W., Drevnick, P.E., Hammerschmidt, C.R., Murphy, C.A., Sandheinrich, M.B., and Wiener, J.G. (2012). Toxicity of dietary methylmercury to fish: Derivation of ecologically meaningful threshold concentrations. *Environmental Toxicology and Chemistry* 31, 1536-1547.

Devlin, E. (2006). Acute Toxicity, Uptake and Histopathology of Aqueous Methyl Mercury to Fathead Minnow Embryos. *Ecotoxicology* 15, 97-110.

Drevnick, P.E., and Sandheinrich, M.B. (2003). Effects of dietary methylmercury on reproductive endocrinology of fathead minnows. *Environmental science & technology* 37, 4390-4396.

Durrieu, G., Maury-Brachet, R., and Boudou, A. (2005). Goldmining and mercury contamination of the piscivorous fish *Hoplias aimara* in French Guiana (Amazon basin). *Ecotoxicology and environmental safety* 60, 315-323.

Easter Jr, S.S., and Nicola, G.N. (1996). The Development of Vision in the Zebrafish (*Danio rerio*). *Developmental biology* 180, 646-663.

Ekino, S., Susa, M., Ninomiya, T., Imamura, K., and Kitamura, T. (2007). Minamata disease revisited: an update on the acute and chronic manifestations of methyl mercury poisoning. *Journal of the neurological sciences* 262, 131-144.

Emran, F., Rihel, J., and Dowling, J.E. (2008). A Behavioral Assay to Measure Responsiveness of Zebrafish to Changes in Light Intensities. *Journal of Visualized Experiments : JoVE*, 923.

Fredslund, J., Schauser, L., Madsen, L.H., Sandal, N., and Stougaard, J. (2005). PriFi: using a multiple alignment of related sequences to find primers for amplification of homologs. *Nucleic Acids Research* 33, W516-W520.

Gahtan, E., Tanger, P., and Baier, H. (2005). Visual prey capture in larval zebrafish is controlled by identified reticulospinal neurons downstream of the tectum. *The Journal of neuroscience* 25, 9294-9303.

Gimenez-Llort, L., Ahlbom, E., Dare, E., Vahter, M., Ögren, S.-O., and Ceccatelli, S. (2001). Prenatal exposure to methylmercury changes dopamine-modulated motor activity during early ontogeny: age and gender-dependent effects. *Environmental toxicology and pharmacology* 9, 61-70.

Giménez-Llort, L., Ahlbom, E., Daré, E., Vahter, M., Ögren, S.O., and Ceccatelli, S. (2001). Prenatal exposure to methylmercury changes dopamine-modulated

motor activity during early ontogeny: age and gender-dependent effects. *Environmental Toxicology and Pharmacology* 9, 61-70.

Gonzalez, P., Dominique, Y., Massabuau, J., Boudou, A., and Bourdineaud, J. (2005). Comparative effects of dietary methylmercury on gene expression in liver, skeletal muscle, and brain of the zebrafish (*Danio rerio*). *Environmental Science & Technology* 39, 3972-3980.

Goto, Y., Shigematsu, J., Tobimatsu, S., Sakamoto, T., Kinukawa, N., and Kato, M. (2001). Different vulnerability of rat retinal cells to methylmercury exposure. *Current eye research* 23, 171-178.

Grandjean, P., Satoh, H., Murata, K., and Eto, K. (2010). Adverse Effects of Methylmercury: Environmental Health Research Implications. *Environmental Health Perspectives* 118, 1137-1145.

Gribble, E.J., Hong, S.W., and Faustman, E.M. (2005). The magnitude of methylmercury-induced cytotoxicity and cell cycle arrest is p53-dependent. *Birth Defects Research Part A: Clinical and Molecular Teratology* 73, 29-38.

Grunwald, D.J., and Eisen, J.S. (2002). Headwaters of the zebrafish [mdash] emergence of a new model vertebrate. *Nat Rev Genet* 3, 717-724.

Guo, S. (2004). Linking genes to brain, behavior and neurological diseases: what can we learn from zebrafish? *Genes, Brain and Behavior* 3, 63-74.

Hammerschmidt, C.R., and Sandheinrich, M.B. (2005). Maternal diet during oogenesis is the major source of methylmercury in fish embryos. *Environmental science & technology* 39, 3580-3584.

Hammerschmidt, C.R., Sandheinrich, M.B., Wiener, J.G., and Rada, R.G. (2002). Effects of dietary methylmercury on reproduction of fathead minnows. *Environmental science & technology* 36, 877-883.

Hammerschmidt, C.R., Wiener, J.G., Frazier, B.E., and Rada, R.G. (1999). Methylmercury content of eggs in yellow perch related to maternal exposure in four Wisconsin lakes. *Environmental Science & Technology* 33, 999-1003.

Harris, R.C., and Bodaly, R.D. (1998). Temperature, growth and dietary effects on fish mercury dynamics in two Ontario lakes. *Biogeochemistry* 40, 175-187.

Hedges, S.B., Dudley, J., and Kumar, S. (2006). TimeTree: a public knowledge-base of divergence times among organisms. *Bioinformatics* 22, 2971-2972.

Heiden, T.K., Hutz, R.J., and Carvan, M.J. (2005). Accumulation, tissue distribution, and maternal transfer of dietary 2, 3, 7, 8,-tetrachlorodibenzo-p-dioxin: impacts on reproductive success of zebrafish. *Toxicological Sciences* 87, 497-507.

Hill, A.J., Teraoka, H., Heideman, W., and Peterson, R.E. (2005). Zebrafish as a model vertebrate for investigating chemical toxicity. *Toxicological Sciences* 86, 6-19.

Ho, N.Y., Yang, L., Legradi, J., Armant, O., Takamiya, M., Rastegar, S., and Strähle, U. (2013). Gene Responses in the Central Nervous System of Zebrafish Embryos Exposed to the Neurotoxicant Methyl Mercury. *Environmental Science & Technology* 47, 3316-3325.

Kakita, A., Wakabayashi, K., Su, M., Yoneoka, Y., Sakamoto, M., Ikuta, F., and Takahashi, H. (2000). Intrauterine methylmercury intoxication: consequence of the inherent brain lesions and cognitive dysfunction in maturity. *Brain research* 877, 322-330.

Kalueff, A.V., Echevarria, D.J., and Stewart, A.M. (2014). Gaining translational momentum: more zebrafish models for neuroscience research. *Progress in Neuro-Psychopharmacology and Biological Psychiatry* 55, 1-6.

Kalueff, A.V., Gebhardt, M., Stewart, A.M., Cachat, J.M., Brimmer, M., Chawla, J.S., Craddock, C., Kyzar, E.J., Roth, A., and Landsman, S. (2013). Towards a comprehensive catalog of zebrafish behavior 1.0 and beyond. *Zebrafish* 10, 70-86.

Kane, A., Salierno, J., and Brewer, S. (2005). Fish models in behavioral toxicology: automated techniques, updates and perspectives. *Methods in aquatic toxicology* 2, 559-590.

Kim, D., Perteza, G., Trapnell, C., Pimentel, H., Kelley, R., and Salzberg, S.L. (2013). TopHat2: accurate alignment of transcriptomes in the presence of insertions, deletions and gene fusions. *Genome Biol* 14, R36.

Klaper, R., Carter, B.J., Richter, C., Drevnick, P., Sandheinrich, M., and Tillitt, D. (2008). Use of a 15 k gene microarray to determine gene expression changes in response to acute and chronic methylmercury exposure in the fathead minnow *Pimephales promelas* Rafinesque. *Journal of Fish Biology* 72, 2207-2280.

Klaper, R., Rees, C.B., Drevnick, P., Weber, D., Sandheinrich, M., and Carvan, M.J. (2006). Gene Expression Changes Related to Endocrine Function and Decline in Reproduction in Fathead Minnow (*Pimephales promelas*) after Dietary Methylmercury Exposure. *Environmental Health Perspectives* 114, 1337-1343.

Korbas, M., Krone, P.H., Pickering, I.J., and George, G.N. (2010). Dynamic accumulation and redistribution of methylmercury in the lens of developing zebrafish embryos and larvae. *JBIC Journal of Biological Inorganic Chemistry* 15, 1137-1145.

- Korbas, M., Lai, B., Vogt, S., Gleber, S.-C., Karunakaran, C., Pickering, I.J., Krone, P.H., and George, G.N. (2013). Methylmercury targets photoreceptor outer segments. *ACS chemical biology* 8, 2256-2263.
- Latif, M., Bodaly, R., Johnston, T., and Fudge, R. (2001). Effects of environmental and maternally derived methylmercury on the embryonic and larval stages of walleye (*Stizostedion vitreum*). *Environmental pollution* 111, 139-148.
- Lieschke, G.J., and Currie, P.D. (2007). Animal models of human disease: zebrafish swim into view. *Nat Rev Genet* 8, 353-367.
- Little, E.E., and Finger, S.E. (1990). Swimming behavior as an indicator of sublethal toxicity in fish. *Environmental Toxicology and Chemistry* 9, 13-19.
- Liu, Q., Basu, N., Goetz, G., Jiang, N., Hutz, R.J., Tonellato, P.J., and Carvan III, M.J. (2013). Differential gene expression associated with dietary methylmercury (MeHg) exposure in rainbow trout (*Oncorhynchus mykiss*) and zebrafish (*Danio rerio*). *Ecotoxicology* 22, 740-751.
- Louis W, C. (1977). Neurotoxic effects of mercury—A review. *Environmental Research* 14, 329-373.
- MacPhail, R., Brooks, J., Hunter, D., Padnos, B., Irons, T., and Padilla, S. (2009). Locomotion in larval zebrafish: influence of time of day, lighting and ethanol. *Neurotoxicology* 30, 52-58.
- Mansueti, A.J. (1964). Early development of the yellow perch, *Perca flavescens*. *Chesapeake Science* 5, 46-66.
- Marsden, J.E., and Robillard, S.R. (2004). Decline of Yellow Perch in Southwestern Lake Michigan, 1987–1997. *North American Journal of Fisheries Management* 24, 952-966.
- Martin, M. (2011). Cutadapt removes adapter sequences from high-throughput sequencing reads. *EMBnet journal* 17, pp. 10-12.
- Mason, R., Reinfelder, J., and Morel, F. (1995). Bioaccumulation of mercury and methylmercury. In *Mercury as a Global Pollutant* (Springer), pp. 915-921.
- Mohammed, A. (2013). Why are Early Life Stages of Aquatic Organisms more Sensitive to Toxicants than Adults? *New Insights into Toxicity and Drug Testing*, InTech, Rijeka, Croatia.
- Monson, B.A. (2009a). Trend Reversal of Mercury Concentrations in Piscivorous Fish from Minnesota Lakes: 1982–2006. *Environmental Science & Technology* 43, 1750-1755.

Monson, B.A. (2009b). Trend reversal of mercury concentrations in piscivorous fish from Minnesota Lakes: 1982– 2006. *Environmental science & technology* 43, 1750-1755.

Montgomery, K.S., Mackey, J., Thuett, K., Ginestra, S., Bizon, J.L., and Abbott, L.C. (2008). Chronic, low-dose prenatal exposure to methylmercury impairs motor and mnemonic function in adult C57/B6 mice. *Behavioural Brain Research* 191, 55-61.

Neuhauss, S.C. (2003). Behavioral genetic approaches to visual system development and function in zebrafish. *Journal of neurobiology* 54, 148-160.

O'brien, W.J., Browman, H.I., and Evans, B.I. (1990). Search strategies of foraging animals. *American Scientist* 78, 152-160.

Oshima, Y., Kang, I.J., Kobayashi, M., Nakayama, K., Imada, N., and Honjo, T. (2003). Suppression of sexual behavior in male Japanese medaka (*Oryzias latipes*) exposed to 17 β -estradiol. *Chemosphere* 50, 429-436.

Pelkowski, S.D., Kapoor, M., Richendfer, H.A., Wang, X., Colwill, R.M., and Creton, R. (2011). A novel high-throughput imaging system for automated analyses of avoidance behavior in zebrafish larvae. *Behavioural Brain Research* 223, 135-144.

Petzold, A.M., Balciunas, D., Sivasubbu, S., Clark, K.J., Bedell, V.M., Westcot, S.E., Myers, S.R., Moulder, G.L., Thomas, M.J., and Ekker, S.C. (2009). Nicotine response genetics in the zebrafish. *Proceedings of the National Academy of Sciences* 106, 18662-18667.

Pierce, L.R., Willey, J.C., Crawford, E.L., Palsule, V.V., Leaman, D.W., Faisal, M., Kim, R.K., Shepherd, B.S., Stanoszek, L.M., and Stepien, C.A. (2013). A new StaRT-PCR approach to detect and quantify fish Viral Hemorrhagic Septicemia virus (VHSV): Enhanced quality control with internal standards. *Journal of virological methods* 189, 129-142.

Pierron, F., Bourret, V., St-Cyr, J., Campbell, P.G., Bernatchez, L., and Couture, P. (2009). Transcriptional responses to environmental metal exposure in wild yellow perch (*Perca flavescens*) collected in lakes with differing environmental metal concentrations (Cd, Cu, Ni). *Ecotoxicology* 18, 620-631.

Provencher, B., and Bishop, R.C. (1997). An Estimable Dynamic Model of Recreation Behavior with an Application to Great Lakes Angling. *Journal of Environmental Economics and Management* 33, 107-127.

Reich, M., Liefeld, T., Gould, J., Lerner, J., Tamayo, P., and Mesirov, J.P. (2006). GenePattern 2.0. *Nature genetics* 38, 500-501.

Ribera, A.B., and Nüsslein-Volhard, C. (1998). Zebrafish Touch-Insensitive Mutants Reveal an Essential Role for the Developmental Regulation of Sodium Current. *The Journal of Neuroscience* 18, 9181-9191.

Risch, M.R., DeWild, J.F., Krabbenhoft, D.P., Kolka, R.K., and Zhang, L. (2012a). Litterfall mercury dry deposition in the eastern USA. *Environmental Pollution* 161, 284-290.

Risch, M.R., Gay, D.A., Fowler, K.K., Keeler, G.J., Backus, S.M., Blanchard, P., Barres, J.A., and Dvonch, J.T. (2012b). Spatial patterns and temporal trends in mercury concentrations, precipitation depths, and mercury wet deposition in the North American Great Lakes region, 2002–2008. *Environmental pollution* 161, 261-271.

Roberts, A., Pimentel, H., Trapnell, C., and Pachter, L. (2011). Identification of novel transcripts in annotated genomes using RNA-Seq. *Bioinformatics* 27, 2325-2329.

Rose, T.M., Henikoff, J.G., and Henikoff, S. (2003). CODEHOP (COnsensus-DEgenerate hybrid oligonucleotide primer) PCR primer design. *Nucleic Acids Research* 31, 3763-3766.

Saglio, P., and Trijasse, S. (1998). Behavioral responses to atrazine and diuron in goldfish. *Archives of environmental contamination and toxicology* 35, 484-491.

Saint-Amant, L., and Drapeau, P. (1998). Time course of the development of motor behaviors in the zebrafish embryo. *Journal of neurobiology* 37, 622-632.

Saint-Amant, L., and Drapeau, P. (2000). Motoneuron Activity Patterns Related to the Earliest Behavior of the Zebrafish Embryo. *The Journal of Neuroscience* 20, 3964-3972.

Samson, J.C., and Shenker, J. (2000). The teratogenic effects of methylmercury on early development of the zebrafish, *Danio rerio*. *Aquatic toxicology* 48, 343-354.

Sandheinrich, M.B., Bhavsar, S.P., Bodaly, R., Drevnick, P.E., and Paul, E.A. (2011). Ecological risk of methylmercury to piscivorous fish of the Great Lakes region. *Ecotoxicology* 20, 1577-1587.

Sandheinrich, M.B., and Miller, K.M. (2006). Effects of dietary methylmercury on reproductive behavior of fathead minnows (*Pimephales promelas*). *Environmental Toxicology and Chemistry* 25, 3053-3057.

Scheuhammer, A.M., Meyer, M.W., Sandheinrich, M.B., and Murray, M.W. (2007a). Effects of environmental methylmercury on the health of wild birds, mammals, and fish. *AMBIO: A Journal of the Human Environment* 36, 12-19.

Scheuhammer, A.M., Meyer, M.W., Sandheinrich, M.B., and Murray, M.W. (2007b). Effects of environmental methylmercury on the health of wild birds, mammals, and fish. *Ambio* 36, 12-18.

Shroyer, S.M., and McComish, T.S. (2000). Relationship between Alewife Abundance and Yellow Perch Recruitment in Southern Lake Michigan. *North American Journal of Fisheries Management* 20, 220-225.

Smith, L.E., Carvan Iii, M.J., Dellinger, J.A., Ghorai, J.K., White, D.B., Williams, F.E., and Weber, D.N. (2010). Developmental selenomethionine and methylmercury exposures affect zebrafish learning. *Neurotoxicology and Teratology* 32, 246-255.

Spitsbergen, J.M., and Kent, M.L. (2003). The State of the Art of the Zebrafish Model for Toxicology and Toxicologic Pathology Research—Advantages and Current Limitations. *Toxicologic Pathology* 31, 62-87.

Stringari, J., Meotti, F.C., Souza, D.O., Santos, A.R., and Farina, M. (2006). Postnatal methylmercury exposure induces hyperlocomotor activity and cerebellar oxidative stress in mice: dependence on the neurodevelopmental period. *Neurochemical research* 31, 563-569.

Subramanian, A., Tamayo, P., Mootha, V.K., Mukherjee, S., Ebert, B.L., Gillette, M.A., Paulovich, A., Pomeroy, S.L., Golub, T.R., and Lander, E.S. (2005). Gene set enrichment analysis: a knowledge-based approach for interpreting genome-wide expression profiles. *Proceedings of the National Academy of Sciences of the United States of America* 102, 15545-15550.

Thomas, L.T., Welsh, L., Galvez, F., and Svoboda, K.R. (2009). Acute nicotine exposure and modulation of a spinal motor circuit in embryonic zebrafish. *Toxicology and applied pharmacology* 239, 1-12.

Thomas, M.A., Joshi, P.P., and Klaper, R.D. (2012). Gene-class analysis of expression patterns induced by psychoactive pharmaceutical exposure in fathead minnow (*Pimephales promelas*) indicates induction of neuronal systems. *Comparative Biochemistry and Physiology Part C: Toxicology & Pharmacology* 155, 109-120.

Trapnell, C., Pachter, L., and Salzberg, S.L. (2009). TopHat: discovering splice junctions with RNA-Seq. *Bioinformatics* 25, 1105-1111.

Trapnell, C., Roberts, A., Goff, L., Pertea, G., Kim, D., Kelley, D.R., Pimentel, H., Salzberg, S.L., Rinn, J.L., and Pachter, L. (2012). Differential gene and transcript expression analysis of RNA-seq experiments with TopHat and Cufflinks. *Nature protocols* 7, 562-578.

Uchida, Y., Hirayama, J., and Nishina, H. (2010). A common origin: signaling similarities in the regulation of the circadian clock and DNA damage responses. *Biological and Pharmaceutical Bulletin* 33, 535-544.

Vitalone, A., Catalani, A., Chiodi, V., Cinque, C., Fattori, V., Goldoni, M., Matteucci, P., Poli, D., Zuena, A.R., and Costa, L.G. (2008). Neurobehavioral assessment of rats exposed to low doses of PCB126 and methyl mercury during development. *Environmental toxicology and pharmacology* 25, 103-113.

von Herbing, I.H., and Gallager, S. (2000). Foraging behavior in early Atlantic cod larvae (*Gadus morhua*) feeding on a protozoan (*Balanion sp.*) and a copepod nauplius (*Pseudodiaptomus sp.*). *Marine Biology* 136, 591-602.

Weber, D. (2006). Dose-dependent effects of developmental mercury exposure on C-start escape responses of larval zebrafish *Danio rerio*. *Journal of fish biology* 69, 75-94.

Weber, D.N., Connaughton, V.P., Dellinger, J.A., Klemer, D., Udvardia, A., and Carvan Iii, M.J. (2008). Selenomethionine reduces visual deficits due to developmental methylmercury exposures. *Physiology & Behavior* 93, 250-260.

Weis, J.S., Smith, G., Zhou, T., Santiago-Bass, C., and Weis, P. (2001). Effects of Contaminants on Behavior: Biochemical Mechanisms and Ecological Consequences, *Bioscience* 51, 209-217.

Weis, J.S., Smith, G.M., and Zhou, T. (1999). Altered predator/prey behavior in polluted environments: implications for fish conservation. *Environmental Biology of Fishes* 55, 43-51.

Weis, J.S., and Weis, P. (1995a). Effects of embryonic exposure to methylmercury on larval prey-capture ability in the mummichog, *fundulus heteroclitus*. *Environmental Toxicology and Chemistry* 14, 153-156.

Weis, J.S., and Weis, P. (1995b). Swimming performance and predator avoidance by mummichog (*Fundulus heteroclitus*) larvae after embryonic or larval exposure to methylmercury. *Canadian Journal of Fisheries and Aquatic Sciences* 52, 2168-2173.

Whalley, K. (2015). Psychiatric disorders: A zebrafish model of ADHD. *Nature Reviews Neuroscience* 16, 188-188.

Wiener, J.G., Sandheinrich, M.B., Bhavsar, S.P., Bohr, J.R., Evers, D.C., Monson, B.A., and Schrank, C.S. (2012). Toxicological significance of mercury in yellow perch in the Laurentian Great Lakes region. *Environmental Pollution* 161, 350-357.

Wilberg, M.J., Bence, J.R., Eggold, B.T., Makauskas, D., and Clapp, D.F. (2005). Yellow Perch Dynamics in Southwestern Lake Michigan during 1986–2002. *North American Journal of Fisheries Management* 25, 1130-1152.

Zhang, B., Kirov, S., and Snoddy, J. (2005). WebGestalt: an integrated system for exploring gene sets in various biological contexts. *Nucleic Acids Research* 33, W741-W748.

APPENDICES

Appendix 1: Maternal MeHg transfer from ovaries to zebrafish embryos

Exposure group and replicate	Ovary THg (ppm, wet weight)	Embryo THg (ppm, wet weight)	Proportion of ovary [Hg] present in embryos (%)
0ppm - 1	0.1381	0.0081	5.85%
0ppm - 2	0.0745	0.0074	9.90%
0ppm - 3	0.0462	0.0047	10.09%
1ppm - 1	0.8372	0.0733	8.75%
1ppm - 2	0.8500	0.0753	8.86%
1ppm - 3	0.7992	0.0717	8.97%
3ppm - 1	2.0001	0.1903	9.51%
3ppm - 2	2.1071	0.1901	9.02%
3ppm - 3	2.2983	0.1817	7.91%
10ppm - 1	5.6685	0.5774	10.19%
10ppm - 2	7.0758	0.6465	9.14%
10ppm - 3	9.3564	0.6442	6.89%

Appendix 2: Fecundity of MeHg exposed zebrafish females and mortality of their offspring

MeHg exposure group	Fecundity	Total mortality at 24 hpf	%Mortality at 24 hpf
0ppm	2051.00±724.83	350.33±78.15	19.09% ±2.98
1ppm	2829.00±491.66	429.33±60.46	15.98% ±2.83
3ppm	2482.67±843.79	409.33±139.71	16.91% ±2.27
10ppm	2668.33±713.22	770.66±480.37	24.44% ±9.68
ANOVA			
F	0.223	0.555	0.501
P	0.878	0.659	0.690

Note: Values are given as the mean ± SE

Appendix 3: ELS tox scores of embryonic zebrafish from MeHg exposed parents

MeHg exposure group	ELS tox score at 24 hpf	ELS tox score at 72 hpf	ELS tox score at 144 hpf
0ppm	0.04±0.01	0.06±0.02	0.24±0.08
1ppm	0.11±0.05	0.12±0.03	0.28±0.01
3ppm	0.09±0.01	0.14±0.05	0.15±0.06
10ppm	0.05±0.03	0.12±0.03	0.19±0.01
ANOVA			
F	1.21	1.02	1.27
P	0.36	0.43	0.35

Note: Values are given as the mean ± SE

Appendix 4: Significantly up-regulated genes in 1ppm MeHg treated zebrafish embryos.

ZFIN gene ID	ENSEMBL gene ID	0ppm FPKM	1ppm FPKM	log ₂ (fold change)	q value
vwa2	ENSDARG00000075441	4.37	18.80	2.1	0.006
tubb4b	ENSDARG00000091444	1.26	4.08	1.7	0.011
gck	ENSDARG00000068006	0.79	2.39	1.6	0.016
pmaip1	ENSDARG00000089307	9.11	26.40	1.5	0.027
slc38a9	ENSDARG00000032769	2.14	4.92	1.2	0.006
si:ch211-13o20.3	ENSDARG00000091871	18.91	42.46	1.2	0.016
zgc:113232	ENSDARG00000040118	6.36	13.43	1.1	0.006
duox	ENSDARG00000062632	0.73	1.48	1.0	0.024
zgc:92590	ENSDARG00000040282	35.95	70.28	1.0	0.006
si:dkey-14d8.6	ENSDARG00000045835	337.06	622.79	0.9	0.006
matn3a	ENSDARG00000069245	16.32	29.66	0.9	0.006
nupr1	ENSDARG00000094557	111.50	195.52	0.8	0.006
col9a1	ENSDARG00000031483	15.25	25.80	0.8	0.030
itga10	ENSDARG00000002507	8.03	13.45	0.7	0.027
serpinh1b	ENSDARG00000019949	15.15	24.30	0.7	0.016
pdia2	ENSDARG00000018263	47.89	76.61	0.7	0.011
si:dkey-14d8.7	ENSDARG00000045834	69.32	110.23	0.7	0.024
zgc:153968	ENSDARG00000061858	40.01	60.95	0.6	0.034

Appendix 5: Significantly down-regulated genes in 1ppm MeHg treated zebrafish embryos.

ZFIN gene ID	ENSEMBL gene ID	0ppm FPKM	1ppm FPKM	log ₂ (fold change)	q value
cux2b	ENSDARG00000086345	2.55	0.30	-3.1	0.011
sema7a	ENSDARG00000078707	18.78	2.38	-3.0	0.006
fkbp5	ENSDARG00000028396	29.82	4.99	-2.6	0.006
gpr112b	ENSDARG00000094386	2.36	0.52	-2.2	0.006
klf9	ENSDARG00000068194	31.90	7.72	-2.0	0.006
zgc:153932	ENSDARG00000052779	4.35	1.19	-1.9	0.006
zgc:162509	ENSDARG00000070604	2.86	0.90	-1.7	0.006
per1a	ENSDARG00000056885	3.86	1.31	-1.6	0.006
cnga3b	ENSDARG00000012297	1.50	0.53	-1.5	0.039
hamp2	ENSDARG00000053227	27.67	9.85	-1.5	0.006
nr1d1	ENSDARG00000033160	42.38	15.34	-1.5	0.006
si:dkey-206d17.5	ENSDARG00000089204	20.35	7.64	-1.4	0.006
papd4	ENSDARG00000055385	2.38	0.92	-1.4	0.034
bahcc1	ENSDARG00000080009	12.36	4.91	-1.3	0.006
ucp3	ENSDARG00000091209	34.56	14.72	-1.2	0.006
nr1d2a	ENSDARG00000003820	39.03	16.76	-1.2	0.006
si:ch211-121a2.2	ENSDARG00000039682	71.84	32.94	-1.1	0.006
cyp24a1	ENSDARG00000070420	16.32	7.93	-1.0	0.006
mgat4a	ENSDARG00000063330	16.83	8.61	-1.0	0.006
pfkfb4l	ENSDARG00000029075	24.73	12.73	-1.0	0.006
rn7sk	ENSDARG00000081270	83.26	43.88	-0.9	0.020
zgc:172246	ENSDARG00000090722	51.43	27.96	-0.9	0.011
f5	ENSDARG00000055705	4.52	2.50	-0.9	0.006
guca1c	ENSDARG00000030758	19.25	10.64	-0.9	0.036
nfil3-6	ENSDARG00000087188	15.09	8.40	-0.8	0.006
nr4a1	ENSDARG00000000796	7.56	4.23	-0.8	0.011
rel	ENSDARG00000055276	7.12	4.01	-0.8	0.016
lpin1	ENSDARG00000020239	57.37	32.48	-0.8	0.006
zgc:171497	ENSDARG00000090578	2.27	1.29	-0.8	0.030
bfb	ENSDARG00000005616	7.90	4.51	-0.8	0.042
si:ch211-132b12.7	ENSDARG00000068374	17.04	9.73	-0.8	0.034

Appendix 5 (Continued)

ZFIN gene ID	ENSEMBL gene ID	0ppm FPKM	1ppm FPKM	log ₂ (fold change)	q value
si:dkey-52d15.1	ENSDARG00000077872	8.60	4.99	-0.8	0.047
birc7	ENSDARG00000058082	4.30	2.54	-0.8	0.011
zgc:110354	ENSDARG00000043093	5.67	3.34	-0.8	0.030
cish	ENSDARG00000060316	34.15	20.32	-0.7	0.011
mych	ENSDARG00000077473	38.24	23.11	-0.7	0.006
plcd3a	ENSDARG00000052957	8.84	5.36	-0.7	0.006
zgc:112265	ENSDARG00000024928	103.93	63.52	-0.7	0.024
si:dkey-162h11.2	ENSDARG00000091715	3.33	2.05	-0.7	0.020
klf3	ENSDARG00000015495	15.66	9.67	-0.7	0.006
a2ml	ENSDARG00000056314	15.11	9.37	-0.7	0.006
slc3a2b	ENSDARG00000037012	93.93	58.52	-0.7	0.011
zgc:110843	ENSDARG00000073845	9.21	5.76	-0.7	0.034
prkacbb	ENSDARG00000059125	4.11	2.57	-0.7	0.024
abcb11b	ENSDARG00000070078	5.41	3.43	-0.7	0.011
ces3	ENSDARG00000041595	37.01	23.65	-0.6	0.030
bfsp2	ENSDARG00000011998	58.98	38.53	-0.6	0.042

Appendix 6: Significantly up-regulated genes in 3ppm MeHg treated zebrafish embryos.

ZFIN gene ID	ENSEMBL gene ID	0ppm FPKM	3ppm FPKM	log ₂ (fold change)	q value
vwa2	ENSDARG00000075441	4.37	63.52	3.9	0.006
spsb3b	ENSDARG00000077487	3.12	15.59	2.3	0.006
opn1lw1	ENSDARG00000044862	6.24	20.94	1.7	0.006
ccdc64	ENSDARG00000074761	0.39	1.26	1.7	0.020
cdkn1d	ENSDARG00000088020	34.84	103.82	1.6	0.011
nfil3-2	ENSDARG00000043237	13.39	38.61	1.5	0.006
nfil3-5	ENSDARG00000094965	26.85	77.00	1.5	0.006
klf2a	ENSDARG00000042667	14.71	39.66	1.4	0.006
prdm1b	ENSDARG00000053592	5.52	14.78	1.4	0.006
tfc2l1	ENSDARG00000029497	1.59	4.14	1.4	0.006
rorcb	ENSDARG00000017780	9.14	23.23	1.3	0.006
slc1a7a	ENSDARG00000034940	1.31	3.29	1.3	0.006
xkr8.2	ENSDARG00000076820	1.12	2.81	1.3	0.027
slc38a9	ENSDARG00000032769	2.14	5.20	1.3	0.006
guca1e	ENSDARG00000078384	2.25	5.28	1.2	0.006
aanat2	ENSDARG00000079802	2.68	6.27	1.2	0.006
asb15a	ENSDARG00000045633	1.60	3.67	1.2	0.006
nr1d4b	ENSDARG00000059370	1.43	3.28	1.2	0.006
arntl2	ENSDARG00000041381	1.85	4.23	1.2	0.011
si:dkey-283b15.2	ENSDARG00000041382	7.00	15.94	1.2	0.006
ampd3b	ENSDARG00000032469	21.49	48.52	1.2	0.006
ndrg1b	ENSDARG00000010420	34.41	77.26	1.2	0.006
slc34a2b	ENSDARG00000036864	4.50	10.07	1.2	0.006
inhbb	ENSDARG00000040777	4.92	10.79	1.1	0.006
kera	ENSDARG00000056938	16.28	35.10	1.1	0.006
asb10	ENSDARG00000071419	3.69	7.94	1.1	0.006
dok7	ENSDARG00000060236	1.92	3.97	1.0	0.006
arntl1b	ENSDARG00000035732	6.50	13.41	1.0	0.006
klhl30	ENSDARG00000076094	1.47	3.03	1.0	0.006
gpr124	ENSDARG00000076994	2.42	4.89	1.0	0.006
fbxo32	ENSDARG00000040277	33.53	66.97	1.0	0.006
hlfb	ENSDARG00000061011	5.37	10.62	1.0	0.006
ankrd33ba	ENSDARG00000058357	4.23	8.35	1.0	0.011

Appendix 6 (Continued)

ZFIN gene ID	ENSEMBL gene ID	0ppm FPKM	3ppm FPKM	log ₂ (fold change)	q value
si:dkey-72114.3	ENSDARG00000061044	1.71	3.37	1.0	0.036
plbd1	ENSDARG00000063313	3.03	5.74	0.9	0.006
si:dkey-89f23.3	ENSDARG00000088774	1.63	3.07	0.9	0.024
itga7	ENSDARG00000089083	22.61	42.45	0.9	0.006
usp28	ENSDARG00000088880	13.59	25.44	0.9	0.006
rd3	ENSDARG00000031600	8.16	15.04	0.9	0.024
slc6a19a	ENSDARG00000018621	2.12	3.88	0.9	0.006
lrp6	ENSDARG00000076053	6.23	11.31	0.9	0.030
mxd3	ENSDARG00000057432	11.67	21.14	0.9	0.006
cdh15	ENSDARG00000068191	3.99	7.22	0.9	0.006
alp3	ENSDARG00000039048	5.98	10.79	0.9	0.016
slc16a12b	ENSDARG00000089885	10.31	18.56	0.8	0.006
si:dkey-14d8.6	ENSDARG00000045835	337.06	598.48	0.8	0.006
zmiz1b	ENSDARG00000076477	1.35	2.39	0.8	0.045
cacna1sb	ENSDARG00000042552	7.62	13.32	0.8	0.006
sema6d	ENSDARG00000002748	7.18	12.50	0.8	0.006
cyp24a1	ENSDARG00000070420	16.32	28.37	0.8	0.020
cyp2k18	ENSDARG00000038366	5.74	9.95	0.8	0.011
npas2	ENSDARG00000016536	3.56	6.16	0.8	0.006
kbtbd12	ENSDARG00000001882	13.03	22.55	0.8	0.006
vapa	ENSDARG00000004312	93.46	161.67	0.8	0.006
mtp	ENSDARG00000008637	4.27	7.38	0.8	0.039
pygl	ENSDARG00000002197	23.48	40.59	0.8	0.006
c3b	ENSDARG00000087359	3.51	6.05	0.8	0.011
mmp15a	ENSDARG00000051962	4.19	7.11	0.8	0.006
npc111	ENSDARG00000077891	4.42	7.51	0.8	0.011
cry4	ENSDARG00000011890	10.51	17.84	0.8	0.006
inpp1b	ENSDARG00000001442	2.67	4.50	0.8	0.036
sb:cb472	ENSDARG00000060238	15.82	26.61	0.8	0.006
qsox1	ENSDARG00000039459	8.53	14.33	0.7	0.011
gadd45ba	ENSDARG00000027744	37.84	63.42	0.7	0.006
abcd1	ENSDARG00000074876	1.32	2.20	0.7	0.006
ppp1r27	ENSDARG00000052591	16.35	27.27	0.7	0.027
nr5a5	ENSDARG00000039116	9.37	15.54	0.7	0.006

Appendix 6 (Continued)

ZFIN gene ID	ENSEMBL gene ID	0ppm FPKM	3ppm FPKM	log ₂ (fold change)	q value
agt	ENSDARG00000016412	24.81	41.12	0.7	0.006
trim63	ENSDARG00000028027	83.41	137.74	0.7	0.011
neurod	ENSDARG00000019566	84.09	138.76	0.7	0.006
ccdc88aa	ENSDARG00000078440	3.82	6.28	0.7	0.016
hbp1	ENSDARG00000028517	15.84	25.88	0.7	0.006
hmox1a	ENSDARG00000027529	17.69	28.88	0.7	0.011
adh8b	ENSDARG00000024278	50.49	82.36	0.7	0.006
klhl38b	ENSDARG00000040278	15.15	24.50	0.7	0.020
ctsc	ENSDARG00000018806	9.47	15.29	0.7	0.006
prnpa	ENSDARG00000026229	27.92	45.04	0.7	0.020
alas1	ENSDARG00000021059	49.27	79.29	0.7	0.027
abcc2	ENSDARG00000014031	11.31	18.19	0.7	0.006
rimk1a	ENSDARG00000016830	39.30	63.14	0.7	0.016
ndrg1a	ENSDARG00000032849	54.75	87.96	0.7	0.011
arntl1a	ENSDARG00000006791	11.19	17.92	0.7	0.036
apoea	ENSDARG00000086370	161.94	257.68	0.7	0.020
txlnba	ENSDARG00000020594	20.08	31.89	0.7	0.016
mybpha	ENSDARG00000058799	10.21	16.19	0.7	0.020
srebf1	ENSDARG00000067607	4.85	7.70	0.7	0.011
slc43a2b	ENSDARG00000061120	42.46	66.72	0.7	0.027
col9a1	ENSDARG00000031483	15.25	23.79	0.6	0.024
pla2g12b	ENSDARG00000015662	26.44	41.17	0.6	0.016
fgf6a	ENSDARG00000009351	11.07	17.21	0.6	0.034
spsb3a	ENSDARG00000077737	8.39	13.05	0.6	0.034
cenpf	ENSDARG00000055133	2.35	3.65	0.6	0.036
acbd5a	ENSDARG00000034883	12.46	19.26	0.6	0.020
gngt2a	ENSDARG00000010680	64.64	99.59	0.6	0.027
ddit4	ENSDARG00000037618	18.04	27.74	0.6	0.042
top2a	ENSDARG00000024488	11.67	17.88	0.6	0.036
aoc1	ENSDARG00000061355	21.09	32.32	0.6	0.027
atp8b5b	ENSDARG00000079235	7.39	11.27	0.6	0.034
fbn2b	ENSDARG00000016744	5.00	7.61	0.6	0.011
helz	ENSDARG00000030560	7.46	11.33	0.6	0.036
epb41l3b	ENSDARG00000019917	26.81	40.51	0.6	0.036
ddb1	ENSDARG00000089106	19.62	29.64	0.6	0.036
zbtb4	ENSDARG00000061827	4.93	7.42	0.6	0.045

Appendix 7: Significantly down-regulated genes in 3ppm MeHg treated zebrafish embryos.

ZFIN gene ID	ENSEMBL gene ID	0ppm FPKM	3ppm FPKM	log ₂ (fold change)	q value
nr1d1	ENSDARG00000033160	42.38	0.69	-5.9	0.006
si:dkey-18a10.3	ENSDARG00000090814	8.05	0.27	-4.9	0.006
per1a	ENSDARG00000056885	3.86	0.22	-4.1	0.006
per1b	ENSDARG00000012499	10.84	1.31	-3.0	0.006
rpe65a	ENSDARG00000007480	39.09	5.73	-2.8	0.006
cry5	ENSDARG00000019498	9.29	1.40	-2.7	0.006
dbpb	ENSDARG00000057652	8.96	1.51	-2.6	0.006
nr1d2b	ENSDARG00000009594	59.66	13.00	-2.2	0.006
tefa	ENSDARG00000039117	91.65	20.12	-2.2	0.006
per3	ENSDARG00000010519	10.02	2.30	-2.1	0.006
dbpa	ENSDARG00000063014	11.51	2.67	-2.1	0.006
prkacbb	ENSDARG00000059125	4.11	1.00	-2.0	0.006
ankrd33ab	ENSDARG00000002508	1.82	0.47	-2.0	0.020
guca1c	ENSDARG00000030758	19.25	5.17	-1.9	0.006
cry-dash	ENSDARG00000002396	23.68	6.57	-1.8	0.006
rn7sk	ENSDARG00000081270	83.26	23.91	-1.8	0.006
guca1g	ENSDARG00000045737	16.36	4.80	-1.8	0.006
hsp90aa1.1	ENSDARG00000010478	31.72	9.36	-1.8	0.006
hsf2	ENSDARG00000053097	25.87	7.65	-1.8	0.006
bhlhe41	ENSDARG00000041691	14.89	4.43	-1.7	0.006
gabrr1	ENSDARG00000043902	5.74	1.80	-1.7	0.006
samsn1b	ENSDARG00000078647	6.56	2.12	-1.6	0.006
ggact.1	ENSDARG00000070581	3.18	1.07	-1.6	0.006
cabp5b	ENSDARG00000028485	21.20	7.21	-1.6	0.006
ankrd33aa	ENSDARG00000055638	5.44	1.96	-1.5	0.006
mgat4a	ENSDARG00000063330	16.83	6.06	-1.5	0.006
arr3a	ENSDARG00000056511	377.02	139.19	-1.4	0.006
gstp2	ENSDARG00000057338	31.84	11.85	-1.4	0.006
snx8b	ENSDARG00000077708	3.53	1.37	-1.4	0.006
cdkn1a	ENSDARG00000076554	6.95	2.72	-1.4	0.006
znf395b	ENSDARG00000024195	31.51	12.38	-1.3	0.006
si:dkey-104n9.1	ENSDARG00000093042	16.30	6.43	-1.3	0.006
hig1	ENSDARG00000022303	23.30	9.24	-1.3	0.006

Appendix 7 (Continued)

ZFIN gene ID	ENSEMBL gene ID	0ppm FPKM	3ppm FPKM	log ₂ (fold change)	q value
si:dkey-33i22.3	ENSDARG00000088377	1.97	0.79	-1.3	0.006
slc1a8b	ENSDARG00000032465	8.04	3.24	-1.3	0.006
ddb2	ENSDARG00000041140	29.72	12.08	-1.3	0.006
pde6h	ENSDARG00000070439	2186.10	890.13	-1.3	0.006
naf1	ENSDARG00000057929	3.88	1.60	-1.3	0.011
grk7a	ENSDARG00000020602	54.98	22.83	-1.3	0.006
rbp4l	ENSDARG00000044684	274.73	115.51	-1.3	0.006
ppm1na	ENSDARG00000010231	5.67	2.45	-1.2	0.006
nmrk2	ENSDARG00000067848	83.62	36.26	-1.2	0.006
ncaldb	ENSDARG00000011334	16.78	7.52	-1.2	0.006
slc1a2a	ENSDARG00000052138	9.75	4.37	-1.2	0.006
rhcgl1	ENSDARG00000007080	25.29	11.58	-1.1	0.006
atp8b2	ENSDARG00000079259	1.26	0.58	-1.1	0.006
rhcga	ENSDARG00000003203	53.63	24.68	-1.1	0.006
caspb	ENSDARG00000052039	22.98	10.59	-1.1	0.006
oaz2b	ENSDARG00000059815	10.52	4.97	-1.1	0.006
urb2	ENSDARG00000003217	3.10	1.47	-1.1	0.034
bhlhe40	ENSDARG00000004060	80.68	39.03	-1.0	0.006
mylipb	ENSDARG00000055118	11.43	5.71	-1.0	0.006
hsp90aa1.2	ENSDARG00000024746	25.19	12.64	-1.0	0.006
si:dkey-21a6.6	ENSDARG00000053544	14.38	7.24	-1.0	0.006
rdh5	ENSDARG00000008306	8.66	4.43	-1.0	0.016
ipo4	ENSDARG00000041493	4.58	2.35	-1.0	0.027
pprc1	ENSDARG00000090337	3.71	1.91	-1.0	0.036
muc5b	ENSDARG00000058556	2.88	1.50	-0.9	0.006
sybu	ENSDARG00000060112	17.92	9.36	-0.9	0.006
mob1bb	ENSDARG00000012953	14.43	7.58	-0.9	0.006
rgra	ENSDARG00000054890	20.20	10.65	-0.9	0.011
tcap	ENSDARG00000007344	11.44	6.06	-0.9	0.011
unc45b	ENSDARG00000008433	6.68	3.54	-0.9	0.006
si:dkey-23o4.6	ENSDARG00000034577	7.05	3.75	-0.9	0.047
cdca7a	ENSDARG00000077620	13.45	7.17	-0.9	0.006
lactbl1a	ENSDARG00000089063	7.66	4.10	-0.9	0.011
ttc19	ENSDARG00000074435	9.64	5.18	-0.9	0.036

Appendix 7 (Continued)

ZFIN gene ID	ENSEMBL gene ID	0ppm FPKM	3ppm FPKM	log ₂ (fold change)	q value
ptgr1	ENSDARG00000024877	8.38	4.51	-0.9	0.042
nfil3-6	ENSDARG000000087188	15.09	8.22	-0.9	0.006
homer1b	ENSDARG000000007517	5.47	2.98	-0.9	0.020
pyya	ENSDARG000000053449	19.66	10.78	-0.9	0.042
prlra	ENSDARG000000016570	6.15	3.40	-0.9	0.006
tfr1b	ENSDARG000000012552	3.46	1.92	-0.9	0.027
nr1d2a	ENSDARG000000003820	39.03	21.76	-0.8	0.006
cdk5r2b	ENSDARG000000078671	12.61	7.08	-0.8	0.006
tefb	ENSDARG000000038401	31.87	18.00	-0.8	0.006
mid1ip1l	ENSDARG000000018145	33.61	19.04	-0.8	0.006
sst3	ENSDARG000000031649	27.98	15.86	-0.8	0.011
ankrd1b	ENSDARG000000076192	45.99	26.11	-0.8	0.006
aldocb	ENSDARG000000019702	217.02	123.67	-0.8	0.006
lrit1a	ENSDARG000000019179	4.84	2.78	-0.8	0.016
cox17	ENSDARG000000069920	92.48	53.06	-0.8	0.006
mylk4a	ENSDARG000000091260	10.99	6.33	-0.8	0.006
xpc	ENSDARG000000039754	6.51	3.76	-0.8	0.024
nop2	ENSDARG000000043304	12.15	7.06	-0.8	0.006
adkb	ENSDARG000000018258	15.64	9.10	-0.8	0.011
eif1axa	ENSDARG000000029003	23.37	13.66	-0.8	0.016
hspe1	ENSDARG000000056167	113.24	66.36	-0.8	0.006
per2	ENSDARG000000034503	17.94	10.55	-0.8	0.006
imp1b	ENSDARG000000074839	6.93	4.11	-0.8	0.006
dct	ENSDARG000000006008	16.30	9.72	-0.7	0.039
slmo2	ENSDARG000000009505	41.50	24.75	-0.7	0.006
ppm1nb	ENSDARG000000057032	14.79	8.84	-0.7	0.006
agr2	ENSDARG000000070480	27.38	16.40	-0.7	0.016
slc25a28	ENSDARG000000074297	5.29	3.17	-0.7	0.047
sh3gl2	ENSDARG000000023600	45.22	27.17	-0.7	0.006
stxbp5l	ENSDARG000000006383	14.98	9.02	-0.7	0.030
mcm2	ENSDARG000000015911	13.28	8.02	-0.7	0.006
cx32.3	ENSDARG000000041787	13.23	8.01	-0.7	0.047
nhp2l1b	ENSDARG000000023299	42.61	25.87	-0.7	0.042
lar4ab	ENSDARG000000074979	7.58	4.62	-0.7	0.006
tyrp1b	ENSDARG000000056151	31.71	19.39	-0.7	0.020
dusp4	ENSDARG000000044688	8.85	5.46	-0.7	0.039

Appendix 7 (Continued)

ZFIN gene ID	ENSEMBL gene ID	0ppm FPKM	3ppm FPKM	log ₂ (fold change)	q value
mt,mt2	ENSDARG00000041623	119.50	73.91	-0.7	0.011
pdcd11	ENSDARG00000052480	8.15	5.06	-0.7	0.016
timm13	ENSDARG00000058297	26.88	16.75	-0.7	0.034
cycsb	ENSDARG00000044562	186.81	117.45	-0.7	0.006
fbl	ENSDARG00000053912	54.36	34.31	-0.7	0.006
mcm4	ENSDARG00000040041	11.60	7.33	-0.7	0.024
dkc1	ENSDARG00000016484	21.83	13.79	-0.7	0.024
mcm5	ENSDARG00000019507	13.23	8.39	-0.7	0.036
slc32a1	ENSDARG00000059775	19.06	12.09	-0.7	0.006
si:dkey- 162h11.2	ENSDARG00000091715	3.33	2.12	-0.7	0.036
cry1b	ENSDARG00000011583	12.17	7.86	-0.6	0.036
hspd1	ENSDARG00000056160	27.25	17.63	-0.6	0.042
desi1a	ENSDARG00000033140	17.91	11.68	-0.6	0.047
glula	ENSDARG00000069054	176.68	116.22	-0.6	0.039
pcsk1	ENSDARG00000002600	10.27	6.81	-0.6	0.039
slc24a3	ENSDARG00000006760	8.98	5.98	-0.6	0.024
cry1a	ENSDARG00000045768	38.26	25.93	-0.6	0.047

Appendix 8. Significantly up-regulated genes in 10ppm MeHg treated zebrafish embryos.

ZFIN gene ID	ENSEMBL gene ID	0ppm FPKM	10ppm FPKM	log ₂ (fold change)	q value
vwa2	ENSDARG00000075441	4.37	52.81	3.6	0.006
haus6	ENSDARG00000068210	2.53	16.35	2.7	0.006
opn1lw1	ENSDARG00000044862	6.24	27.32	2.1	0.006
spsb3b	ENSDARG00000077487	3.12	12.30	2.0	0.006
nfil3-2	ENSDARG00000043237	13.39	51.12	1.9	0.006
nfil3-5	ENSDARG00000094965	26.85	97.57	1.9	0.006
nr1d4b	ENSDARG00000059370	1.43	4.99	1.8	0.006
xkr8.2	ENSDARG00000076820	1.12	3.91	1.8	0.006
cdkn1d	ENSDARG00000088020	34.84	119.41	1.8	0.006
prdm1b	ENSDARG00000053592	5.52	18.46	1.7	0.006
tfcp2l1	ENSDARG00000029497	1.59	5.28	1.7	0.006
rn7sk	ENSDARG00000081270	83.26	248.90	1.6	0.006
slc1a7a	ENSDARG00000034940	1.31	3.79	1.5	0.006
agnr	ENSDARG00000096339	2.00	5.78	1.5	0.036
aanat2	ENSDARG00000079802	2.68	7.24	1.4	0.006
fkbp5	ENSDARG00000028396	29.82	79.39	1.4	0.006
arntl2	ENSDARG00000041381	1.85	4.92	1.4	0.006
rorcb	ENSDARG00000017780	9.14	24.08	1.4	0.006
ndrg1b	ENSDARG00000010420	34.41	86.12	1.3	0.006
inhbb	ENSDARG00000040777	4.92	11.90	1.3	0.006
hlfb	ENSDARG00000061011	5.37	12.83	1.3	0.006
ampd3b	ENSDARG00000032469	21.49	48.54	1.2	0.006
cyp11c1	ENSDARG00000042014	0.94	2.12	1.2	0.034
mxd3	ENSDARG00000057432	11.67	26.18	1.2	0.006
kera	ENSDARG00000056938	16.28	36.14	1.2	0.011
slc34a2b	ENSDARG00000036864	4.50	9.91	1.1	0.006
guca1e	ENSDARG00000078384	2.25	4.85	1.1	0.006
mxra5b	ENSDARG00000076309	0.59	1.21	1.0	0.006
rab14	ENSDARG00000074246	4.19	8.51	1.0	0.006
klf2a	ENSDARG00000042667	14.71	28.14	0.9	0.006
arntl1b	ENSDARG00000035732	6.50	12.24	0.9	0.006
mep1b	ENSDARG00000037533	5.67	10.65	0.9	0.006
slc25a25a	ENSDARG00000010572	5.55	10.43	0.9	0.006
cyp2k18	ENSDARG00000038366	5.74	10.70	0.9	0.006

Appendix 8 (Continued)

ZFIN gene ID	ENSEMBL gene ID	Oppm FPKM	10ppm FPKM	log ₂ (fold change)	q value
pik3r3a	ENSDARG00000071219	9.21	17.10	0.9	0.006
jam2b	ENSDARG00000079071	5.29	9.62	0.9	0.030
fbxo32	ENSDARG00000040277	33.53	60.18	0.8	0.006
b4galt1	ENSDARG00000002634	8.55	15.30	0.8	0.006
slc6a19a	ENSDARG00000018621	2.12	3.73	0.8	0.036
npas2	ENSDARG00000016536	3.56	6.21	0.8	0.006
tsc22d2	ENSDARG00000041839	13.76	23.94	0.8	0.006
agt	ENSDARG00000016412	24.81	42.91	0.8	0.006
slc16a12b	ENSDARG00000089885	10.31	17.76	0.8	0.006
arntl1a	ENSDARG00000006791	11.19	19.12	0.8	0.016
ccdc88aa	ENSDARG00000078440	3.82	6.52	0.8	0.011
rimk1a	ENSDARG00000016830	39.30	66.47	0.8	0.006
inpp1b	ENSDARG00000001442	2.67	4.52	0.8	0.036
klf3	ENSDARG00000015495	15.66	26.25	0.7	0.006
cry4	ENSDARG00000011890	10.51	17.58	0.7	0.006
pfkfb4l	ENSDARG00000029075	24.73	41.32	0.7	0.020
trim63	ENSDARG00000028027	83.41	138.93	0.7	0.006
csrn1a	ENSDARG00000031426	6.49	10.78	0.7	0.036
c3b	ENSDARG00000087359	3.51	5.78	0.7	0.016
txlnba	ENSDARG00000020594	20.08	32.97	0.7	0.006
hsd11b2	ENSDARG00000001975	11.11	18.05	0.7	0.011
kbtbd12	ENSDARG00000001882	13.03	20.94	0.7	0.006
r3hdm4	ENSDARG00000063254	9.50	15.24	0.7	0.020
cd99	ENSDARG00000051975	21.46	34.40	0.7	0.042
klhl38b	ENSDARG00000040278	15.15	24.24	0.7	0.030
slc34a2a	ENSDARG00000012903	10.04	16.05	0.7	0.027
gngt2a	ENSDARG00000010680	64.64	102.11	0.7	0.011
zyg11	ENSDARG00000007737	12.48	19.36	0.6	0.030
col9a1	ENSDARG00000031483	15.25	23.41	0.6	0.039
adh8b	ENSDARG00000024278	50.49	76.96	0.6	0.011
zbtb4	ENSDARG00000061827	4.93	7.52	0.6	0.016
tcf12	ENSDARG00000004714	19.38	29.01	0.6	0.047

Appendix 9. Significantly down-regulated genes in 10ppm MeHg treated zebrafish embryos.

ZFIN gene ID	ENSEMBL gene ID	0ppm FPKM	10ppm FPKM	log ₂ (fold change)	q value
nr1d1	ENSDARG00000033160	42.38	1.54	-4.8	0.006
per1b	ENSDARG00000012499	10.84	1.04	-3.4	0.006
sema7a	ENSDARG00000078707	18.78	1.93	-3.3	0.006
cry5	ENSDARG00000019498	9.29	1.18	-3.0	0.006
rpe65a	ENSDARG00000007480	39.09	5.01	-3.0	0.006
per3	ENSDARG00000010519	10.02	1.58	-2.7	0.006
gabrr1	ENSDARG000000043902	5.74	1.09	-2.4	0.006
ankrd33ab	ENSDARG00000002508	1.82	0.37	-2.3	0.006
nr1d2b	ENSDARG00000009594	59.66	12.49	-2.3	0.006
dbpb	ENSDARG000000057652	8.96	1.92	-2.2	0.006
cry-dash	ENSDARG00000002396	23.68	5.77	-2.0	0.006
tefa	ENSDARG000000039117	91.65	22.51	-2.0	0.006
hsf2	ENSDARG000000053097	25.87	6.68	-2.0	0.006
lama1	ENSDARG000000056043	4.44	1.24	-1.8	0.011
samsn1b	ENSDARG000000078647	6.56	1.89	-1.8	0.006
arr3a	ENSDARG000000056511	377.02	110.27	-1.8	0.006
dbpa	ENSDARG000000063014	11.51	3.44	-1.7	0.006
prkg2	ENSDARG000000054741	1.28	0.39	-1.7	0.006
hsp90aa1.1	ENSDARG000000010478	31.72	9.60	-1.7	0.006
ankrd33aa	ENSDARG000000055638	5.44	1.67	-1.7	0.006
slc1a2a	ENSDARG000000052138	9.75	3.02	-1.7	0.006
gstp2	ENSDARG000000057338	31.84	10.15	-1.6	0.006
bhlhe41	ENSDARG000000041691	14.89	4.77	-1.6	0.006
grk7a	ENSDARG000000020602	54.98	17.89	-1.6	0.006
cabp5b	ENSDARG000000028485	21.20	6.91	-1.6	0.006
pde6h	ENSDARG000000070439	2186.10	724.46	-1.6	0.006
cdca7a	ENSDARG000000077620	13.45	4.74	-1.5	0.006
guca1c	ENSDARG000000030758	19.25	6.83	-1.5	0.006
bhlhe40	ENSDARG000000004060	80.68	29.27	-1.5	0.006
znf395b	ENSDARG000000024195	31.51	11.72	-1.4	0.006
sdr42e1	ENSDARG000000003397	1.92	0.72	-1.4	0.039
prkacbb	ENSDARG000000059125	4.11	1.56	-1.4	0.006
ncaldb	ENSDARG000000011334	16.78	6.46	-1.4	0.006

Appendix 9 (Continued)

ZFIN gene ID	ENSEMBL gene ID	0ppm FPKM	10ppm FPKM	log ₂ (fold change)	q value
foxq1a	ENSDARG00000030896	15.35	5.95	-1.4	0.006
ddb2	ENSDARG00000041140	29.72	12.04	-1.3	0.006
sqlea	ENSDARG00000079946	2.48	1.01	-1.3	0.011
naf1	ENSDARG00000057929	3.88	1.63	-1.3	0.011
tyrp1a	ENSDARG00000029204	5.70	2.40	-1.2	0.006
pcyt1bb	ENSDARG00000044456	5.61	2.40	-1.2	0.006
impg1b	ENSDARG00000074839	6.93	2.99	-1.2	0.006
hig1	ENSDARG00000022303	23.30	10.07	-1.2	0.006
guca1g	ENSDARG00000045737	16.36	7.13	-1.2	0.034
neto2b	ENSDARG00000063293	1.40	0.62	-1.2	0.030
gbp	ENSDARG00000040059	19.85	8.83	-1.2	0.006
urb2	ENSDARG00000003217	3.10	1.39	-1.2	0.020
mcm2	ENSDARG00000015911	13.28	5.93	-1.2	0.006
snx8b	ENSDARG00000077708	3.53	1.59	-1.2	0.006
lactbl1a	ENSDARG00000089063	7.66	3.45	-1.1	0.006
mcm5	ENSDARG00000019507	13.23	6.00	-1.1	0.006
slc2a1a	ENSDARG00000001437	11.16	5.14	-1.1	0.006
rbp4l	ENSDARG00000044684	274.73	127.19	-1.1	0.006
odam	ENSDARG00000074476	14.73	6.89	-1.1	0.020
bahcc1	ENSDARG00000080009	12.36	5.81	-1.1	0.006
gabrr2a	ENSDARG00000052982	2.83	1.35	-1.1	0.042
atp8b2	ENSDARG00000079259	1.26	0.60	-1.1	0.006
rdh5	ENSDARG00000008306	8.66	4.13	-1.1	0.006
ppm1na	ENSDARG00000010231	5.67	2.75	-1.0	0.006
nle1	ENSDARG00000057105	4.43	2.15	-1.0	0.006
rx1	ENSDARG00000071684	15.62	7.64	-1.0	0.006
cdk5r2b	ENSDARG00000078671	12.61	6.22	-1.0	0.006
dct	ENSDARG00000006008	16.30	8.09	-1.0	0.006
mgat4a	ENSDARG00000063330	16.83	8.36	-1.0	0.006
mcm4	ENSDARG00000040041	11.60	5.83	-1.0	0.006
anxa11b	ENSDARG00000002632	93.75	47.18	-1.0	0.006
ptgs2b	ENSDARG00000010276	3.47	1.75	-1.0	0.020
npas4a	ENSDARG00000055752	3.87	1.96	-1.0	0.006
slc1a8b	ENSDARG00000032465	8.04	4.10	-1.0	0.020
mcm6	ENSDARG00000057683	9.55	4.92	-1.0	0.006
gale	ENSDARG00000002401	6.90	3.57	-1.0	0.034

Appendix 9 (Continued)

ZFIN gene ID	ENSEMBL gene ID	Oppm FPKM	10ppm FPKM	log ₂ (fold change)	q value
tyrp1b	ENSDARG00000056151	31.71	16.67	-0.9	0.006
acap3a	ENSDARG00000075990	55.78	29.62	-0.9	0.006
per2	ENSDARG00000034503	17.94	9.54	-0.9	0.006
hells	ENSDARG00000057738	4.45	2.37	-0.9	0.006
crcp	ENSDARG00000069373	17.84	9.53	-0.9	0.011
pdc11	ENSDARG00000052480	8.15	4.40	-0.9	0.006
scpp5	ENSDARG00000078622	15.54	8.44	-0.9	0.047
homer1b	ENSDARG00000007517	5.47	2.97	-0.9	0.006
muc5b	ENSDARG00000058556	2.88	1.60	-0.8	0.034
agr2	ENSDARG00000070480	27.38	15.24	-0.8	0.006
mthfr	ENSDARG00000053087	5.05	2.82	-0.8	0.020
polr1c	ENSDARG00000039400	11.20	6.26	-0.8	0.036
mt,mt2	ENSDARG00000041623	119.50	66.90	-0.8	0.006
hspd1	ENSDARG00000056160	27.25	15.36	-0.8	0.006
xpc	ENSDARG00000039754	6.51	3.71	-0.8	0.011
rab14	ENSDARG00000045261	12.09	6.89	-0.8	0.006
mylipb	ENSDARG00000055118	11.43	6.54	-0.8	0.011
aldoeb	ENSDARG00000019702	217.02	124.40	-0.8	0.006
ttc19	ENSDARG00000074435	9.64	5.54	-0.8	0.034
bbox1	ENSDARG00000036135	12.52	7.21	-0.8	0.006
nfil3-6	ENSDARG00000087188	15.09	8.83	-0.8	0.006
nhp211b	ENSDARG00000023299	42.61	24.96	-0.8	0.016
mob1bb	ENSDARG00000012953	14.43	8.47	-0.8	0.006
nol6	ENSDARG00000059711	5.02	2.95	-0.8	0.027
acaca	ENSDARG00000078512	8.88	5.32	-0.7	0.020
slc25a28	ENSDARG00000074297	5.29	3.17	-0.7	0.042
pdc1b	ENSDARG00000017634	53.34	32.02	-0.7	0.006
egr1	ENSDARG00000037421	26.63	16.05	-0.7	0.006
txnipb	ENSDARG00000070000	34.89	21.23	-0.7	0.011
gatm	ENSDARG00000036239	103.99	63.39	-0.7	0.034
adkb	ENSDARG00000018258	15.64	9.55	-0.7	0.024
pdca	ENSDARG00000011886	6.81	4.17	-0.7	0.024
dkc1	ENSDARG00000016484	21.83	13.43	-0.7	0.011
prlra	ENSDARG00000016570	6.15	3.79	-0.7	0.034
atp1a2a	ENSDARG00000010472	15.47	9.55	-0.7	0.011
fts1	ENSDARG00000076761	8.35	5.17	-0.7	0.047

Appendix 9 (Continued)

ZFIN gene ID	ENSEMBL gene ID	0ppm FPKM	10ppm FPKM	log ₂ (fold change)	q value
ankrd1b	ENSDARG00000076192	45.99	28.57	-0.7	0.039
oat	ENSDARG00000078425	14.95	9.30	-0.7	0.024
cry1b	ENSDARG00000011583	12.17	7.58	-0.7	0.020
gc3	ENSDARG00000026820	10.66	6.67	-0.7	0.020
aqp8a.1	ENSDARG00000045141	60.20	37.76	-0.7	0.016
nat10	ENSDARG00000054259	8.96	5.62	-0.7	0.011
sagb	ENSDARG00000038378	143.52	91.17	-0.7	0.020
abcc4	ENSDARG00000058953	7.97	5.07	-0.7	0.020
hspe1	ENSDARG00000056167	113.24	72.46	-0.6	0.045
sybu	ENSDARG00000060112	17.92	11.47	-0.6	0.030
larp4ab	ENSDARG00000074979	7.58	4.87	-0.6	0.027
hmgcra	ENSDARG00000052734	10.31	6.66	-0.6	0.036
mybbp1a	ENSDARG00000028323	15.61	10.12	-0.6	0.016

Appendix 10: Gene ontology (GO) enrichment analysis of biological functions affected by MeHg exposure in zebrafish embryos.

Biological function	Source	Number of genes	Adjusted P
response to light stimulus	GO:0009416	17	5.87E-15
response to radiation	GO:0009314	18	1.44E-14
Photoperiodism	GO:0009648	9	7.09E-13
response to abiotic stimulus	GO:0009628	18	2.16E-09
circadian rhythm	GO:0007623	7	3.14E-07
rhythmic process	GO:0048511	7	1.07E-05
nucleic acid metabolic process	GO:0090304	57	7.53E-05
cellular biosynthetic process	GO:0044249	62	0.0002
cellular nitrogen compound metabolic process	GO:0034641	67	0.0002
nucleobase-containing compound metabolic process	GO:0006139	64	0.0003
biosynthetic process	GO:0009058	64	0.0003
cellular nitrogen compound biosynthetic process	GO:0044271	48	0.0004
heterocycle metabolic process	GO:0046483	65	0.0005
cellular aromatic compound metabolic process	GO:0006725	65	0.0005
organic cyclic compound metabolic process	GO:1901360	66	0.0005
nitrogen compound metabolic process	GO:0006807	68	0.0009
organic substance biosynthetic process	GO:1901576	61	0.001
organic cyclic compound biosynthetic process	GO:1901362	47	0.001
aromatic compound biosynthetic process	GO:0019438	46	0.0011
nucleobase-containing compound biosynthetic process	GO:0034654	45	0.0012
transcription, DNA-dependent	GO:0006351	41	0.0014
RNA metabolic process	GO:0016070	48	0.0014
heterocycle biosynthetic process	GO:0018130	46	0.0015
RNA biosynthetic process	GO:0032774	41	0.0015
regulation of transcription, DNA-dependent	GO:0006355	39	0.0027
regulation of RNA biosynthetic process	GO:2001141	39	0.0028
regulation of RNA metabolic process	GO:0051252	39	0.0037
regulation of cellular biosynthetic process	GO:0031326	40	0.0053
regulation of biosynthetic process	GO:0009889	40	0.0056
single-organism metabolic process	GO:0044710	114	0.0056
regulation of nitrogen compound metabolic process	GO:0051171	41	0.0064
metabolic process	GO:0008152	122	0.0064

Appendix 10 (Continued)

Biological function	Source	Number of genes	Adjusted P
response to oxidative stress	GO:0006979	5	0.0073
DNA-dependent DNA replication	GO:0006261	5	0.0073
regulation of cellular macromolecule biosynthetic process	GO:2000112	39	0.0087
regulation of macromolecule biosynthetic process	GO:0010556	39	0.0092
cellular process	GO:0009987	149	0.0093
regulation of nucleobase-containing compound metabolic process	GO:0019219	40	0.0136
primary metabolic process	GO:0044238	101	0.0192
cellular macromolecule biosynthetic process	GO:0034645	48	0.0208
regulation of gene expression	GO:0010468	40	0.0208
cellular metabolic process	GO:0044237	96	0.0416
regulation of primary metabolic process	GO:0080090	42	0.0416
regulation of macromolecule metabolic process	GO:0060255	42	0.0416
anion transport	GO:0006820	8	0.0416
response to stress	GO:0006950	20	0.0416
macromolecule biosynthetic process	GO:0009059	48	0.0416
regulation of cellular metabolic process	GO:0031323	42	0.0416
response to chemical stimulus	GO:0042221	17	0.0416
regulation of metabolic process	GO:0019222	45	0.0416

Appendix 11: Gene set enrichment analysis (GSEA) results for each MeHg exposure concentration tested in zebrafish embryos.

C2: Curated gene set collection

<i>Gene set description</i>	<i>Source</i>	<i>1ppm MeHg</i>	<i>3ppm MeHg</i>	<i>10ppm MeHg</i>
Acetylcholine neurotransmitter release cycle	REACTOME			
Axon guidance	KEGG		NES=1.642 P=0.033 q=0.305	NES=2.812 P=0.000 q=0.000
Axon guidance	REACTOME		NES=1.472 P=0.065 q=0.159	
Dopamine neurotransmitter release cycle	REACTOME			
Glutamate neurotransmitter release cycle	REACTOME			
Glutathione conjugation	REACTOME			
Glutathione metabolism	KEGG			
NaCl dependent neurotransmitter transporters	REACTOME			
Neuroactive ligand receptor interaction	KEGG		NES=-1.685 P=0.035 q=0.043	NES=1.560 P=0.035 q=0.292
Neurotransmitter receptor binding and downstream transmission in the postsynaptic cell	REACTOME		NES=-2.676 P=0.000 q=0.003	
Neurotransmitter release cycle	REACTOME	NES=-1.633 P=0.044 q=0.296	NES=-1.874 P=0.008 q=0.024	
Norepinephrine neurotransmitter release cycle	REACTOME			

Appendix 11 (Continued)

C2: Curated gene set collection

<i>Gene set description</i>	<i>Source</i>	<i>1ppm MeHg</i>	<i>3ppm MeHg</i>	<i>10ppm MeHg</i>
Parkinson's disease	KEGG		NES=-3.047 P=0.000 q=0.000	NES=-2.867 P=0.000 q=0.000
SEMA3A pak dependent axon repulsion	REACTOME			
Parkinson's disease	KEGG		NES=-3.047 P=0.000 q=0.000	NES=-2.867 P=0.000 q=0.000
SEMA3A pak dependent axon repulsion	REACTOME			

C5: GO Biological process collection

<i>Gene set description</i>	<i>Source</i>	<i>1ppm MeHg</i>	<i>3ppm MeHg</i>	<i>10ppm MeHg</i>
Axon guidance	GO:0007411		NES=-1.648 P=0.038 q=0.048	
Axonogenesis	GO:0007409		NES=-1.848 P=0.008 q=0.026	
Brain development	GO:0007420		NES=-1.323 P=0.154 q=0.186	
Central nervous system development	GO:0007417		NES=-1.295 P=0.171 q=0.198	
Generation of neurons	GO:0048699		NES=-2.138 P=0.006 q=0.007	
Nervous system development	GO:0007399		NES=-1.786 P=0.018 q=0.031	

Appendix 11 (Continued)

C5: GO Biological process collection

<i>Gene set description</i>	<i>Source</i>	<i>1ppm MeHg</i>	<i>3ppm MeHg</i>	<i>10ppm MeHg</i>
Peripheral nervous system development	GO:0007422			
Phototransduction	GO:0007602			
Regulation of axonogenesis	GO:0050770			
Regulation of neurogenesis	GO:0050767			
Regulation of neuron apoptosis	GO:0043523			
Regulation of neurotransmitter levels	GO:0001505		NES=-1.736	P=0.026 q=0.035
Synapse organization and biogenesis	GO:0050808			
Transmission of nerve impulse	GO:0019226		NES=-2.532	P=0.000 q=0.002

C5: GO Cellular component collection

<i>Gene set description</i>	<i>Source</i>	<i>1ppm MeHg</i>	<i>3ppm MeHg</i>	<i>10ppm MeHg</i>
Focal adhesion	GO:0005925			
Neuron projection	GO:0043005		NES=-1.966	P=0.006 q=0.015

Appendix 11 (Continued)

C5: GO Molecular function collection

<i>Gene set description</i>	<i>Source</i>	<i>1ppm MeHg</i>	<i>3ppm MeHg</i>	<i>10ppm MeHg</i>
Acetylcholine binding	GO:0042166			
Glutamate receptor activity	GO:0008066		NES=-1.780 P=0.020 q=0.029	
Glutathione transferase activity	GO:0004364			
Neuropeptide binding	GO:0042923			
Neuropeptide hormone activity	GO:0005184			
Neuropeptide receptor activity	GO:0008188			
Neurotransmitter binding	GO:0042165			
Neurotransmitter receptor activity	GO:0030594			
Serotonin receptor activity	GO:0004993			

HPO: Human phenotype ontology collection

<i>Gene set description</i>	<i>Source</i>	<i>1ppm MeHg</i>	<i>3ppm MeHg</i>	<i>10ppm MeHg</i>
Abnormal lower motor neuron morphology	HP:0002366			
Abnormal neuron morphology	HP:0012757		NES=-1.760 P=0.017 q=0.077	
Abnormal upper motor neuron morphology	HP:0002127			
Abnormality of neural tube closure	HP:0045005			

Appendix 11 (Continued)

HPO: Human phenotype ontology collection

<i>Gene set description</i>	<i>Source</i>	<i>1ppm MeHg</i>	<i>3ppm MeHg</i>	<i>10ppm MeHg</i>
Abnormality of neuronal migration	HP:0002269			
Abnormality of vision	HP:0000504			NES=-1.680 P=0.029 q=0.182
Abnormality of vision evoked potentials	HP:0000649			
Ataxia	HP:0001251		NES=-2.079 P=0.000 q=0.020	
Attention deficit hyperactivity disorder	HP:0007018	NES=1.838 P=0.011 q=0.167		
Autism	Wall, et al. (2008)		NES=-2.094 P=0.000 q=0.040	NES=1.535 P=0.065 q=0.242
Autistic behavior	HP:0000729			
Bilateral convulsive seizures	HP:0007334			
Decreased motor nerve conduction velocity	HP:0003431			
Epileptic encephalopathy	HP:0200134		NES=-1.802 P=0.024 q=0.083	
Epileptic spasms	HP:0011097			
Epileptiform EEG discharges	HP:0011182		NES=-1.451 P=0.097 q=0.209	

Appendix 11 (Continued)

HPO: Human phenotype ontology collection

<i>Gene set description</i>	<i>Source</i>	<i>1ppm MeHg</i>	<i>3ppm MeHg</i>	<i>10ppm MeHg</i>
Episodic ataxia	HP:0002131			
Focal motor seizures	HP:0011153			
Functional motor problems	HP:0004302			
Gait ataxia	HP:0002066			
Generalized seizures	HP:0002197			
Limb ataxia	HP:0002070			
Motor neuron atrophy	HP:0007373		NES=-1.650 P=0.030 q=0.102	
Motor tics	HP:0100034			
Neurodegeneration	HP:0002180			
Neurodevelopmental delay	HP:0012758			NES=-2.246 P=0.000 q=0.012
Neuronal loss in central nervous system	HP:0002529			
Oculomotor apraxia	HP:0000657			
Optic neuropathy	HP:0001138			
Paresthesia	HP:0003401			
Parkinsonism	HP:0001300			

Appendix 11 (Continued)

HPO: Human phenotype ontology collection

<i>Gene set description</i>	<i>Source</i>	<i>1ppm MeHg</i>	<i>3ppm MeHg</i>	<i>10ppm MeHg</i>
Peripheral axonal degeneration	HP:0000764	NES=-1.576 P=0.039 q=0.443		
Peripheral axonal neuropathy	HP:0003477			
Peripheral neuropathy	HP:0009830			
Poor fine motor coordination	HP:0007010			
Progressive cerebellar ataxia	HP:0002073			
Progressive gait ataxia	HP:0007240			
Progressive neurologic deterioration	HP:0002344			
Progressive visual loss	HP:0000529			
Seizures	HP:0001250			NES=-2.500 P=0.000 q=0.003
Sensorimotor neuropathy	HP:0007141			
Sensory impairment	HP:0003474			
Sensory neuropathy	HP:0000763			

Appendix 12: RNA yields and RIN values of zebrafish whole-embryo RNA extractions

Sample ID	ng/ μ l	Total RNA (μ g)	260/280	260/230	RIN
CTRL1	161.47	3.23	1.99	2.24	7.3
CTRL2	68.25	1.37	2	2.13	8.9
CTRL3	69.17	1.38	2.03	2.11	9.5
1PPMHg1	82.97	1.66	2.09	2.14	9.5
1PPMHg2	120.75	2.42	2.01	2.17	7.7
1PPMHg3	102.87	2.06	2.08	2.2	9.6
3PPMHg1	116.09	2.32	2.09	1.97	9.5
3PPMHg2	81.26	1.63	2.07	2.15	9.9
3PPMHg3	91.15	1.82	2.09	2.18	9.7
10PPMHg1	160.82	3.22	2.01	2.26	9.5
10PPMHg2	78.57	1.57	2.07	2.13	9.7
10PPMHg3	91.96	1.84	2.03	2.12	9.5

Appendix 13: RNA yields and RIN values of yellow perch whole-embryo RNA extractions

Sample ID	Total RNA (μg)	260/280	260/230	RIN
Ctrl 17 dpf Perch #1 - Replicate 1	0.66	2.04	2.08	9.3
Ctrl 17 dpf Perch #2 - Replicate 1	1.80	2.12	2.19	9.8
Ctrl 17 dpf Perch #3 - Replicate 1	1.62	2.1	2.04	9.2
Ctrl 17 dpf Perch #4 - Replicate 1	0.64	1.76	1.88	10
Ctrl 17 dpf Perch #5 - Replicate 1	1.96	2.09	2.16	9.5
Ctrl 17 dpf Perch #6 - Replicate 1	1.30	2.32	2.26	8.5
Ctrl 17 dpf Perch #7 - Replicate 1	2.27	2.03	2.18	9
Ctrl 17 dpf Perch #8 - Replicate 1	0.85	1.95	2.15	9.2
Ctrl 17 dpf Perch #1 - Replicate 2	1.51	2.1	2.17	9
Ctrl 17 dpf Perch #2 - Replicate 2	1.87	2.05	2.12	8.8
Ctrl 17 dpf Perch #3 - Replicate 2	1.52	2.1	2.09	9.2
Ctrl 17 dpf Perch #4 - Replicate 2	1.81	2.11	2.19	8.9
Ctrl 17 dpf Perch #5 - Replicate 2	2.25	2.06	2.18	8.6
Ctrl 17 dpf Perch #6 - Replicate 2	1.92	2	2.07	8
Ctrl 17 dpf Perch #7 - Replicate 2	1.67	1.91	2.07	7.8
Ctrl 17 dpf Perch #8 - Replicate 2	1.77	1.93	2.06	7.6
Ctrl 17 dpf Perch #1 - Replicate 3	1.91	2.03	2.15	7.8
Ctrl 17 dpf Perch #2 - Replicate 3	2.19	2.02	2.07	8.6
Ctrl 17 dpf Perch #3 - Replicate 3	1.58	1.88	2.03	8.8
Ctrl 17 dpf Perch #4 - Replicate 3	2.03	1.95	2.16	8
Ctrl 17 dpf Perch #5 - Replicate 3	1.75	2.07	2.07	8.4
Ctrl 17 dpf Perch #6 - Replicate 3	1.12	1.9	1.92	7.2
Ctrl 17 dpf Perch #7 - Replicate 3	1.71	1.99	1.89	7.9
Ctrl 17 dpf Perch #8 - Replicate 3	2.03	2.03	2.1	7.9
0.03 μM MeHg 17 dpf Perch #1 - Replicate 1	2.25	2.05	2.18	8.8
0.03 μM MeHg 17 dpf Perch #2 - Replicate 1	1.81	2.03	2.06	8.7
0.03 μM MeHg 17 dpf Perch #3 - Replicate 1	2.72	2.08	2.24	9.1
0.03 μM MeHg 17 dpf Perch #4 - Replicate 1	1.97	2.01	2.01	8.7
0.03 μM MeHg 17 dpf Perch #5 - Replicate 1	2.73	2.06	2.23	8.8
0.03 μM MeHg 17 dpf Perch #6 - Replicate 1	2.18	2.03	2.16	8.3
0.03 μM MeHg 17 dpf Perch #7 - Replicate 1	2.03	2.01	2.13	7.4
0.03 μM MeHg 17 dpf Perch #8 - Replicate 1	0.94	2.05	2.22	9.1
0.03 μM MeHg 17 dpf Perch #1 - Replicate 2	2.16	2.03	2.22	8.9
0.03 μM MeHg 17 dpf Perch #2 - Replicate 2	2.77	2.06	2.24	8.5
0.03 μM MeHg 17 dpf Perch #3 - Replicate 2	2.89	2.08	2.22	8.7
0.03 μM MeHg 17 dpf Perch #5 - Replicate 2	2.24	2.12	2.19	8
0.03 μM MeHg 17 dpf Perch #6 - Replicate 2	1.58	2.12	2.08	9.1
0.03 μM MeHg 17 dpf Perch #7 - Replicate 2	0.96	2.08	2.02	9.4

0.03µM MeHg 17 dpf Perch #8 - Replicate 2	1.90	2.1	2.2	8.7
0.03µM MeHg 17 dpf Perch #1 - Replicate 3	1.33	2.14	2.22	9.1
0.03µM MeHg 17 dpf Perch #2 - Replicate 3	1.50	2.15	2.19	9.2
0.03µM MeHg 17 dpf Perch #3 - Replicate 3	1.47	2.09	2.17	9.4
0.03µM MeHg 17 dpf Perch #4 - Replicate 3	1.30	2.08	2.08	9.1
0.03µM MeHg 17 dpf Perch #5 - Replicate 3	1.76	2.08	2.26	8.8
0.03µM MeHg 17 dpf Perch #6 - Replicate 3	1.96	2.08	2.24	9
0.03µM MeHg 17 dpf Perch #7 - Replicate 3	1.14	1.99	2.14	8.5
0.03µM MeHg 17 dpf Perch #8 - Replicate 3	1.30	2.05	2.15	9
0.03µM MeHg 17 dpf Perch #4 - Replicate 2	2.00	2.07	2.21	7.8
0.1µM MeHg 17 dpf Perch #1 - Replicate 1	1.20	2.05	2.19	10
0.1µM MeHg 17 dpf Perch #2 - Replicate 1	1.93	2.04	2.1	9.4
0.1µM MeHg 17 dpf Perch #3 - Replicate 1	1.83	2.09	2.16	9.3
0.1µM MeHg 17 dpf Perch #4 - Replicate 1	1.85	2.03	2.22	9.3
0.1µM MeHg 17 dpf Perch #5 - Replicate 1	1.64	2.06	2.19	9.1
0.1µM MeHg 17 dpf Perch #6 - Replicate 1	1.92	2.06	2.18	9.1
0.1µM MeHg 17 dpf Perch #7 - Replicate 1	1.87	2.08	2.22	9
0.1µM MeHg 17 dpf Perch #8 - Replicate 1	0.60	1.93	2.07	9.6
0.1µM MeHg 17 dpf Perch #1 - Replicate 2	1.91	2.08	2.19	9.3
0.1µM MeHg 17 dpf Perch #2 - Replicate 2	2.27	2.07	2.17	9.4
0.1µM MeHg 17 dpf Perch #3 - Replicate 2	1.77	2.04	2.21	9.7
0.1µM MeHg 17 dpf Perch #4 - Replicate 2	1.75	2.11	2.17	9.5
0.1µM MeHg 17 dpf Perch #5 - Replicate 2	1.97	2.08	2.11	9.7
0.1µM MeHg 17 dpf Perch #6 - Replicate 2	2.33	2.07	2.15	9.6
0.1µM MeHg 17 dpf Perch #7 - Replicate 2	1.79	2.07	2.18	10
0.1µM MeHg 17 dpf Perch #8 - Replicate 2	0.83	2.01	2.12	9.8
0.1µM MeHg 17 dpf Perch #1 - Replicate 3	1.41	1.95	2.08	9.2
0.1µM MeHg 17 dpf Perch #2 - Replicate 3	1.77	2	2.1	8.9
0.1µM MeHg 17 dpf Perch #3 - Replicate 3	1.49	2.04	2.18	9.1
0.1µM MeHg 17 dpf Perch #4 - Replicate 3	1.32	2	2.11	9.2
0.1µM MeHg 17 dpf Perch #5 - Replicate 3	1.47	2.02	2.18	9.2
0.1µM MeHg 17 dpf Perch #6 - Replicate 3	1.76	1.98	2.13	9.3
0.1µM MeHg 17 dpf Perch #7 - Replicate 3	1.54	2.04	2.06	9
0.1µM MeHg 17 dpf Perch #8 - Replicate 3	1.64	2.07	2.19	9.4
0.3µM MeHg 17 dpf Perch #1 - Replicate 1	2.58	2.03	2.23	8.7
0.3µM MeHg 17 dpf Perch #2 - Replicate 1	1.90	2.11	2.15	9.5
0.3µM MeHg 17 dpf Perch #3 - Replicate 1	1.63	2.08	2.15	9.6
0.3µM MeHg 17 dpf Perch #4 - Replicate 1	1.78	2.06	2.12	9.9
0.3µM MeHg 17 dpf Perch #5 - Replicate 1	2.07	2.14	2.2	9.6
0.3µM MeHg 17 dpf Perch #6 - Replicate 1	1.86	2.06	2.13	9.8
0.3µM MeHg 17 dpf Perch #7 - Replicate 1	2.02	2.07	2.2	9.3

0.3µM MeHg 17 dpf Perch #8 - Replicate 1	0.72	1.97	2.07	9.2
0.3µM MeHg 17 dpf Perch #1 - Replicate 2	2.32	2.01	2.2	8.7
0.3µM MeHg 17 dpf Perch #2 - Replicate 2	2.83	2.07	2.22	8.9
0.3µM MeHg 17 dpf Perch #3 - Replicate 2	3.06	2.06	2.23	8.9
0.3µM MeHg 17 dpf Perch #4 - Replicate 2	1.95	2.01	2.19	8.9
0.3µM MeHg 17 dpf Perch #5 - Replicate 2	2.61	2.09	2.23	9
0.3µM MeHg 17 dpf Perch #6 - Replicate 2	2.47	2.1	2.24	9.2
0.3µM MeHg 17 dpf Perch #7 - Replicate 2	2.45	2.05	2.21	9.1
0.3µM MeHg 17 dpf Perch #8 - Replicate 2	2.55	2.03	2.25	8.9
0.3µM MeHg 17 dpf Perch #1 - Replicate 3	1.80	2.05	2.23	8.6
0.3µM MeHg 17 dpf Perch #2 - Replicate 3	1.86	1.95	2.21	8.2
0.3µM MeHg 17 dpf Perch #3 - Replicate 3	1.27	2.03	2.05	8.6
0.3µM MeHg 17 dpf Perch #4 - Replicate 3	1.43	2.05	2.19	9
0.3µM MeHg 17 dpf Perch #5 - Replicate 3	1.63	2.02	2.21	8.9
0.3µM MeHg 17 dpf Perch #6 - Replicate 3	1.68	1.97	2.2	8.7
0.3µM MeHg 17 dpf Perch #7 - Replicate 3	0.81	2.1	2.19	9.5
0.3µM MeHg 17 dpf Perch #8 - Replicate 3	0.80	2.15	2.23	9.4

Appendix 14: RT-qPCR primers utilized for the analysis of gene expression in yellow perch embryos

Gene symbol	Primer ID	Primer Sequence (5'–3')	Efficiency (%)	Concentration
<i>l13a</i>	l13a_FW	CTGAAGCCAACTCGCAAGTTC	97.21	1 μ M
	l13a_RV	GGTCAGCTTGATCAGTGTCTTTTTC		
<i>ef1a</i>	ef1a_FW	CGACAAGATGAGCTGGTTCAAG	97.51	0.75 μ M
	ef1a_RV	ACAGTTCCGATACCGCCAATC		
<i>ef2</i>	ef2_FW	GATGAGGCTGCCATGGGTATC	98.06	2 μ M
	ef2_RV	CCTTCTTTCCAGGGACATAGTTTG		
<i>cry1a</i>	cry1a_FW	ATGGGATTGTCTGTCTCGAGGC	96.72	1 μ M
	cry1a_RV	GAGTGGTGCAGTGGAGTTCA		
<i>per3</i>	per3_FW	CTGTGCACCGGAAAGTGTTG	95.20	2 μ M
	per3_RV	TCAGTGGACTCGTCCTGACT		
<i>slc1a2a</i>	slc1a2a_FW	TCACTCGTTTTGTGCTCCCA	92.62	1 μ M
	slc1a2a_RV	GGGTCAAGTACGATGCCGTT		
<i>prkacbb</i>	prkacbb_FW	CCCGAGATCATCCTCAGCAAGG	95.61	1 μ M
	prkacbb_RV	CCTCAGCAGATCCTTCAG		
<i>opn1lw1</i>	opn1lw1_FW	ACACTGTCGCATGTTGTGGT	92.67	1 μ M
	opn1lw1_RV	AGTCCATGAGGCCAGTACCT		

Appendix 15: Accession numbers of proteins used to perform alignments in order to create degenerate primer pairs for yellow perch

Target gene	Organism	Accession number
opn1lw	<i>Danio rerio</i>	NP_571250.1
	<i>Carassius auratus</i>	ACZ97946.1
	<i>Cyprinus carpio</i>	BAB32496.1
	<i>Gasterosteus aculeatus</i>	AGL76517.1
	<i>Poecilia reticulata</i>	BAM74441.1
per3	<i>Danio rerio</i>	NP_571659.1
	<i>Solea senegalensis</i>	CAQ68365.1
	<i>Oryzias latipes</i> (PREDICTED)	XP_004069203.1
	<i>Poecilia reticulata</i> (PREDICTED)	XP_008407502.1
slc1a2a	<i>Danio rerio</i>	NP_001177234.1
	<i>Astyanax mexicanus</i> (PREDICTED)	XP_007228216.1
	<i>Takifugu rubripes</i> (PREDICTED)	XP_011616643

Appendix 16: Degenerate primers for yellow perch obtained from protein alignment.

Gene symbol	Primer_ID	Primer Sequence (5'–3')
<i>opn1lw</i>	opn1lw_FW	GGTGGCCACCGCCAARTTYAARAA
	opn1lw_RV	CGGAACTGCCGGTTCATRAANAC
<i>per3</i>	per3_FW	CCTCGGATCCCCATGGAYAARMG
	per3_RV	AGGTACCTGATGATGTTGTCCACRCARTTDAT
<i>slc1a2a</i>	slc1a2a_FW	GCACCCGGGCCATGRTNTAYTA
	slc1a2a_RV	CGGAACCGGTCCAGCARCCARTCNAC

Curriculum vitae

Francisco Xavier Mora-Zamorano

PLACE OF BIRTH: Tijuana, Baja California, Mexico

EDUCATION

PhD in Freshwater Sciences

University of Wisconsin-Milwaukee

2011/9- 2015/9; Advisor: Dr. Michael Carvan III

Dissertation Title: Neurobehavioral and gene expression effects of early embryonic methylmercury exposure in yellow perch (*Perca flavescens*) and zebrafish (*Danio rerio*) larvae.

B.S. in Aquaculture (2007-2011)

Autonomous University of Baja California, Mexico; 2007/2- 2011/2

HONORS AND AWARDS

University of Wisconsin – Milwaukee Chancellor’s Graduate Student Award (2014)

Society of Environmental Toxicology and Chemistry (SETAC) Travel Award for best poster presentation (2014)

Graduate traineeship in Oceans and Human Health, from the NOAA Center of Excellence for Great Lakes and Human Health (2011 – 2013)

Watertech of America Scholarship in Memory of Eugene VandenHeuvel (2014)

Watertech of America Scholarship in Memory of Eugene VandenHeuvel (2012)

Bachelors of Science in Marine Science with Honors from the Autonomous University of Baja California (2011)

PRESENTATIONS

Platform: FX Mora-Zamorano, CA Murphy, N Basu, J Head, R Goetz, MJ Carvan III “Effects of methylmercury on behavior and gene expression of larval yellow perch (*Perca flavescens*) and zebrafish (*Danio rerio*): a comparative study”,

SETAC North America 35th annual meeting, Vancouver, Canada, November 11, 2014.

Poster: FX Mora-Zamorano, CA Murphy, N Basu, J Head, R Goetz, MJ Carvan III, "Effects of methylmercury on the swimming kinematics and foraging of larval yellow perch (*Perca flavescens*) and zebrafish (*Danio rerio*)", SETAC Midwest chapter meeting, Chicago, Illinois, March 21, 2014.

Poster: FX Mora-Zamorano, CA Murphy, N Basu, J Head, R Goetz, MJ Carvan III "Effects of methylmercury on the swimming kinematics and foraging of larval yellow perch (*Perca flavescens*) and zebrafish (*Danio rerio*)", SETAC Midwest chapter meeting, Chicago, Illinois, March 21, 2014.

Invited talk: "Effects of methylmercury on the behavior of larval yellow perch and zebrafish: a comparative study", University of Wisconsin – Milwaukee, School of Freshwater Sciences, March 13, 2014.

Poster: FX Mora-Zamorano, MJ Carvan III, K Svoboda, "Novel, low-cost setup allows simultaneous tracking of multiple groups of zebrafish eleutheroembryos", Aquatic Animal Models for Human Disease 6th annual meeting, Milwaukee, Wisconsin, July 1, 2013.

Poster: FX Mora-Zamorano, CA Murphy, N Basu, J Head, R Goetz, MJ Carvan III "Assessing the neurobehavioral effects of methylmercury on yellow perch (*Perca flavescens*) and zebrafish (*Danio rerio*)", SETAC Midwest chapter meeting, La Crosse, Wisconsin, March 19, 2013.

Platform: FX Mora-Zamorano, CA Murphy, AD Deardorff, N Basu, J Head, R Goetz, MJ Carvan III "Behavioral effects of MeHg on larval yellow perch (*Perca flavescens*) and zebrafish (*Danio rerio*): implications for recruitment", SETAC North America 33rd annual meeting, Long Beach, California, November 15, 2012.

MANUSCRIPTS IN PREPARATION

FX Mora-Zamorano, K Svoboda, MJ Carvan III, "The nicotine evoked locomotor response: A tool for the early detection of locomotor abnormalities in zebrafish embryos".

FX Mora-Zamorano, R Klingler, CA Murphy, N Basu, J Head, MJ Carvan III, "Parental whole life cycle dietary exposure to methylmercury in zebrafish (*Danio rerio*) affects visualmotor response, locomotion and foraging of offspring".

FX Mora-Zamorano, R Klingler, CA Murphy, N Basu, J Head, MJ Carvan III, “Embryonic methylmercury exposure affects swimming behavior and foraging of yellow perch (*Perca flavescens*) larvae”.

FX Mora-Zamorano, ME Waltz, R Klingler, CA Murphy, N Basu , J Head, P Tonellato, MJ Carvan III, “Effects of embryonic methylmercury exposure in the gene expression of larval zebrafish (*Danio rerio*) and yellow perch (*Perca flavescens*)”.

T Kalluvila, R Klingler, MC Pickens, FX Mora-Zamorano, VP Connaughton, MJ Carvan III, “Ancestral developmental exposure to methylmercury induces transgenerational inheritance of visual and neurobehavioral deficits”

PROFFESIONAL MEMBERSHIPS

Society of Environmental Toxicology and Chemistry (SETAC)

Society of Toxicology (SOT)